Scuola Universitaria Superiore IUSS Pavia

Regional Seismic Risk Assessment for Integrated Loss–Based Prioritisation of Bridge Portfolios

A Thesis Submitted in Partial Fulfilment of the Requirements
for the Degree of Doctor of Philosophy in

EARTHQUAKE ENGINEERING AND ENGINEERING SEISMOLOGY

Obtained in the framework of the Doctoral Programme in
Understanding and Managing Extremes

by

Andres Abarca Jimenez

April, 2022

Scuola Universitaria Superiore IUSS Pavia

Regional Seismic Risk Assessment for Integrated Loss–Based Prioritisation of Bridge Portfolios

A Thesis Submitted in Partial Fulfilment of the Requirements
for the Degree of Doctor of Philosophy in

EARTHQUAKE ENGINEERING AND ENGINEERING SEISMOLOGY

Obtained in the framework of the Doctoral Programme in
Understanding and Managing Extremes

by

Andres Abarca Jimenez

Supervisors:
Ricardo Monteiro PhD (IUSS Pavia)
Gerard O'Reilly PhD (IUSS Pavia)

April 2022

ABSTRACT

In recent years, regional seismic risk assessment has seen a growing interest as a tool for stakeholders to quantify the expected performance of infrastructure inventories, providing useful information for efficient resource allocation and an overall increase in resilience of the systems analyzed. However, despite this being a frontline topic of research, there are multiple setbacks on the application side that have prevented a well-established uniform approach to follow being formalised when an assessment of this type needs to be performed. Researchers and practitioners tasked with such an assignment can become overwhelmed by questions that have not been addressed so far, such as: How to efficiently account for the seismic hazard of a regionally distributed inventory? How much knowledge of the inventory is required to attain adequate results? What is the uncertainty in the final results that derive from the lack of complete knowledge of the inventory? How to consider indirect losses when network traffic information is unavailable? How to prioritize resource allocation within a bridge inventory?

Within this thesis, these questions are tackled within an application setting, using a database of real bridges from the Italian road network that are located in synthetic case studies to represent real-life bridge networks. The overall objective is to quantify the impact on the overall results of typical and innovative decisions made for regional assessment purposes, as well as to provide recommendations on specific topics that will aid in the determination of guidelines for future projects.

Initially, the hazard component is addressed by evaluating the intensity measure that should be used in regional seismic assessment of bridges, to efficiently and accurately account for the fragility of the assets. In terms of exposure, the uncertainty that derives from the lack of structural information when performing risk assessment of large bridge portfolios is quantified and explored. In terms of seismic vulnerability, specifically the losses that can be associated with the complete disruption of each bridge in the inventory, the calculation of indirect losses with a view to their use within prioritization schemes is addressed. Finally, recognizing the practical need for management agencies to define methodologies with which to optimize asset maintenance and to effectively utilise their limited resources, a prioritization methodology is defined and evaluated. Overall, the methodologies implemented and results obtained, represent a useful contribution towards the practical implementation of regional seismic risk assessment and prioritization of bridge inventories.

Keywords: regional seismic risk, bridges, intensity measure, average spectral acceleration, ground motion record selection, network analysis, taxonomy-based assessment, machine learning

ACKNOWLEDGEMENTS

First, I would like to thank both my supervisors, Ricardo Monteiro and Gerard O'Reilly, for their incredible guidance and support provided throughout the last four years. Your dedication, patience and friendship made a great impact in the way that I see research and will be an example that I will continue to recall fondly for years to come.

This experience would never have happened, in any shape or form, without the help of my beautiful, strong and intelligent wife Maria Jose. Her drive, support and encouragement, in all aspects of life, was fundamental in accomplishing my goals during these last challenging years.

I share the credit of this work with all my friends and collegues all over the world that, one way or another, provided the support I needed, in times both good and bad. Special mention goes out to Camilo Perdomo, Lucho Alvarez and Theo Famprikis; for all the long conversations we had that have shaped my perpective in academic and (mostly) real life. I hope the future brings many, many more.

Finally, I would like to thank musicians Dallas Green and Adele, as well as the band Daft Punk, for providing the main soundtrack used to write this thesis. Though we are strangers, their work constantly inspires me and serves as a reminder that applying passion and dedication to your work, can lead to life changing outcomes.

TABLE OF CONTENTS

LIST OF FIGURES

LIST OF TABLES

LIST OF SYMBOLS AND ACRONYMS

AAL	= Average Annual Loss
A_c	= Gross area of the element
ANAS	= Azienda Nazionale Autonoma delle Strade
APE	= Annual Probability of Exceedance
A_{sl}	= Area of longitudinal steel
A_{st}	= Area of transverse steel
AvgSa	= Average Spectral Acceleration
BDC	= Baseline Daily Cost
BRITNEY	= BRIdge auTomatic Nonlinear analysis-based Earthquake fragilitY
BVHT	= Baseline Vehicle Hours Travelled
C	= Capacity
CS	= Conditional Spectrum
D	= Demand
DOC	= Daily Operation Cost
EAL	= Expected Annual Loss
EDP	= Engineering Demand Parameter
€RC	= Bridge replacement cost

$€L|LS_C$ = Direct economic losses associated to LSC

$€L|LS_D$ = Direct economic losses associated to LSD

FE = Finite Element

f_c = Concrete compression strength

f_y = Steel yield strength

GMPE = Ground Motion Prediction Equation

IM = Intensity Measure

IML = Intensity Measure Level

I_v = Fafjar index

LS = Limit State

LS_C = Collapse Limit State

LS_D = Damage Limit State

L_p = Plastic hinge length

L_v = Shear length

MAE = Mean Absolute Error

MAFE = Mean Annual Frequency of Exceedance

MC = Multiple Column

MDF = Modified Daily Cost

MedAE = Median Absolute Error

MIT = Ministero delle Intrastrutture e dei Trasporti

ML = Machine Learning

$MDF|LS_C$ = Mean damage factor for LSC

$MDF|LS_D$ = Mean damage factor for LSD

MVHT = Modified Vehicle Hours Travelled

N = Axial load

NLTHA = Non-linear Time-History Analysis

OSM = OpenStreetMap

PGA = Peak Ground Acceleration

PGV = Peak Ground Velocity

POE = Probability of Exceedance

PSHA = Probabilistic Seismic Hazard Analysis

R^2 = Coefficient of Determination

RC = Reinforced Concrete

RMSD = Root Mean Squared Error

Sa(T1) = Spectral Acceleration at first modal period

Sa_{1s} = Spectral Acceleration at 1 second

SC = Single Column

SSHA = Scenario-based Seismic Hazard Analysis

STA = Static Traffic Assingment

T_1 = First modal period of vibration

$T_{85\%}$ = Modal period at which 85% of the modal mass is obtained

VDT = Vehicle Distance Travelled

VHT = Vehicle Hours Travelled

V_N = Axial load contribution to shear resistance

V_c = Concrete shear resistance

V_s = Transverse steel shear resistance

V_u = Ultimate shear resistance

W = Wall

μ_{lnY} = Fragility curve median

β_{lnY} = Fragility curve dispersion

$\beta_{Y/IML}$ = Structural performance dispersion given an intensity measure level

θ_u = Ultimate rotation

θ_y = Yield rotation

ϕ_u = Ultimate curvature

ϕ_y = Yield curvature

$k(\mu_\Delta)$ = Ductility based reduction factor as per NTC2008

$p(LS_C)$ = Annual probability of occurrence of LSC

$p(LS_D)$ = Annual probability of occurrence of LSD

1. INTRODUCTION

1.1 RESEARCH MOTIVATION

The motivation for the chosen line of research comes from the aknowledgemnt that, within regional seismic risk assessment of buildings and bridges, even though this type of large scale assessments have been performed successfully for several years, the practical implementation of its underlying concepts to real-life case studies can bring multiple challenges. These often force practitioners to make difficult decisions with little data that will have an unknown impact in the final results; something that is sometimes not accurately communicated to the stakeholders.

While for the most part, regional seismic risk assessment is in general seen favourably as a tool for stakeholders to quantify the expected performance of their infrastructure inventories, several setbacks can arise on the application side that cloud the theoretical background of its concepts. This leads to confusion as to what are acceptable guidelines that can be followed when parts of the baseline information that is ideally required is unavailable, or when there are not sufficient resources to procure and process it. Furthermore, even though this topic is on the forefront of research efforts and many innovations are being made (e.g. the calculation of indirect losses and the prioritization of assets), no consensus currently exists on what an acceptable methodology would be to carry out these tasks. With this in mind, it was seen as an opportunity to use the vast information and knowledge acquired during the INFRA-NAT Project (www.infranat-eu.org), a European Union funded research project that dealt with the regional seismic risk of bridges in Italy, North Macedonia and Israel. The bridge data collected during this project was used to create synthetic case studies with fully-known information to mimic a real-life practical setting. Current and innovative risk assessment methodologies could then be carried out and used as a benchmark to evaluate the impact of some of the common decisions made during this type of project, thus determining recommendations and best practices for their development, while also identifying their limitations and, when possible, calculating their associated uncertainty.

Overall, it is intended that the research efforts presented in this thesis will be useful to practitioners in the field of regional assessment of bridges, while also making significant research contributions that can help to push both the state-of-the-art and the standard-of-practice in a positive direction.

1.2 SCOPE

Considering the many topics within regional risk assessment of bridges, the work presented in this thesis aims to answer a set of specific research questions using available information and databases. Accordingly, the scope of this thesis can be summarized by the research questions posed, which have been separated in each of the primary components of risk: hazard, exposure and vulnerability.

Within the hazard component, the research question was stated as: ***How to efficiently account for the seismic hazard of a regionally distributed inventory?*** For this part, even though there are many possible ways to address this question, focus was given to the evaluation of intensity measures (IM), specifically the use of the recently developed average spectral acceleration (AvgSa) and its comparison to the more traditional use of peak ground acceleration (PGA). State-of-the-art risk assessment requires the use of fragility functions, derived using non-linear time-history analysis with earthquake records that are compatible with the site hazard and characterized via an IM suitable for the structures to be analysed, which poses a challenge given the wide variety of structural characteristics found in bridge inventories. Given the lack of consensus on a suitable IM, regional studies are often performed using PGA, which, despite being recognized as a poor indicator of structural performance, remains a common denominator in earthquake response characterization. AvgSa has recently gained popularity as an alternative since it describes earthquake intensity over a range of pertinent periods of vibration, however, its suitability as an IM has not been demonstrated on real bridge inventories with a wide variety of structural characteristics.

For the exposure component, two main questions were posed: ***How much knowledge of the inventory is required to attain adequate results?*** and ***what is the uncertainty in the final results that derives from the lack of complete knowledge of the inventory?*** In this case, these questions emerged from the lack of bridge structural information that analysts usually encounter when dealing with the regional assessment of bridge inventories. In most regions, the bridge inventory is composed of structures built over decades and detailed structural information of the existing configurations is difficult to obtain and can be expensive to survey. Most of the regional risk studies for bridges are done with incomplete exposure knowledge and usually rely on macro taxonomy-based approaches that average fragility information of assets with similar configurations. This leads to an unknown level of uncertainty in the results that is commonly not quantified or accurately communicated to the stakeholders. Accordingly, there is a need for a better understanding on how much uncertainty can be expected in results using such approaches, as well as for recommendations to those dealing with this type of assessment to define an appropriate required minimum knowledge of the inventory to obtain reasonable results. With this in mind, a study was conducted by creating a case study of 617 bridges with full information and systematically removing portions of the inventory to quantify uncertainty, thus deriving

recommendations for minimum exposure knowledge and the associated uncertainty of specific known percentages of the inventory.

In terms of the vulnerability component: ***How to consider indirect losses when network traffic information is unavailable?*** This question derives from the difficulty that currently exists in characterizing the losses experienced by users of a road network when the links provided by bridges become unavailable. These losses are recognised to be of greater relative importance than their direct counterpart, associated with the cost of the infrastructure, however, while the theoretical background for such calculations exists, the associated methodologies require a great amount of information on the overall network and the demands of the users, as well as a multi-disciplinarily skilled team, both of which can be difficult to procure. With this in mind, a review of currently used methodologies was made and used to develop two methodologies, one that includes most of the recommended components and allows the calculation of monetary losses; and a second simplified alternative that does not rely on traffic information and can be used to approximate the relative importance of bridges in a network in terms of indirect losses.

Finally, more on the general risk management side: ***How to prioritize resource allocation within a bridge inventory?*** This question was addressed after the main findings, relating to the components of risk previously mentioned were obtained, and utilizes the majority of the results and insights attained throughout the research. The idea behind it is to determine an efficient way to perform resource prioritization when only specific key aspects of all elements in a bridge portfolio are available, a very real and common situation that bridge management authorities must face. When looking for decision variables to perform this prioritisation, seismic risk assessment metrics, such as average annual losses (AAL), are an appealing choice. However, obtaining this metric for a large bridge inventory is technically challenging and requires large amounts of information that are seldom available. This promotes the development of practical approaches that can predict the relative priority of assets within a portfolio, based on processing simple indicators with acceptable accuracy. For this question, the main elements that drive the seismic risk of a bridge portfolio in terms of AAL were identified, and their relative importance was used to calibrate a proposal for modification of a set of guidelines recently published by the Italian government.

1.3 THESIS OUTLINE

The main body of this thesis is formed around four peer-reviewed journal publications, one for each of the main key topics described in the previous section, and each one forming a chapter in the current thesis. Readers are advised to keep this in mind since, to aid in the standalone clarity of each of the main four chapters, some statements may seem repetitive throughout the entire document. Furthermore, with the same purpose of aiding in clarity

while avoiding repetitiveness, the literature review of the state-of-the-art for each topic was included in the introduction sections of their respective chapters.

Chapter 1: Introduction, this chapter is made with the intention of clarifying the motivation and reasoning behind the topics and strategies selected for detailed study, while also briefly introducing an overview of the research performed. The detailed introduction of each of the research efforts that resulted in the journal publications, will be provided in its respective chapter to assist readers that are only focused on a single part of the study performed.

Chapter 2: Case Study Portfolio, Fragility Assessment Methodology and Seismic Hazard Assessment presents a detailed account of the information, methodologies and hazard results used throughout the overall research. Initially, a main overview of the existing bridge database that was used to create the different synthetic case studies database and its structural characteristics is present, followed by a description of the process used to define the case studies and their resulting properties. A following subsection details the main methodology used in this thesis to perform numerical modelling of the bridges in the database, as well as the assumptions made to characterize the seismic performance and obtain fragility curves of each asset. Finally in this chapter, the seismic hazard present in each of the case study location selected was characterized, as well as a description of the ground motion selection process used to perform non-linear time-history analysis of the bridge inventory.

Chapter 3: Hazard – Effect of Choice of Intensity Measure, relates to the comparison of average spectral acceleration with peak ground acceleration as intensity measures for regional seismic assessment of bridges. This is the first of the main four chapters that have a standalone structure, with individual introductions and its own set of conclusions. Its respective publication is entitled ***"Evaluation of intensity measure performance in the regional assessment of reinforced concrete bridge inventories"***, published in the journal Structure and Infrastructure Engineering.

Chapter 4: Exposure – Effect of Knowledge Level, represents the second of the main four chapters, and deals with study performed to characterize the uncertainty associated to the lack of exposure knowledge and the consequences of using traditional taxonomy-based fragility curves in comparison to individual and machine-learning predicted ones. Its respective publication is entitled ***"Exposure Knowledge Impact on Regional Seismic Risk Assessment of Bridge Portfolios"***, and is under review for publication in the Bulletin of Earthquake Engineering.

Chapter 5: Vulnerability – Simplified Indirect Loss Assessment, represents the third of the main four chapters, and deals with the definition of a detailed methodology and a simplified alternative to account for indirect losses in bridge portfolios with limited information. Its respective publication is entitled ***"Simplified Indirect Loss Characterization for the***

Risk Assessment of Roadway Bridge Networks", and is being revised for publication in the International Journal of Disaster Risk Reduction.

Chapter 6: Risk Management – Prioritization Framework, represents the last of the main four chapters, and deals with the identification of the main parameters that drive the seismic losses of bridge portfolios, information used to calibrate a methodology that can help determine the relative urgency of intervention of assets in the inventory, based on limited parameters. Its respective publication is entitled ***"Seismic Risk Prioritisation Schemes for Reinforced Concrete Bridge Portfolios"*** and is under review for publication in the journal Structure and Infrastructure Engineering.

Finally, Chapter 7: Overall Conclusions and Future Developments, serves as a summary of the main findings of the overall research, taking the key points and insights from each of the chapters in the thesis. Also, it presents recommendations for further developments that were identified in the topic.

2.CASE STUDY PORTFOLIO, FRAGILITY ASSESSMENT METHODOLOGY AND SEISMIC HAZARD ANALYSIS

2.1 CASE STUDY BRIDGE PORTFOLIO

A bridge database comprising 308 bridges from the National Autonomous Roads Corporation ANAS (*Azienda Nazionale Autonoma delle Strade)* inventory, collected and managed by the Eucentre Foundation, was considered to develop two case studies: one in Campania with 165 assets and one in Salerno with 617 assets bootstrapped sampled from the 308-bridge database. These bridge assets form a part of the Italian road network and their geographic location is scattered along the primary highway grid of Italy, as shown in Figure 2.1.

Figure 2.1. Location of 308 bridges in the database

The information considered in the database comprises a practically complete account of geometrical and structural properties of the bridges, allowing a detailed structural numerical model of each asset to be created. Each asset in the database is a reinforced concrete (RC) bridge with two or more spans, which is a predominant configuration in the Italian road network (Zelaschi, Monteiro, & Pinho, 2016).

2.1.1 Main Characteristics

Within the main class of RC bridges with two or more spans previously mentioned, the assets in the database are very heterogeneous in terms of dimensions and structural configurations. This is considered ideal since it makes the case studies built from the database more representative of real existing road networks that typically include a large range of bridge types.

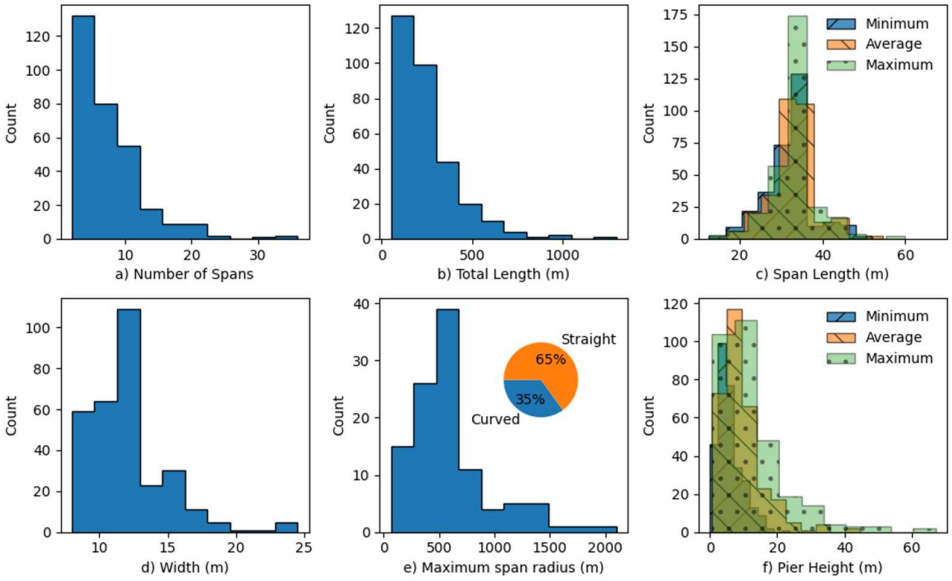

Figure 2.2. Main geometric characteristics of bridge database

In terms of general dimensions, the overall number of spans ranges from 2 to 36, which translates to an overall bridge length range of 50m to 1250m. A large portion of the inventory is not straight in plan, as 35% of the assets have curved decks on at least one of the spans, which sometimes makes it difficult to use the typical definition of longitudinal/transverse directions. The height of piers ranges between 5m and 45m in the overall inventory and it is typical to observe large variation of the pier height within the same asset, leading sometimes to irregular dynamic configurations within straight bridges.

A more complete description of the distributions of these bridge properties is shown in Figure 2.2. In terms of static configuration, the vast majority of the case-study assets have spans that are simply supported upon the piers with thin elastomeric pads, and only a small percentage has continuous deck and bearings that can be either elastomeric or isolators.

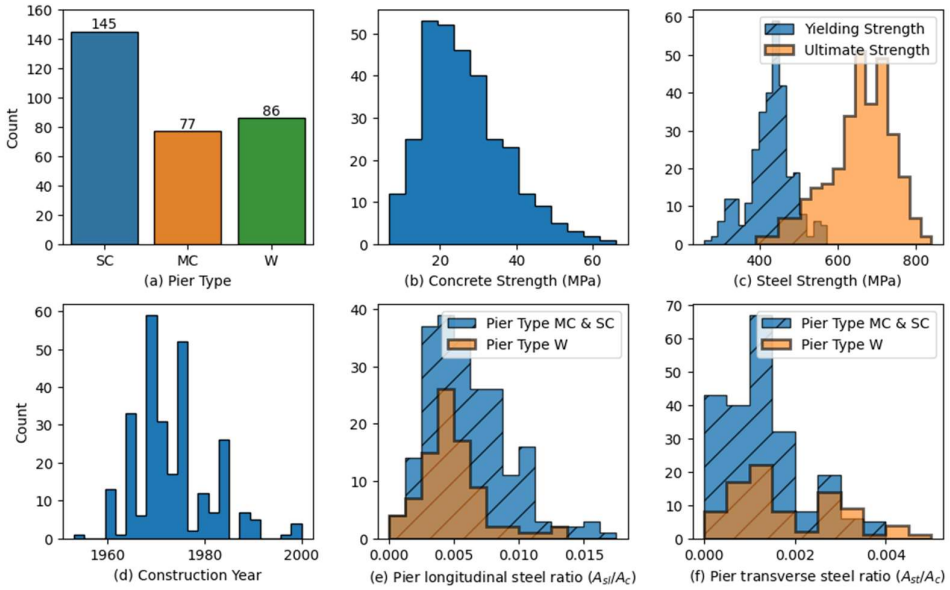

Figure 2.3. Distribution of main material properties of the bridge database (SC: Single Column, MC: Multiple Columns, W: Wall, Asl: Area of longitudinal steel, Ast: Area of transverse steel, Ac: gross area of the element)

In terms of pier sections, the inventory includes multiple configurations, which sometimes change even within the same asset. For simplicity in classification, three main pier types were identified: single column (SC), wall (W) and multiple column (MW) configurations, the distribution of which is shown in Figure 2.3(a). It is important to note that the actual pier cross sections might be composed of circular sections, box sections, elliptical or many other kinds of geometrical configurations; however, it was considered appropriate to aggregate some of these into the pier types to avoid excessive sub-categorisation and having some pier categories with very few assets to analyse.

The construction year was available for all assets, ranging between 1953 and 2000, with most of them built during the 1960s and 1970s, as shown in Figure 2.3 (d). As is common for regular Italian bridges of that period, none of them are expected to have been specifically designed to meet appropriate seismic requirements, especially considering that

the first national seismic regulation in Italy that addressed the entire national territory was instated in 2003 (Consiglio dei Ministri , 2003).

In general, the reinforcement percentages in the piers, both in longitudinal (A_{sl}/A_c) and transverse (A_{st}/A_c) directions, are low in comparison to current design standards and are quite similar across the different pier sections. This is atypical under current design practices, however, both the reinforcement ratios and the properties of the materials used for construction are in line with the age of construction of the inventory. Distributions for the mechanical properties of the materials are shown in Figure 2.3(e) and (f).

2.1.2 Dynamic Characteristics

2.1.2.1 *Modal Analysis*

In terms of dynamic properties, a structural model was created for each asset to determine the modal periods in both orthogonal horizonal directions. Since, for the case of bridges, the first mode does not typically account for a significative percentage of the total modal mass (O'Reilly G. , 2021), an appropriate number of modes were evaluated for each asset to include 85% of the modal mass in each direction. The distributions for the first modal period (T_1) and the modal period at which 85% of the modal mass is obtained ($T_{85\%}$) as shown in Figure 2.4.

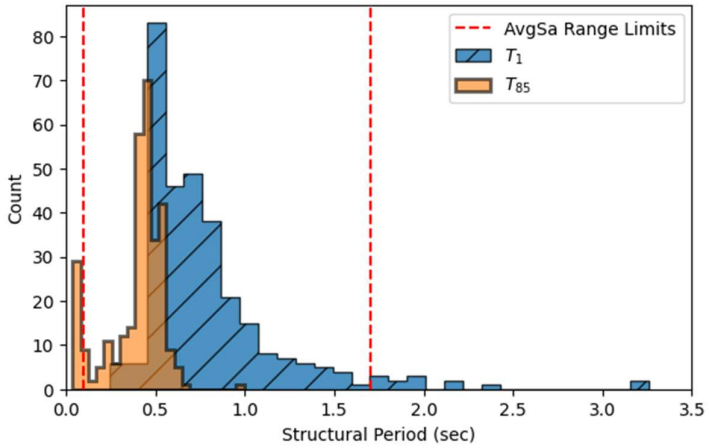

Figure 2.4. Results for modal structural periods of the entire inventory and definition of AvgSa range

The intensity measure chosen to perform hazard and fragility calculations was average spectral acceleration (AvgSa), for which the collective results of T_1 and $T_{85\%}$ were used to define the period range. As shown in Figure 2.11, the selected range was 0.1 seconds to 1.7 seconds, which was defined as per O'Reilly (2021) as 1.5 times the 84th percentile to account

for period elongation of the first mode and 0.5 times the 16th percentile to account for higher mode contributions of the T_1 and $T_{85\%}$ periods, respectively, for the entire inventory.

2.1.2.2 *Simplified Period Range Estimation*

Recognizing the difficulty in performing detailed numerical models of each asset in a portfolio, which would ultimately cause delays in a real risk assessment project since the period range for AvgSa would need to be defined for the hazard component analysis, a simplified period range estimation methodology was developed.

Inspiration was taken from a previous similar exercise made by Zelaschi et al (2016) using a subset of the same case study database used in this thesis. In that previous study, the database was parametrized, and a statistical distribution was fitted to each parameter, then these were used to generate a synthetic population of bridges by randomly sampling from the distributions. The population created was entirely made of straight bridges with single circular columns and each was modelled to determine the first period of vibration in the transversal direction. Finally, the period results were analyzed and a multivariate regression was made to determine a simplified equation to approximate the first period of vibration based on the most correlated parameter, which was determined to be the ratio between the average pier height and the pier cross section diameter.

For the case of this thesis, the decision was made to use the results of the modal analysis of the case study database without going through the parametrization and sampling process, and attempt to find simplified expressions to approximate T_1 and $T_{85\%}$ based on easily obtainable geometrical parameters that are not specific to the pier class of each asset, therefore excluding the geometry of the pier section from the candidate variables. The features for the regression were identified as: total length of the bridge, number of spans, maximum span length, average pier height and maximum pier height. These variables were preselected since they fulfil the requirements of being easily obtainable and general amongst all bridge classes.

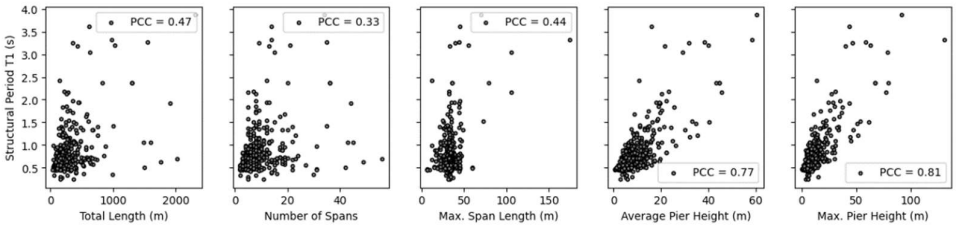

Figure 2.5. Relationship between T_1 and candidate variables

Initially for the first period estimation, the candidate variables were analyzed by searching for individual trends and correlations with the calculated values of T_1. Such an analysis can be seen in Figure 2.5, where the Pearson correlation coefficient (PCC) is indicated as a measure of linear correlation between each variable and the target T_1. It can be seen that the features that are most correlated are the ones relating to the height of the piers, which is in line with the findings of Zelaschi et al al (2016).

Multiple options considering a multivariate regression were evaluated to produce a function to approximate T_1, however, none produced a significant advantage in accuracy in comparison with a simple linear regression performed using the most correlated variable of the maximum pier height, which is what ultimately was used to derive Equation 2.1.

$$\sim T_1 = 0.43 + 0.03 \cdot Max\_Pier\_Height\ (m) \qquad \text{Equation 2.1}$$

The use of this equation is not optimal as a way to determine the first period of individual assets, as evidenced by Figure 2.6(a), where the comparison of predicted and calculated values show a large overall dispersion and a R-squared coefficient on 0.65, which is relatively low. However, when used to calculate the upper limit of the AvgSa range, by taking the same rationale of 1.5 times the 84th percentile over the aggregate predicted results does lead to encouraging results, with an approximation of the upper limit that is only 5% lower than the limit calculated using the modal analysis results.

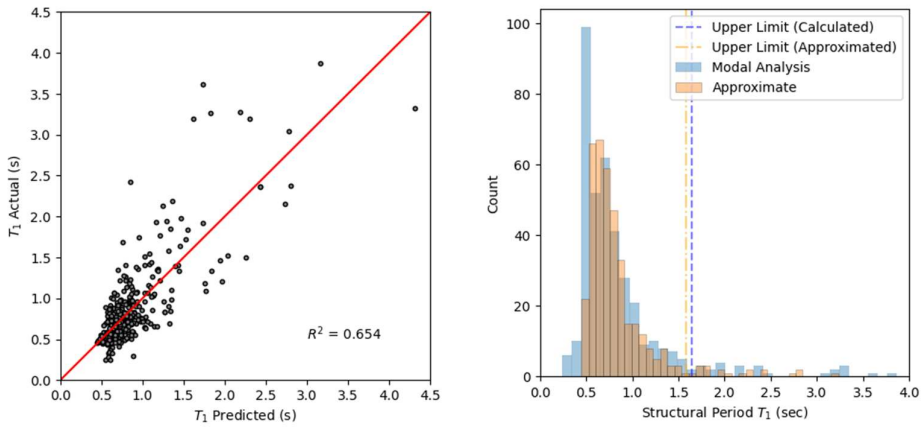

(a) **(b)**

Figure 2.6. Evaluation of Equation 2.1 to approximate T_1: (a) Prediction of individual T_1 results, (b) Histogram of T_1 predictions and determination of AvgSa upper range limit

A similar exercise was carried out to derive an approximate function to estimate $T_{85\%}$, however the correlation analysis provided no apparent trends relating the candidate variables to the calculated ones as can be seen in Figure 2.7. This is attributed to the fact that the number of modes required to obtain such a significant percentage of the total modal mass in both orthogonal directions change significantly between all assets, depending on the size of the bridge and its structural configurations; therefore, the estimation of this attribute might be a far more complicated problem, which would require the addition of extra variables that ultimately would defeat the purpose of the simplified estimation exercise. However, as shown in Figure 2.8, in general it appears that the consideration of enough modes to obtain the 85% mass target will ultimately lead to the calculation of very short periods in comparison to their T_1 counterparts. This in addition to the rationale of using 0.5 times the 16th percentile over the aggregate $T_{85\%}$ results, will most likely lead to estimates of the lower limit for the AvgSa range that vary between 0.1 and 0.2s, which would make the use of 0.1 seconds a conservative generalization that could be made for portfolios of bridges with similar characteristics as the one used herein.

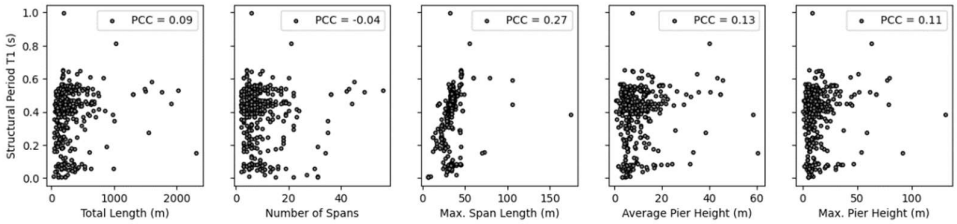

Figure 2.7. Relationship between $T_{85\%}$ and candidate variables (PCC: Pearson Correlation Coefficient)

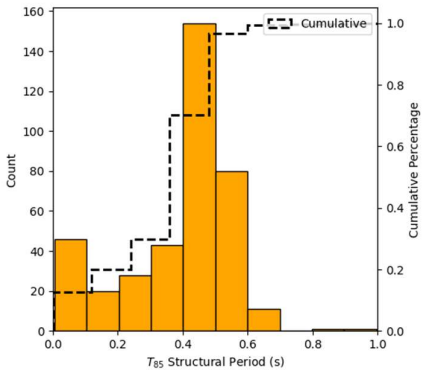

Figure 2.8. Histogram of $T_{85\%}$ structural period of case study portfolio

2.1.3 Case Study 1: Campania

A reduced sample of 163 assets from the main 308 asset database was used to perform the research related to exploring suitable intensity measures as stated previously. This decision to reduce the dataset for the exporation of this aspect of the hazard component was made to minimize the computational burden required to run the NLTHA with multiple intensity measure candidates.

Differences in the number of spans and pier types were used to define six bridge taxonomy branches, listed in Table 2.1. It is important to note that the taxonomy distribution of the bridges in the inventory is not uniform, i.e. some taxonomy branches include fewer assets than others, as shown in Figure 2.9(a). This must be considered when comparing taxonomy-based results, but it is to be expected given that the data represents a real existing inventory of bridges. Furthermore, the decision of dividing the bridges based on the number of spans in two categories, divided at the five-span threshold, could be considered somewhat ambiguous; however, it was determined in this way to allow for a similar amount of assets in both sides of the main taxonomy break, as seen in Figure 2.9(b).

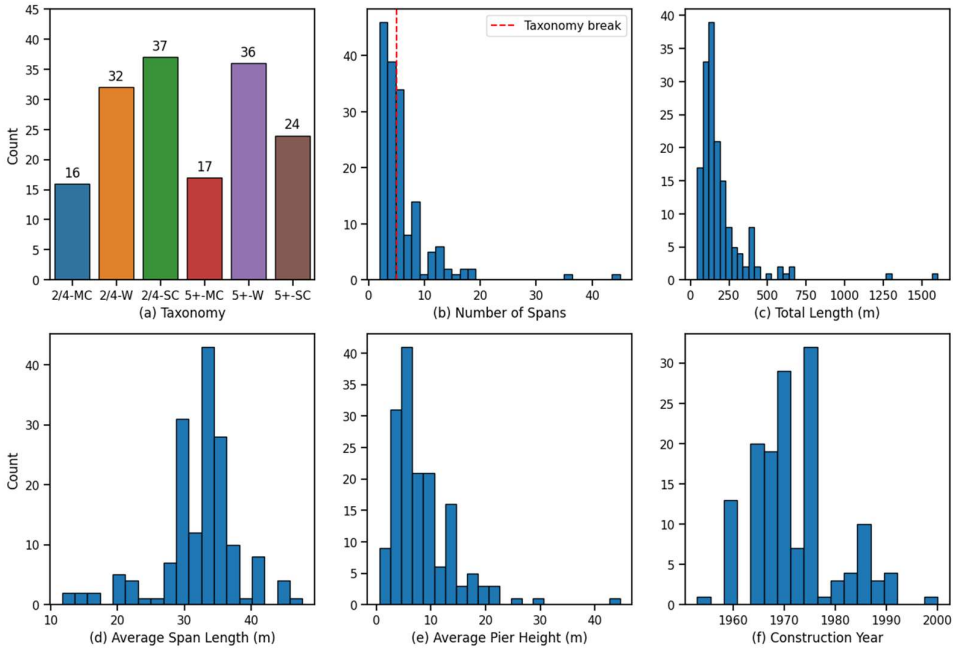

Figure 2.9. Distribution of general and geometrical properties of the reduced 163 bridge database selected for Case Study 1

Table 2.1. Definition of taxonomy branches for Case Study 1 based on key structural parameters

Material	Static Scheme	Spans	Pier Type	Taxonomy Branch
Reinforced Concrete	Simply Supported	2 to 4	Multiple Column	RC-SS-2/4-MC
			Wall	RC-SS-2/4-W
			Single Column	RC-SS-2/4-SC
		Above 5	Multiple Column	RC-SS-5+-MC
			Wall	RC-SS-5+-W
			Single Column	RC-SS-5+-SC

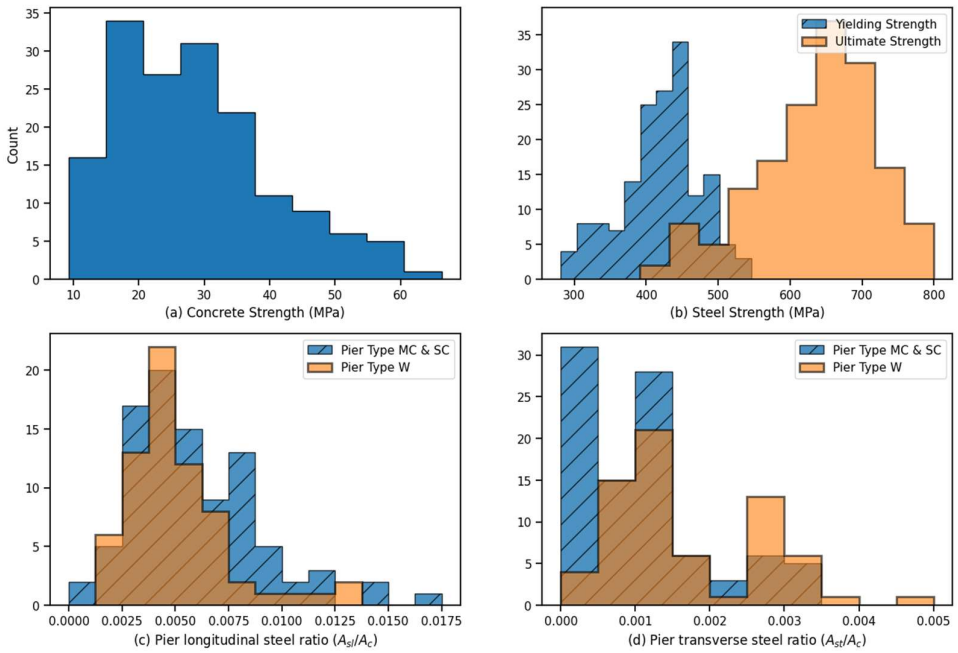

Figure 2.10. Distribution of main material properties of the reduced 163 bridge database selected for Case Study 1

Further detailed information about the distribution of general geometric and material properties of the bridges in the database can be seen in Figure 2.9 and Figure 2.10. Divisions of reinforcement ratios are included through the differentiation between pier types.

Even though the real location of each bridge in the database is known, for this case study, they will all be treated as if subjected to the same seismic demands corresponding to a specific site hazard in specific location in the Campania region. This is another simplification that has been made to reduce the extensive NLTHA burden, described in the following sections, and to evaluate all assets under the same ground motion set. In actual applications, the procedure could be repeated for the different asset sites or a more hybrid means of selecting the ground motions to consider the seismicity of multiple sites could be used (Kohrangi et al., 2017).

Since case study 1 is a subsample from the original database, the modal analysis of the assets chosen, as well as the aggregate analysis of the results, was repeated to define an AvgSa period range that was appropriate for the reduced asset sample. In this case, the modal analysis was carried out to determine the first three structural periods of each bridge. The results from this modal analysis are shown in Figure 2.11(a), classified by taxonomy branch where the height of each bar represents the median period and the black lines the 95% confidence intervals of the data for each case to provide a measure of the period variability within the same group. It can be seen that the taxonomy branches that include more spans present higher overall medians and variations in all periods than their respective counterparts with fewer spans, an intuitive trend since larger bridges are expected to have longer oscillation periods in the transverse direction. Moreover, there is more dispersion in the bridge length for the taxonomy branch with more spans.

The aggregated results of the entire inventory are then used to determine an appropriate range of periods for the AvgSa IM record selection. While a study (Eads et al., 2015) has been made to determine the correct range of periods to use in AvgSa to reduce dispersion of the results, it dealt with the case of single buildings and therefore the recommendations are made in terms of the fundamental period (T_1) of the structure.

In the present case study, the lower limit was defined by 0.5 $T_{3,median}$ and the higher limit as 1.5 $T_{1,median}$, the intention being to use a lower bound that can include higher mode contributions and a higher bound that can account for period elongation in the non-linear range, for the majority of the case study bridges. This rule led to the selection of a range between 0.2 and 1.0 seconds was chosen as shown in Figure 2.11(b) for the definition of the AvgSa record selection, which is considered adequate since it contains most of the period results for the assets in the database.

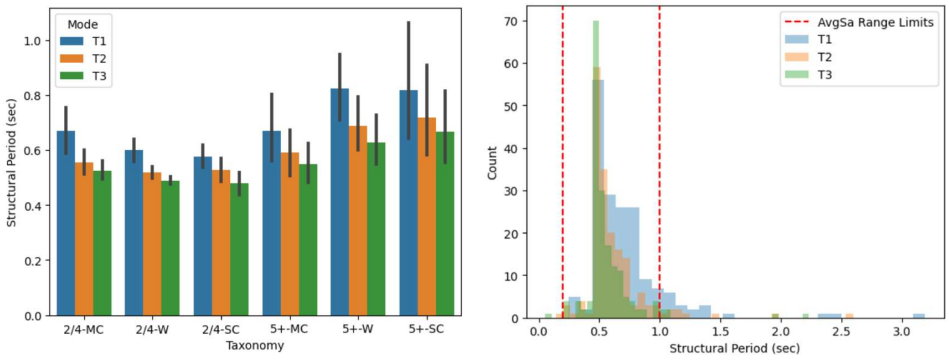

(a) (b)

Figure 2.11. Results of first three structural periods obtained from modal analysis of case study 1 assets: (a) Divided by taxonomy branch, (b) definition of AvgSa period range for case study 1

Readers are advised to note that the decisions made to define the AvgSa range for case study 1 are different that the ones previously described for the entire database. Before, the modal analysis was carried out considering enough modes per model until 85% of the cummulative mass was achieved, then the period range was defined by accounting for the collective results of T_1 and $T_{85\%}$, scaling them to account for period elongation and higher mode contributions as discussed previously. This procedure is preferred here and considered more representative of the overall period range that should be considered when using AvgSa on bridge portfolios. This, however, was not applied to case study 1 since the research related to this case study was performed chronologically much before the rest of the scope for this thesis was defined; therefore, at the time this portion of the research was being conducted, the decision to include only the first three structural periods and defining a range that would confortably contain the majority of the results was considered sufficient.

2.1.4 Case Study 2: Salerno

As shown in Figure 2.1, the bridges in the ANAS database are scattered geographically all over the Italian territory and not directly connected, therefore, their real location is not ideal to define a complete case study, since the consideration of the collective and individual role of each asset in the road network would be an unfeasible exercise. In contrast to the decisions made to define Case Study 1, a secondary case study was defined for the remainder of the research that has the adequate characteristics to account for connectivity and road network effects in the occurrence of a bridge collapse.

Ideally, if a case study of bridges closely connected within the same territory were available, it could be explored and fully analysed to represent a benchmark with which to evaluate the performance of simplified prioritisation frameworks. For this reason, and taking

advantage of the fact that even in locations with different seismic hazard demands, bridge design practices did not vary considerably among the Italian territory for the construction period of the bridges in the database (Borzi, et al., 2015), a semi-synthetic case study was created. To do so, the road network of a region for which the location of bridges and road properties was known was taken, with a bridge from the 308 asset database being randomly sampled and assigned to each location.

Table 2.2. Definition of taxonomy branches for Case Study 2 based on key structural parameters

Material	Spans	Pier Type	Taxonomy Branch
Reinforced Concrete	2 to 4	Single Column	RC-SC-2to4
		Multiple Column	RC-MC-2to4
		Wall	RC-W-2to4
	5 to 8	Single Column	RC-SC-5to8
		Multiple Column	RC-MC-5to8
		Wall	RC-W-5to8
	9 to 36	Single Column	RC-SC-9to36
		Multiple Column	RC-MC-9to36
		Wall	RC-W-9to36

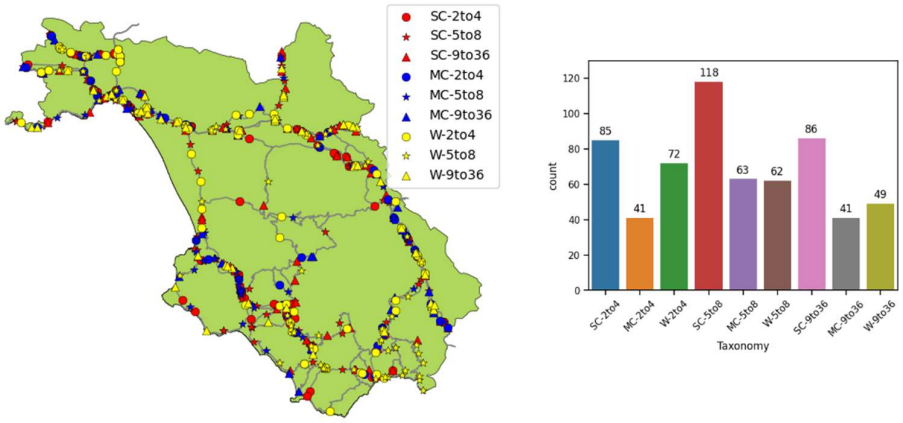

(a) **(b)**

Figure 2.12. Definition of case study 2: (a) Taxonomy of bridges assigned to the locations of bridges in the Salerno road network, (b) Number of assets per taxonomy branch present in case study 2

The Salerno province was selected for having a transportation network that relies heavily on the vehicular road system, a relatively low number of bridges (thus reducing the sampling process) and a varying seismicity level. Information about the road network of Salerno was taken from the OpenStreetMap database (OpenStreetMap contributors, 2020), which comprises all roads within the highway, primary and secondary systems, including a total of 617 bridges. The 308 bridges in the database were thus located randomly within the locations of bridges in the Salerno network using a sampling with replacement scheme. Once the final distribution of assets in the case study was defined and, based on the differences in the number of spans and pier types, the six bridge taxonomy branches listed in Table 2.2 were defined. The locations of the assets based on their respective taxonomy branch are shown in Figure 2.12. The period range of 0.1 to 1.7 seconds defined previously for the AvgSa consideration of the bridge database was maintained for case study 2 since the all the assets in the database were used for the definition of this case study.

2.2 SEISMIC VULNERABILITY ASSESSMENT METHODOLOGY

In this section, the overall methodology, tools and assumptions used to determine the fragility curves of each asset in the case studies will be presented. In general, the methodology relies on NLTHA performed to numerical models created for each bridge, using the ground motion catalogue selected for each case study. Only the detailed account of the methodology will be discussed in this chapter, the associated fragility results obtained will be presented in the following chapters, as they vary for each case study.

2.2.1 Bridge Numerical Modelling Framework

In order to efficiently implement a numerical modelling framework to generate, analyse and process the great amount of bridge information present in the database, a state-of-the-art tool developed by the Eucentre Foundation called BRI.T.N.E.Y (BRIdge auTomatic Nonlinear analysis based Earthquake fragilitY) (Borzi, et al., 2015) was used. The tool creates finite element (FE) models for carrying out NLTHA with OpenSees (McKenna, 2011) and processes the results to characterise the structural response of each bridge.

The model elements are either frame elements, *elastic* for the deck and *BeamWithHinges* (Scott & Fenves, 2006) for the pier segments and the transverse beams, respectively, or *zeroLength* elements for deck connections and *twoNodeLink* elements for bearing devices within super- to sub-structure connections. Nonlinearity is modelled within both frame and *zeroLength* elements. For this purpose, in the *beamWithHinges* elements the cross-section is discretised into fibres. *RigidLink* elements are also used to model connection dimensions. Uniaxial constitutive models employed for the fibre section of inelastic elements are the Scott-Kent-Park concrete model (Kent & Park, 1971) (*Concrete01* in OpenSees) and the bilinear steel model (*Steel01* in OpenSees). Values for the material model parameters are

established for each of them, based on a sample taken from the structural property distributions created for each taxonomy branch.

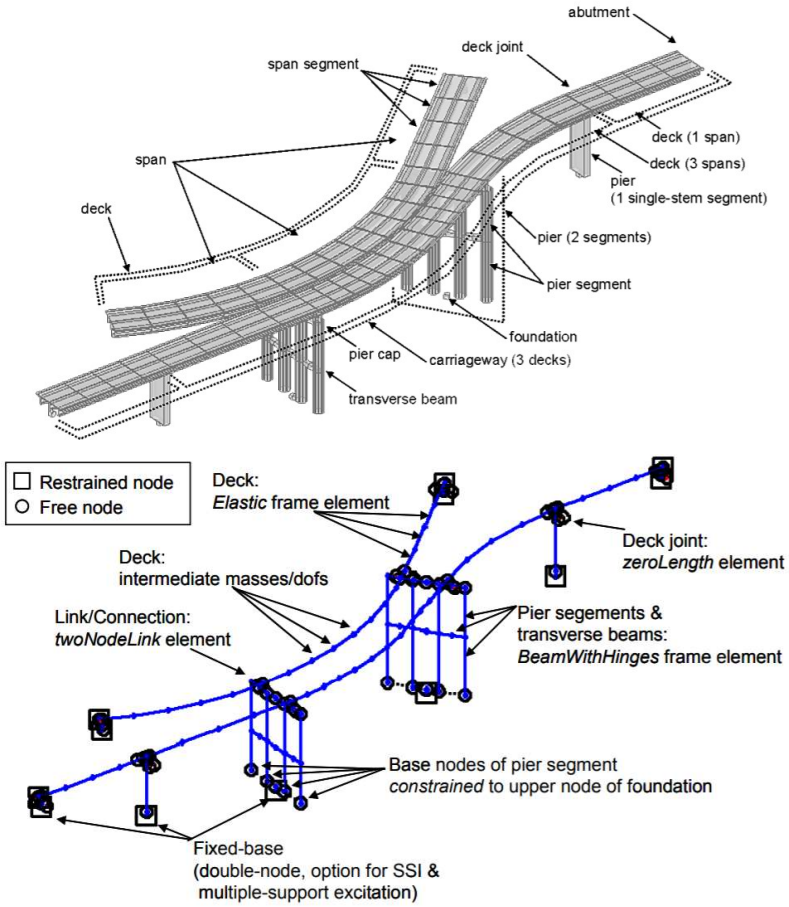

Figure 2.13. Example of finite element model created using BRITNEY with the upper plot showing a simple rendering of the bridge system and the lower plot showing its discretisation within the numerical model. Adapted from Borzi et al (2015)

For the bearing supports and connections between the deck, piers and abutments, available force-deformation laws in OpenSees (e.g. *Elastomeric, FlatSlider, FrictionPendulum*) cover the full spectrum of devices, both traditional and modern, typically found in the bridge stocks

of Italy. The platform also accounts for simple friction support between two surfaces simply supported, as well as monolithic connections.

Even though the tool does allow for foundations and abutments to be explicitly modelled, the lack of the necessary data on the soil system did not allow exploring these aspects in this study. However, this was not considered a major issue for the purpose of the risk assessment of the bridge portfolios since most design practices require that the foundations be capacity-protected which typically leads to significant conservatism in the design of bridge foundations (Chen & Duan, 2014). Furthermore, the tool allows for a great flexibility in geometrical definitions so as to model bridges with complex layouts, such as having curvature, multiple decks sharing piers, Gerber joints, etc. An example of the FE models created by the tool for a bridge from the case study portfolio is shown in Figure 2.13.

2.2.2 Damage Criterion and Limit States

Consistently with the BRITNEY analysis tool (Borzi, et al., 2015) that was used to model and characterise the structural performance of the bridges in the database, two limit states were used for the evaluation of the performance of the assets: a) damage limit state, and b) collapse limit state. In this tool, structural deterioration interactions between elements leading to collapse are not specifically accounted for in the models (i.e. elements will deform beyond the limit response thresholds). Instead of using explicit engineering demand parameters (EDP), a critical demand-to-capacity ratio per component ($y_i = d_i/c_i$) was used as damage measure to reflect how far each critical component is from the threshold of the limit state, which allows to later easily aggregate the state of its components into the global structural state (Jalayer et al., 2007). Local demand over capacity ratios were calculated for piers and bearings and, depending on the values of these ratios, limit states were later assigned in the post-processing stage.

Piers can fail because either shear or deformation capacity, in terms of chord-rotation, has been exceeded. Two response thresholds were considered for chord rotation of the piers (yield θ_y and ultimate θ_u). The shear span L_V was taken equal to the pier height L for single-stem cantilever piers, or in the longitudinal direction, and $L/2$ in the transverse direction of multiple stem piers or piers with monolithic deck connections. Yield and ultimate curvatures were determined automatically from a bilinear fit of a section moment-curvature analysis to deal with general cross-section shapes and reinforcement layouts. In terms of shear failure, given the brittle nature of the phenomenon, only a single threshold was defined and associated with the collapse limit state, with the pier shear capacity calculated according to the NTC 2008 equations (M.I.T., 2008).

Furthermore, to account for uncertainty in the capacity thresholds for pier components, they were modelled as lognormal random variables that are sampled every time an analysis

was conducted. The equations used in the definition of the pier thresholds for chord rotation and shear, as well as the logarithmic standard deviation used for the analyses, are presented in Table 2.3. Further detail on the choice of the different formulations can be found in Borzi et al (2015).

Regarding the bearings, these can suffer from unseating failure, involving the deck and the supporting sub-structure. Bearings can fail due to excessive displacement demand, from simple falling of the deck from the bearing seat or due to the full loss of support from the pier head. The first condition detects a damage LS, while the second a collapse LS. The displacement capacity of the bearings was derived from the pier cap and bearing seats geometry, or directly defined by the user, and was considered as deterministically known.

Table 2.3. Capacity thresholds for pier segments (h and d_b are the section height and longitudinal bar diameter, respectively) adapted from *Borzi et al* (2015)

Limit State	Mechanism	Median	Standard Deviation σ_{ln}
Damage	Flexure	$\theta_y = \frac{\phi_y L_v}{3}$	0.3
Collapse	Flexure	$\theta_u = \theta_y + (\phi_u - \phi_y) L_p \left(1 - \frac{L_p}{2L_v}\right)$ with: $L_p = 0.1L_v + 0.17h + 0.24\left(\frac{d_b f_y}{\sqrt{f_c}}\right)$	0.4
	Shear	$V_u = V_c + V_N + V_s$ with: $V_c = k(\mu_\Delta)0.8A_c\sqrt{f_c}$, $V_s = A_{st}0.9\,hf_y$, $V_N = N\frac{0.8h}{2L_v}$	0.25

θ_y: *Yield rotation*
ϕ_y: *Yield curvature*
L_v: *Shear length*
θ_u: *Ultimate rotation*
ϕ_u: *Ultimate curvature*
L_p: *Plastic hinge length*

V_u: *Ultimate shear resistance*
V_c: *Concrete shear resistance*
V_N: *Axial load contribution to shear resistance*
V_s: *Transverse steel shear resistance*
$k(\mu_\Delta)$: *Ductility based reduction factor as per NTC2008*
A_c: *Concrete shear resistance area*

N: *Axial load*
f_c: *conc. compression strength*
f_y: *Steel yield strength*

To account for the bi-directional response under multi-component seismic input, the local D/C ratios, y_i, were taken as the SRSS combination for the piers and bearings, respectively. For example, the local ratio for flexural deformation at the collapse LS was given in terms

of the responses and capacities in the longitudinal (L) and transverse (T) directions using Equation 2.2.

$$y_{i\_\theta_u} = \sqrt{\left(\frac{\theta_{iL}}{\theta_{uiL}}\right)^2 + \left(\frac{\theta_{iT}}{\theta_{uiT}}\right)^2} \qquad \text{Equation 2.2}$$

2.2.3 NLTHA and Fragility Curve definition

Each bridge model was evaluated using NLTH analysis to each set of 30 bi-directional records, for each of the nine increasing intensity measure levels. Each individual record set provided a small sample of response corresponding to demand values D in each vulnerable component to be compared to its corresponding component capacity values C, sampled from their respective distributions. At each intensity level, the obtained sample of the component demand to capacity ratios $y=D/C$ was used to obtain a global, structural system level D/C ratio, denoted by Y (Jalayer, Franchin, & Pinto, 2007). Making the assumption that bridge components are a part of a series system, where the weakest failure system leads to the overall damage or collapse of the global structure, the global D/C ratio for the j-th intensity level and k-th ground motion is given in terms of the n local D/C ratios by Equation 2.3.

$$Y_{jk} = \max\left(y_{1jk}, \dots, y_{njk}\right) \; j = 1, \dots, 9 \; ; \; k = 1, \dots, 30 \qquad \text{Equation 2.3}$$

The 30 values of Y at each intensity level were used to fit a lognormal distribution to determine the probability of exceedance of the unit value of Y that marks the attainment of the performance level being evaluated, as shown in Figure 2.14.

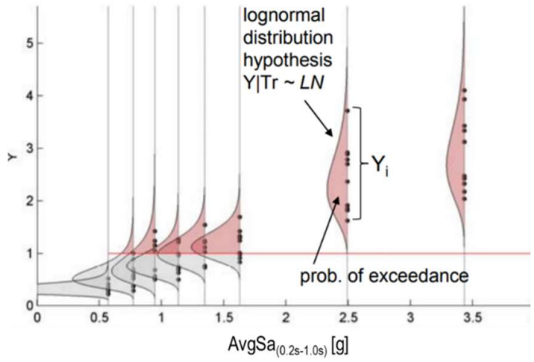

Figure 2.14. Sample values of the global D/C ratio Y being fitted with a lognormal distribution conditional on intensity level). Adapted from Borzi et al (2015)

These values of probability of exceedance form a piecewise fragility function however, since a continuous function is desired for reference and ease of implementation in the platform, the points are assumed to follow a cumulative lognormal distribution. A maximum likelihood estimation fitting algorithm (Baker, Efficient Analytical Fragility Function Fitting Using Dynamic Structural Analysis, 2015) was employed to obtain the exponent of the logarithmic mean μ_{lnY} and dispersion β_{lnY} parameters that describe the fragility curve, as per Equation 2.4. A schematic example of such calculation can be seen in Figure 2.15.

$$p(LS \mid IM{:}\, x) = \Phi\left(\frac{\ln\left(\frac{x}{\mu_{lnY}}\right)}{\beta_{lnY}}\right) \qquad \text{Equation 2.4}$$

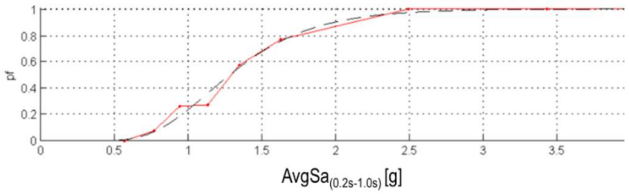

Figure 2.15. Fitting a continuous fragility function as a cumulative log-normal curve based on discrete probability of exceedance observations. Adapted from Borzi et al (2015)

The process is repeated for each bridge model in a specific taxonomy and the results can be processed statistically to obtain a class fragility function. For this purpose, the class lognormal mean is represented by the average of all the means of the synthetic bridge models, as presented in Equation 2.5, while the overall dispersion is given by the square root of the sum of squares of the intra-bridge dispersion and the inter-bridge dispersion, as presented in Equation 2.6.

$$ln\ \mu_{lnY_{tax}} = \frac{1}{N}\sum_{i=1}^{N} ln\ \mu_{lnY_i} \qquad \text{Equation 2.5}$$

$$\beta_{lnY_{tax}} = \sqrt{\beta^2_{lnY_{intra}} + \beta^2_{lnY_{inter}}} \qquad \text{Equation 2.6}$$

where:

$$\beta_{\ln Y_{intra}} = \frac{1}{N}\sum_{i=1}^{N}\beta_{lnY_i} \quad \text{Equation 2.7}$$

$$\beta_{lnY_{inter}} = \sqrt{\frac{\sum_{i=1}^{N}\left(ln\ \mu_{lnY_i} - ln\ \mu_{lnY_{tax}}\right)^2}{N}} \quad \text{Equation 2.8}$$

2.3 SEISMIC HAZARD ASSESSMENT

In this section, the main decisions made to conduct the seismic hazard assessment of each site of the case studies will be presented, along with the results obtained for some illustrative locations and return periods. For both cases, the overall methodology relies in the implementation of probabilistic seismic hazard analysis (PSHA) (Cornell, 1968) to obtain hazard curves, the use of disaggregation results (Bazzurro & Cornell, 1999) to determine the main sources that contribute to the seismic demands of the sites analysed, and the selection of ground motion records using a conditional spectrum approach (Lin, Haselton, & Baker, 2013).

Some differences will be noticed in the hazard analysis of both case studies, readers are advised to keep in mind that this is mainly related to the chronological order in which the case studies were developed. The research related to case study 1 in Campania was performed chronologically much before the one related to the case study in Salerno, therefore, the latter will seem more detailed than the former.

2.3.1 Case Study 1: Campania

A site located in the northern part of the Italian Campania region was chosen to carry out the seismic hazard analysis required to select ground motion records required to run NLTHA of the assets included in case study 1. The OpenQuake engine (Silva, Crowley, Pagani, Monelli, & Pinho, 2014) was used to perform probabilistic seismic hazard analysis (PSHA) calculations using the SHARE source model (Woessner, et al., The 2013 European Seismic Hazard Model: key components and results, 2015) on the selected site. The resulting hazard curves for peak ground acceleration (PGA) and AvgSa are shown in Figure 2.16.

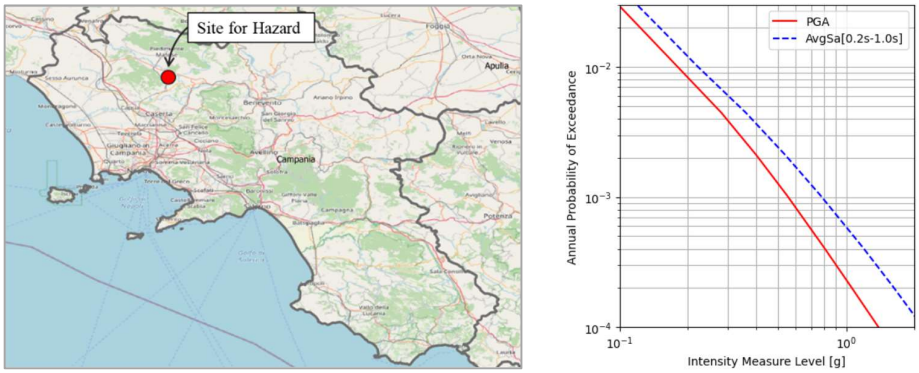

(a) (b)

Figure 2.16. Seismic Hazard Site used for Case Study 1: (a) Site location, (b) Hazard curves for PGA and AvgSa in the 0.2-1.0 secong range.

A selection of 30 bi-directional earthquake records was performed for each of nine considered return periods (30, 50, 98, 224, 475, 975, 2475, 4975 and 9975 years) giving a total of 270 ground motions for each IM. The selection process was carried out using the haselREC tool (Zuccolo, O'Reilly, Poggi, & Monteiro, 2021), which follows a conditional spectrum (CS) approach (Lin, Haselton, & Baker, 2013) where a target response spectrum distribution (with mean and dispersion) is computed for each return period and intensity measure. For the case of AvgSa, the original CS procedure was extended in Kohrangi et al (2017) to define the target spectrum distribution in the AvgSa period range defined. Each of these results were used to screen a composite database made up by the PEER NGAWest2 database (Chiou, Darragh, Gregor, & Silva, 2008) and the Engineering-Strong Motion (ESM) database (Luzi, et al., 2016). In order to select and scale the records in a way that accurately accounts for their bi-directional characteristics, the RotD50 response spectrum (Boore, 2010) of each bi-directional earthquake recording was used to match compatible records with the target CS distribution selected for each return period–IM pair. This response spectrum comprises the median values of response spectra of the two horizontal components projected onto all nonredundant azimuths, both the PGA and AvgSa values of each record used was calculated in this space.

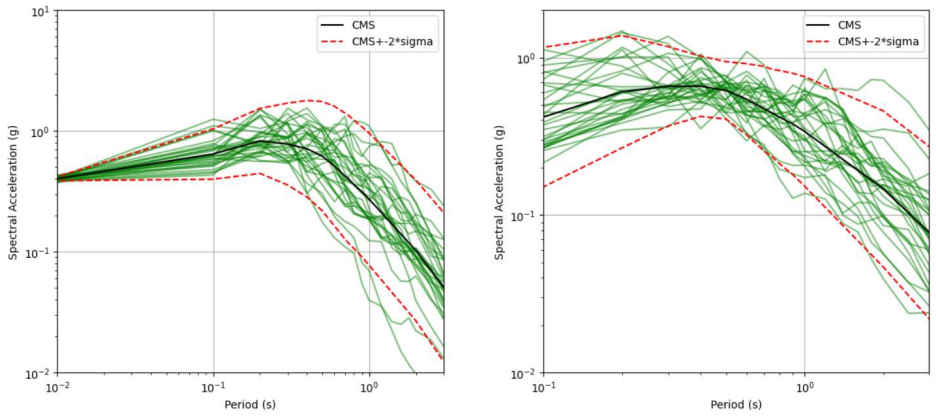

Figure 2.17. Record selection results for 475-year return period: (a) PGA, (b) AvgSa in the 0.2s – 1.0s period range.

An example of the response spectra of a set of selected accelerograms for the 475-year return period can be seen in Figure 2.17 for both PGA and AvgSa. The 30 green lines are the RotD50 response spectra of selected ground motions while the red lines represent the target conditional spectrum (average and ±2 standard deviations).

2.3.2 Case Study 2: Salerno

The Salerno province, as previously described, was selected as the location for case study 2, partly because it has a varied seismic hazard that ranges from low seismicity regions near the coastline, to high seismicity areas near the Southern Apennines Mountain range, which was the location of the M_w 6.9 Irpinia earthquake in 1980, for example. This wide range of seismicity represents an opportunity for this case study, as it allows possible differences in the response of bridges in different seismic demand areas to be investigated.

In terms of hazard curves, same as for case study 1, the SHARE hazard model (Woessner, et al., 2015), implemented in the OpenQuake Engine (Silva, Crowley, Pagani, Monelli, & Pinho, 2014), was used to determine the probability of exceedance of different levels of AvgSa (in this case using the period range of 0.1s -1.7s) for an investigation period of 50 years. The main difference for this case study in comparison to the previous one is that, instead of using the same hazard site for all assets, the PSHA was performed at the location of each bridge in the case study.

In terms of ground motion record selection, the EzGM tool developed by Ozsarac et al. (2021) was used, which follows a conditional spectrum scheme (Lin, Haselton, & Baker, 2013) using a modification that allows the conditioning of the spectra for AvgSa (Kohrangi,

Bazzurro, Vamvatsikos, & Spillatura, 2017). The implementation of the record selection methodology used requires results from a disaggregation analysis to determine the mean magnitude and distance that principally drive the seismic demands at each specific site. However, given the large number of bridge locations, and to minimise the computational burden of performing disaggregation at each location, all assets were assigned to four hazard zones and two soil classes (i.e., soft and stiff soil differentiated by a $V_{s,30}$ threshold of 360 m/s) as illustrated in Figure 2.18. Following this, a complete hazard disaggregation analysis was carried out for the eight possible zone-soil combinations. For each combination, sets of 30 bidirectional ground motion records were selected from the NGA West-2 Strong-motion Database (Ancheta, et al., 2014) for nine return periods ranging from 98 years to 9975 years. An example set of the selected ground motion records is illustrated in Figure 2.19.

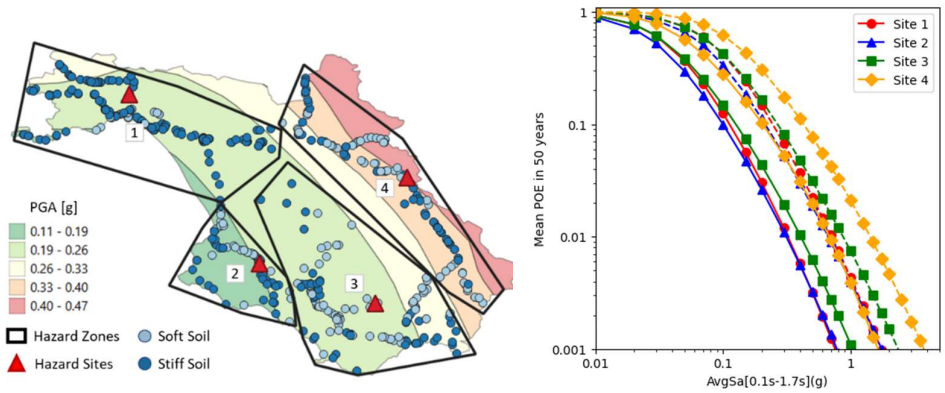

(a) **(b)**

Figure 2.18. Seismic hazard of the case study 2 (Salerno): (a) Hazard zones and soil sites (PGA values for a return period of 475 years are shown for reference), (b) Hazard curves for each hazard zones (dashed lines are soft soil results).

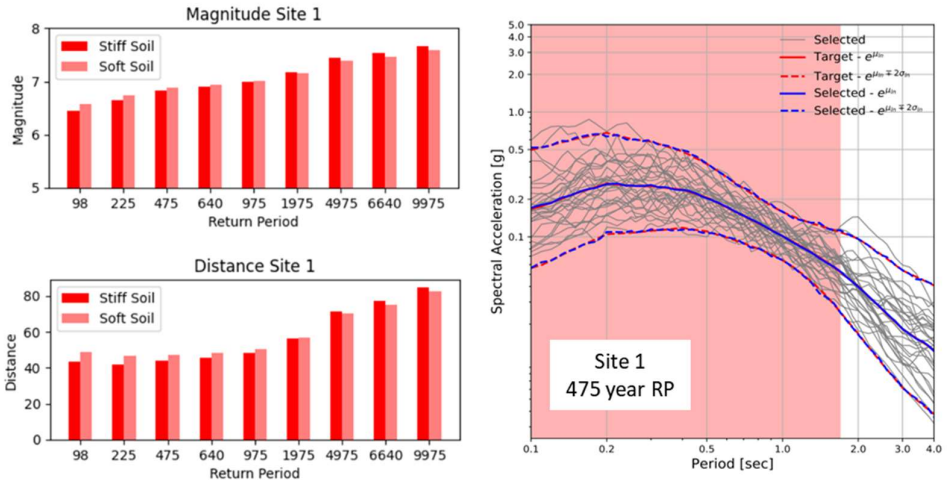

(a) (b)

Figure 2.19. Conditional Spectrum Record Selection for Case Study 2: (a) Disaggregation results for Site 1, (b) Example of record selection for Site 1, 475-year return period, stiff soil.

2.4 CHAPTER SUMMARY

In this chapter, a detailed account of the characteristics of the existing bridge database, as well as the procedure used to create realistic case studies and their resulting properties was presented. Furthermore, the main methodology used in this thesis to perform numerical modelling of the bridges in the database, as well as the assumptions made to characterize the seismic performance and obtain fragility curves of each asset was presented. Finally, the seismic hazard present in each of the case study location selected was characterized, as well as a description of the ground motion selection process used to perform non-linear time-history analysis of the bridge inventory.

3. HAZARD: EFFECT OF CHOICE OF INTENSITY MEASURE

3.1 INTRODUCTION

State-of-the-art seismic risk assessment requires the use of fragility functions typically derived via non-linear time-history analysis (NLTHA). This is done using earthquake records that are both: a) compatible with the site hazard and, b) characterized via an intensity measure (IM) suitable for the structures to be analysed. The latter condition is typically achieved by performing the record selection procedure with an IM that minimises the dispersion in the observed structural behaviour.

For the case of individual building structures, the use of the spectral acceleration at the fundamental period, $Sa(T_1)$, is a typical choice for IM that has proven to minimise the dispersion in the response of a structure to multiple ground motions with the same IM level. This option is based on the notion that the first mode response tends to govern the performance of most regular buildings with short to medium height. However, in the case of bridges or inventories with multiple classes of structures, no single period can be typically chosen to characterise the entire structural behaviour thus no clear answer exists on how to efficiently choose an IM.

Multiple studies have been conducted to address this issue, specifically investigating the impact of the choice of the IM on the development of fragility curves for bridges. Earlier work by Padgett et al (2008) concluded that peak ground acceleration (PGA) is the optimal choice for portfolio analysis since it provides adequate results and does not require consideration of the dynamic characteristics of the inventory. More recent accounts (Monteiro, Zelaschi, Silva, & Pinho, 2017) have determined that some IMs such as peak ground velocity (PGV) and Fajfar index (I_v) show a better performance in comparison to PGA, however, they do not completely disqualify its use and recognize the advantages of its widespread availability and popularity amongst practitioners.

Reaching a consensus on the choice for an optimal IM for analytical fragility calculations remains an open challenge (Silva, et al., 2019) and, therefore, recent regional studies have been many times performed in terms of PGA (Borzi, et al., 2015; Carozza, Jalayer, Miano, & Manfredi, 2017) or spectral acceleration at 1 second (Sa_{1s}) as popularized by HAZUS (Porter K. , 2009), not because of their actually proven accuracy, but because of its convenience as IMs that are readily available in hazard calculations in most regional

contexts. More recently, average spectral acceleration (AvgSa) (Eads, Miranda, & Lignos, 2015) has gained popularity as a promising alternative, given that it describes ground motion intensity in terms of the geometric mean of spectral demand over a range of pertinent periods of vibration. Some recent research has shown encouraging results for its use in portfolio assessment of structures (Kohrangi, Vamvatsikos, & Bazzurro, 2017) and specifically for bridges (O'Reilly & Monteiro, 2019), however, its claims as an efficient IM have not been yet verified on real inventories of bridges with a wide variety of structural characteristics.

In this chapter, the sets of 270 bi-directional hazard-consistent records that were selected previously in Section 2.3.1 for PGA and AvgSa, are used to evaluate the response, through NLTHA, on the case study inventory of 163 existing bridges described in Section 2.1.3. In order to address the abovementioned gap related to the choice of a proper IM in bridge inventories, the results from the extensive analysis campaign were scrutinised using several performance metrics that evaluate the statistical and behavioural performance of the entire set from an individual and taxonomy-based perspective with to quantify the impact of the choice of IM in the results typically obtained in regional risk assessment of bridge inventories. Beyond the comparison between the use of the two aforementioned IMs (PGA and AvgSa) in bridge portfolio risk assessment, this current chapter explains in detail the application of a state-of-the-art methodology for regional seismic risk assessment of bridges and, furthermore, the analysis of the results obtained will permit to gain insights into some practical questions that may arise when performing regional analysis of bridges, such as the applicability of taxonomy-based fragility curves for the calculation of risk assessment results and the mechanisms that govern the exceedance of the types of bridges analysed.

3.2 METHODOLOGY

The adopted methodology for this chapter, shown schematically in Figure 3.1, consists of initially processing the case study bridges to create a series of numerical models as described in Section 2.2. As stated in Section 2.1.3, these models were be used to perform a preliminary analysis to determine the structural modal information used to define a representative period range for the computation of the AvgSa IM. This information is then combined with the seismic hazard analysis described in Section 2.3.1 for a specific site in Campania, taken as characteristic of the seismicity of the area where the bridge inventory was located. Both these results, concerning the definition of the period range of interest and the hazard conditions of the site, were used to perform a hazard-consistent record selection for both PGA and AvgSa in the selected period range, leading to a set of 30 bi-directional earthquake records for return periods of 30, 50, 98, 224, 475, 975, 2475, 4995 and 9975 years, hence, a total of 270 ground motion records for each IM as described in Section 2.3.1.

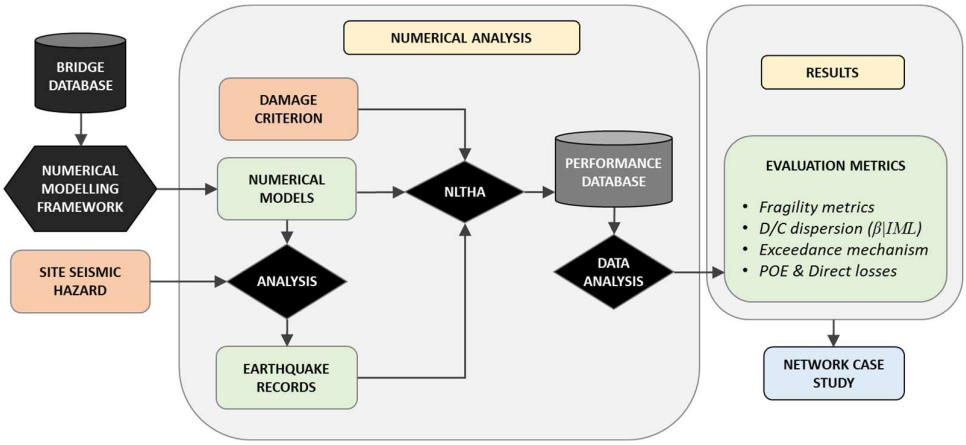

Figure 3.1. Methodology defined to evaluate the choice of IM on a bridge portfolio

Table 3.1. Selected performance metrics to evaluate IM efficiency and result comparison

Performance Metric	Significance
Fragility curve dispersion (β_{lnY})	The dispersion parameter of the continuous fragility curves can be seen as an indicator of efficiency since lower values of β_{lnY} imply a higher probability of reaching a LS for a given IM level.
D/C dispersion ($\beta_{Y\|IML}$)	The dispersion in the demand over capacity ratios obtained for each return period represent a direct indicator of IM efficiency, the lower dispersion associated to an IM the smaller number of records is required to capture the behaviour
Exceedance mechanism	Though not a measure of IM efficiency, it was deemed interesting to investigate if there were differences between the underlying phenomena that cause the exceedance of a LS using records chosen for different IMs
Probabilities of exceedance and direct losses	Thorough comparisons of the mean annual probabilities of exceedance of each LS as well as the resulting average annual losses using both individual and taxonomy-based perspectives were made in order to evaluate the difference in the behaviour obtained by using different IMs

These records are then used to perform NLTHA on each of the 163 bridge structural models to obtain demand over capacity ratios (Y = D/C) of key bridge components that are processed statistically for each return period to determine the exceedance probabilities of specific limit states. These results are then used to fit continuous fragility curves for each bridge in the inventory. The

information obtained from the analysis is later processed to evaluate the efficiency and overall differences resulting from each IM through multiple bridge performance metrics. The selected metrics and their significance in terms of efficiency are presented in

Table 3.1 and will be explained in further detail in the following sections of the present chapter.

Finally, in order to illustrate how the difference in results for both IMs could influence the estimates of road network interruption, a fictitious case study network is evaluated under a seismic event scenario to determine the number of bridges that could be tagged as inoperative. This output represents an additional indirect metric for the evaluation of the relative performance of the IMs.

3.3 RESULTS

3.3.1 Fragility Metrics

Following the procedure described in Section 2.2, for each of the 163 case-study bridges, fragility curves for the damage and collapse limit states were defined as pairs of median (μ_{lnY}) and standard deviation (β_{lnY}) that define a lognormal distribution described by Equation 2.4, for both PGA and AvgSa. All resulting fragility curves, together with the calculated mean group fragility curves, are shown in Figure 3.2 for illustrative purposes alone since these mean curves include bridges from all taxonomy branches. Each individual curve was processed by grouping the results based on the taxonomy branch of each bridge and obtaining the taxonomy-based fragility curves described by the parameters shown in Table 3.2.

Table 3.2. Taxonomy-based fragility curve results

IM	**AvgSa (0.2s-1.0s) [g]**				**PGA [g]**			
LS	**Damage**		**Collapse**		**Damage**		**Collapse**	
Taxonomy	μ_{lnY}	β_{lnY}	μ_{lnY}	β_{lnY}	μ_{lnY}	β_{lnY}	μ_{lnY}	β_{lnY}
2/4-MC	0.185	0.731	1.131	0.540	0.076	0.992	0.694	0.621
2/4-SC	0.191	0.392	1.079	0.496	0.124	0.458	0.752	0.579
2/4-W	0.207	0.340	0.769	0.453	0.119	0.522	0.549	0.590
5+-MC	0.113	0.676	0.787	0.604	0.075	0.763	0.498	0.665
5+-SC	0.127	0.507	0.618	0.497	0.048	0.946	0.428	0.629
5+-W	0.122	0.539	0.847	0.672	0.049	0.960	0.582	0.740

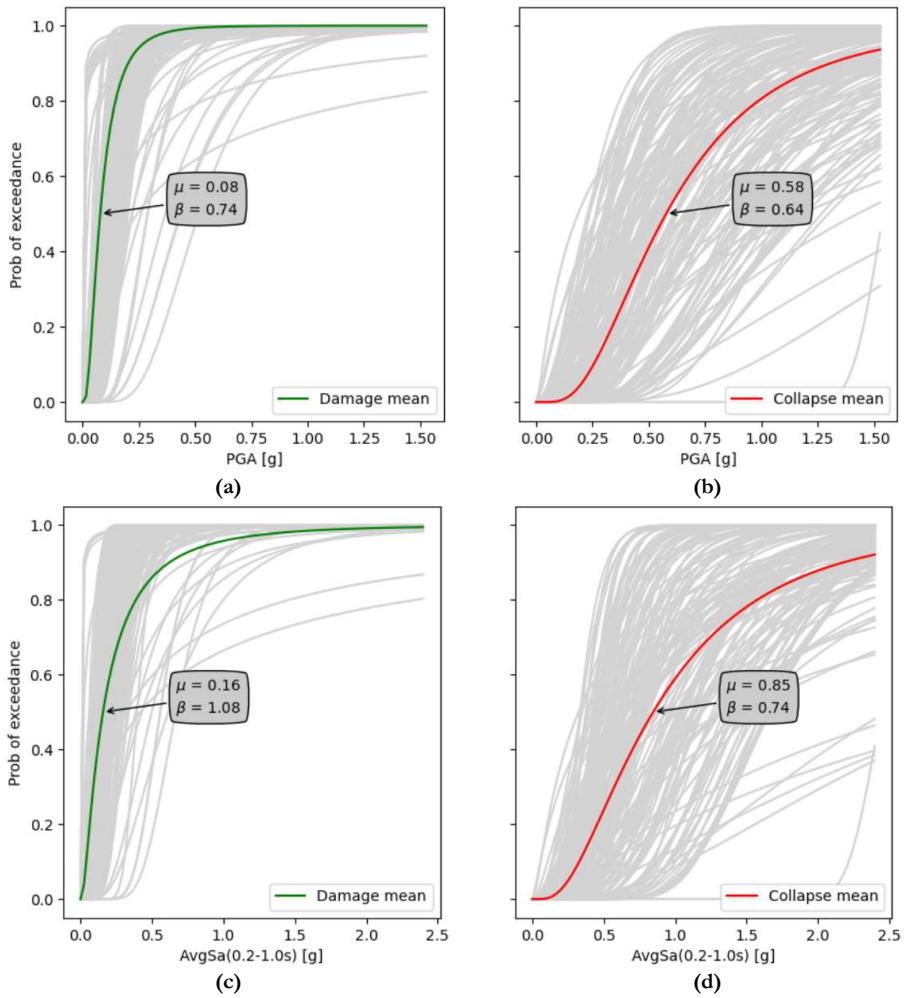

Figure 3.2. Fragility curve results obtained from NLTHA campaign on all 163 assets in the database for: (a) Damage PGA, (b) Collapse PGA, (c) Damage AvgSa, (d) Collapse AvgSa.

From these results, the value of dispersion (β_{lnY}) of the fitted fragility curve can be inferred to be representative of the relative performance of fragility curves calculated with different IM choices since lower values of dispersion are indicative of more abrupt changes between limit states, leading to more certain predictions of performance when compared to curves with higher dispersion values. This is illustrated in Figure 3.3 where, for two curves with similar medians but different dispersions, it can be argued that the IM in curve A is a better

performer in comparison to the one of curve B. Considering these assumptions and comparing the aggregated results obtained from each asset in the database, shown in Figure 3.4, it can be argued that the curves calculated using AvgSa as IM perform better in comparison to the curves calculated with PGA, as they present consistently lower dispersion values for both limit states.

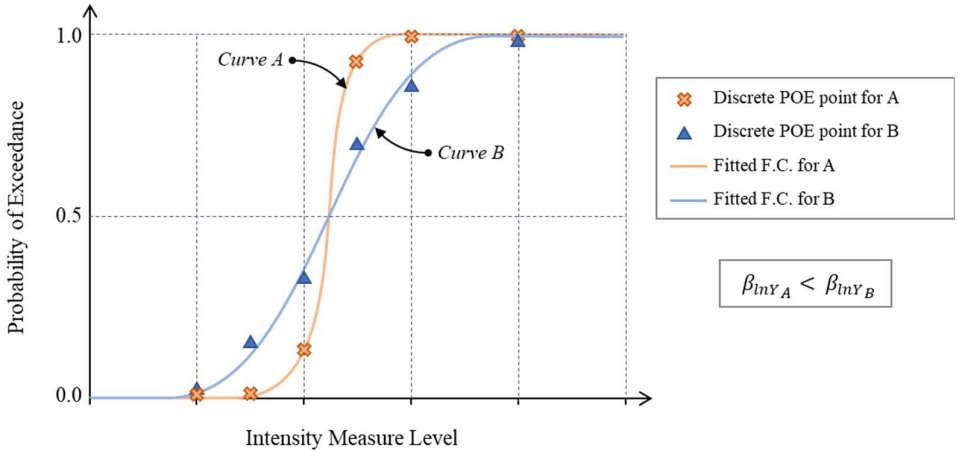

Figure 3.3. Schematic representation of influence of dispersion as metric of performance

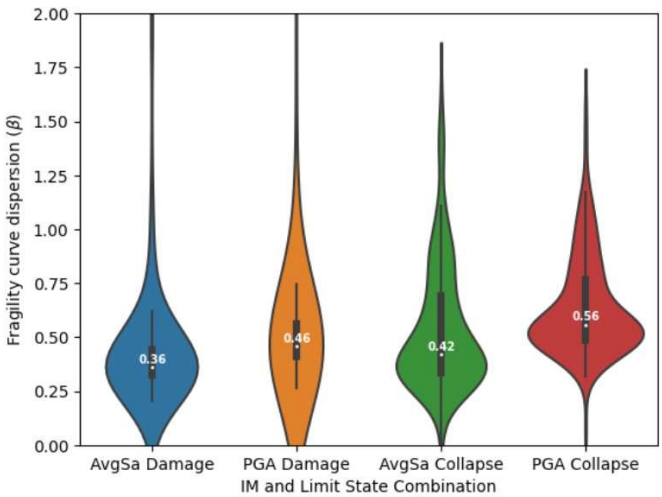

Figure 3.4. Fragility curve dispersion results for all assets, defined as metric to evaluate performance of IM choice

The dispersion results were further investigated to determine if the values were sensitive to the taxonomy branch of each asset; in other words, the results were disaggregated per taxonomy branch and limit state, as shown in Figure 3.5. In this case, it can be seen that there is no apparent trend in the dispersion in terms of taxonomy branch. However, it can also be seen in both plots that, in general, the median dispersion values remain lower when AvgSa is chosen as IM, when compared with their PGA counterparts.

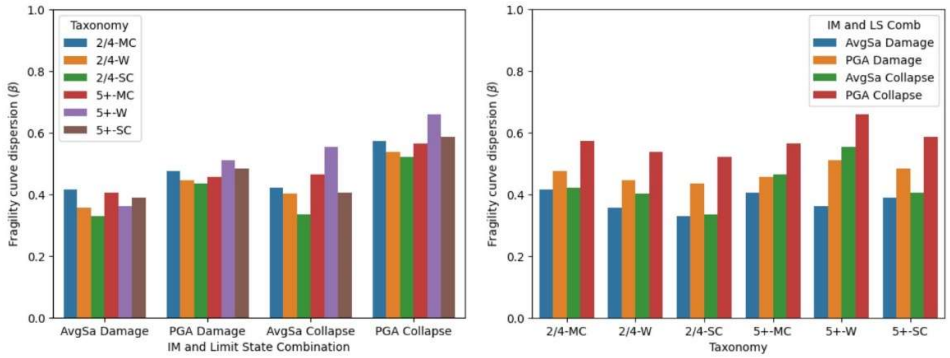

Figure 3.5. Median dispersion values obtained from the results of the entire database, represented in terms of: (a) Limit State and, (b) Taxonomy branch.

3.3.2 Structural Behaviour Dispersion ($\beta_{Y|IML}$)

Another useful metric to evaluate the efficiency of an IM to characterise structural behaviour is the variability observed in the structural demands caused by records representative of the same return period that have been selected and scaled to have the same IM level (record-to-record variability). It is argued that a low variability of structural demand under such conditions is indicative of higher efficiency since it would require fewer records per IM level to capture the resulting behaviour.

As mentioned previously in Section 2.2.3 and illustrated in Figure 2.14, the demand over capacity ratios (Y=D/C) obtained from the NLTHA for each return period are fitted into a lognormal distribution that is used primarily to determine the probability of the structural demands exceeding a limit state threshold. Therefore, values of the median and dispersion per IM level are defined for each return period of which the dispersion value ($\beta_{Y|IML}$) is a direct indicator of the variability observed.

These values were thus retrieved from the structural response database and plotted in terms of their corresponding return period, for both limit states and IMs evaluated. The results

obtained are shown in Figure 3.6, where the bold lines represent the median dispersions obtained from the entire inventory and the shaded areas represent the lower and upper quartiles observed per IML, included as a measure of variability.

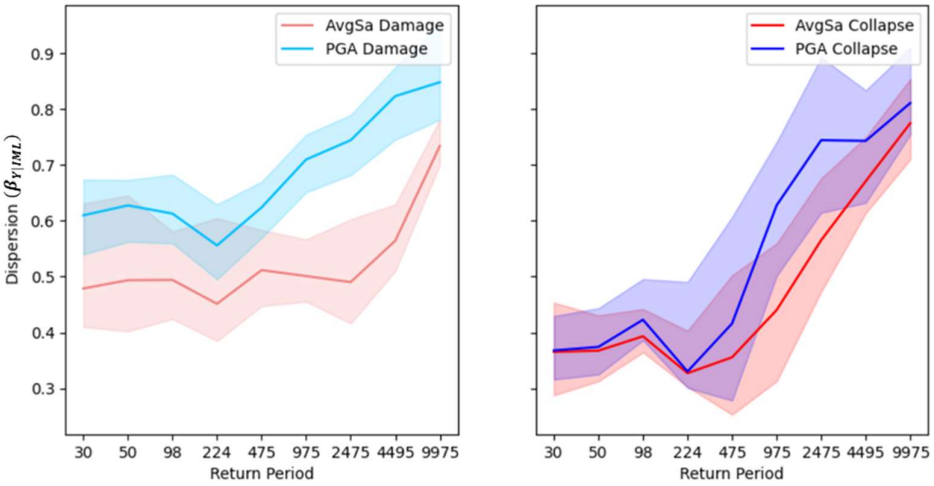

(a) (b)

Figure 3.6. Dispersion of structural demand per IML obtained from the results of the entire database: (a) Damage Limit State, (b) Collapse Limit State.

As it can be seen in Figure 3.6, the dispersion results for PGA and AvgSa show similar trends but with AvgSa always demonstrating lower median values for all return periods and both limit states considered, when compared with its PGA counterpart, leading to the preliminary conclusion that AvgSa is a more efficient choice for IM.

3.3.3 Exceedance Mechanism

As detailed previously in Section 2.2.2, the NLTHA platform takes into account multiple EDPs to determine the probability of exceedance of a specific limit state, with each EDP being used to trigger a limit state based on the exceedance of either flexure, shear or bearing displacement (unseating) capacity.

For simplicity, the fragility curve calculation was made with an enveloping approach, described in Equation 2.3, using the highest D/C ratios obtained throughout the NLTHA campaign for each exceedance mechanism in each asset analysed. However, in order to investigate the mechanism that contributes the most to the fragility of each bridge typology, as well as to determine if the IM choice has any influence in such a mechanism, the structural behaviour database was reanalysed to determine the most recurring mechanism that governs the fragility of each asset in the inventory.

The results of this exercise are shown in Figure 3.7, divided by limit state and taxonomy branch. It can be seen that the exceedance of flexure capacity is the governing mechanism for the majority of assets in all taxonomy branches and that the choice of IM for record selection has very little impact in the overall governing mechanism. This preliminarily indicates that the governing mechanism depends mostly on the particular characteristics (e.g. geometrical layout, materials, structural system) of each asset rather than the employed IM.

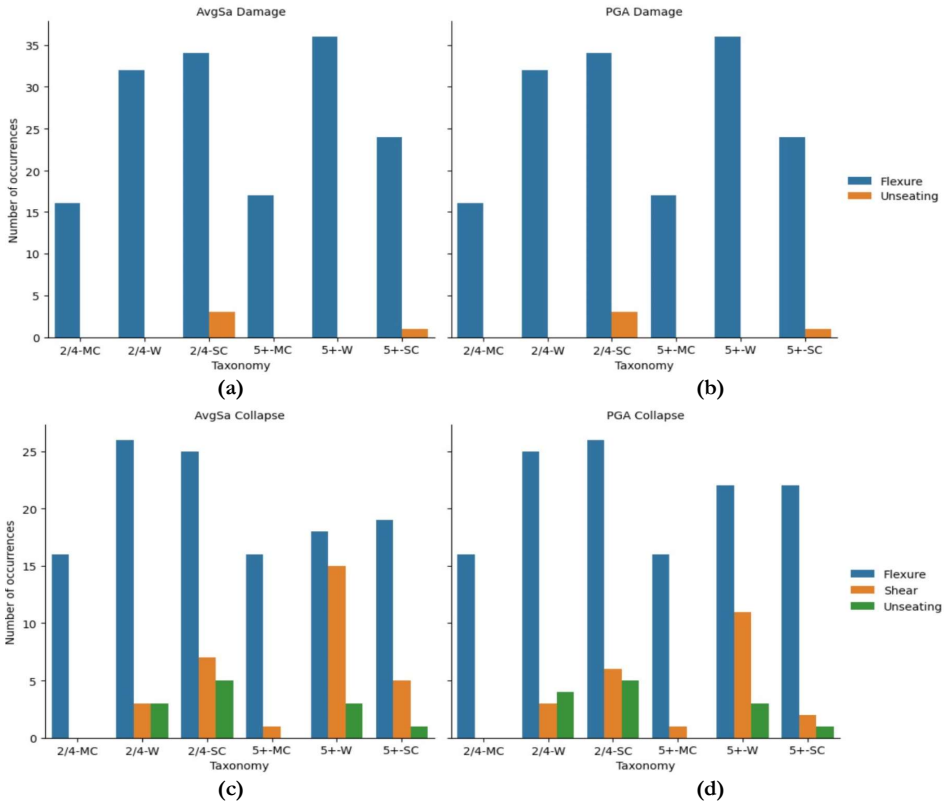

Figure 3.7. Structural mechanism that governs the exceedance of limit states separated by taxonomy branch for: (a) Damage AvgSa, (b) Damage PGA, (c) Collapse AvgSa (d) Collapse PGA.

3.3.4 Limit state Probabilities of Exceedance and Direct Losses

3.3.4.1 *Probability of Exceedance of Limit States*

In order to investigate the influence of the choice of IM in the probabilities of exceedance (POE) of the two limit states for different IM levels, the discrete results obtained from the NLTHA for the nine IM levels were associated with their respective return periods. This was to allow results from both PGA and AvgSa record sets to be plotted together and compared for each asset in the case study. The aggregated results of all bridges in the database can be seen in Figure 3.8, where the bold lines represent the median values of POE for each limit state and return period observed for the entire inventory, while the shaded areas represent the lower and upper quartiles included as a measure of the corresponding variability.

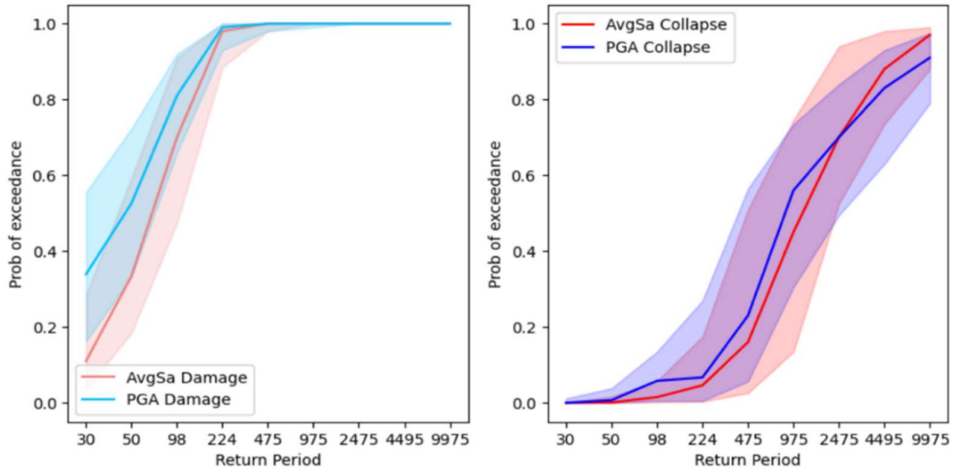

(a) (b)

Figure 3.8. Probability of exceedance versus return period comparison for: (a) Damage Limit State, (b) Collapse Limit State.

It can be seen that the largest differences in probability of exceedance between both choices of IM are present in the lower return period range of the Damage LS, where the results obtained with the PGA selected records show a much higher median and uncertainty in the POE than its AvgSa counterpart. This trend is reduced for higher return periods as the Damage LS becomes exceeded by the entire set of records above a return period of 975 years. In the case of the Collapse LS, as it is shown in Figure 3.8 (b), both IM choices lead to similar median results although, again, the PGA calculations yield a slightly higher POE for lower return periods than its AvgSa counterpart, a trend that is reversed for return periods above 2475 years.

Furthermore, by combining the POE results with the mean annual frequency of exceedance (MAFE) obtained during the hazard analysis for each IM level and integrating over the resulting curve, it is possible to obtain the annual probability of exceeding (APE) a specific limit state, as described schematically in Figure 3.9. This exercise was performed for each asset in the database and each IM choice for both limit states and the results are presented in Figure 3.10.

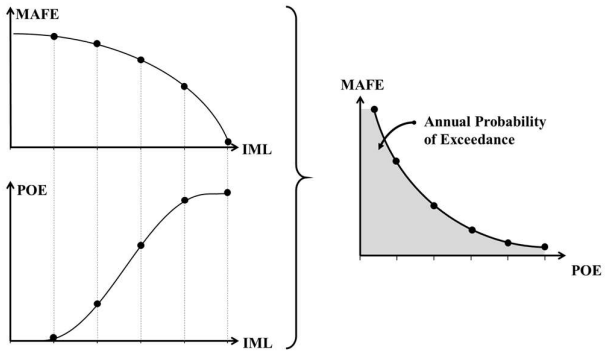

Figure 3.9. Schematic representation of the calculation of the annual probability of exceedance of a specific limit state

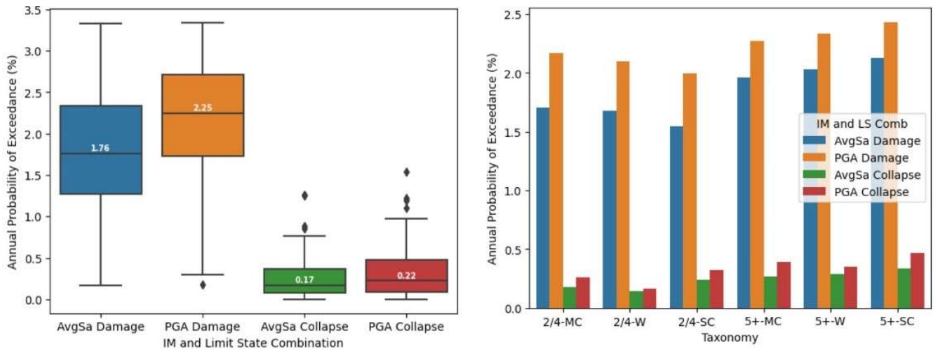

(a) **(b)**

Figure 3.10. Annual probability of exceedance for each limit state and each IM choice: (a) Aggregated results for entire inventory, (b) Disaggregated results by taxonomy branch.

As it can be seen in Figure 3.10 (a), when considering the entire inventory data, the median APE calculated with PGA as the IM was slightly higher for both limit states when

compared to AvgSa. This trend was maintained when disaggregating the results by taxonomy branch, as shown in Figure 3.10 (b), where it can also be seen that taxonomy branches representing bridges with more spans experience higher mean APE than their shorter counterparts with the same pier section types. This is considered an expected result since bridges with more elements are more likely to have any of them exceeding a specific limit state for an IM level.

3.3.4.2 *Direct Losses*

Finally, a simplified methodology was adopted to evaluate the potential impact of the choice of IM on the direct economic losses that can be expected over the entire inventory. This methodology is based on the earlier versions of the Pacific Earthquake Engineering Research Center's Performance Based Earthquake Engineering (PEER PBEE) framework (Porter K. A., 2003) and it aims to calculate the direct Expected Annual Losses (EAL) for each asset in the database by accounting for the percentage of the replacement cost of the bridge associated to each LS, also known as Mean Damage Factor (MDF), together with its probability of occurrence as described by Equation 3.1.

$$\begin{aligned} \text{EAL} &= \begin{bmatrix} p(LS_D) & p(LS_C) \end{bmatrix} \cdot \begin{bmatrix} €L|LS_D \\ €L|LS_D \end{bmatrix} \\ &= \begin{bmatrix} \big((APE, LS_D) - (APE, LS_C)\big) & (APE, LS_C) \end{bmatrix} \cdot \begin{bmatrix} MDF|LS_D \\ MDF|LS_C \end{bmatrix} \cdot €RC \end{aligned} \qquad \text{Equation 3.1}$$

Where:

LS_D: Damage Limit State
LS_C: Collapse Limit State
$p(LS_D)$: annual probability of occurrence of LS_D
$p(LS_C)$: annual probability of occurrence of LS_C
$€L|LS_D$: direct economic losses associated to LS_D
$€L|LS_C$: direct economic losses associated to LS_C
APE, LS_D: annual probability of exceedance of LS_D
APE, LS_C: annual probability of exceedance of LS_C
$MDF|LS_D$: mean damage factor for LS_D
$MDF|LS_C$: mean damage factor for LS_C
€RC: bridge replacement cost

For the purposes of the present research, where the aim is to compare the impact of choice of IM in these calculations, the MDF associated to the occurrence of LS_D and LS_C were considered deterministically known (no uncertainty was considered) and taken respectively as 8% and 100% of the replacement cost of each asset, which are the central MDF values indicated for Moderate and Collapse LS for bridges used previously in Perdomo et al. (2020) and in other studies conducted by PEER (Stergiou & Kiremidjian, 2008). In the same line of thought, the replacement cost of each bridge was taken as proportional to the

deck area, considering a generic cost per square meter. The EAL results, expressed as a percentage of the overall replacement cost of the entire inventory, are shown in Table 3.3.

Table 3.3. Results for Expected Annual Losses as percentage of the replacement cost of the entire inventory

IM	EAL Individual	EAL Taxonomy-Based	EAL Ind/Tax
AvgSa	0.406%	0.407%	0.996
PGA	0.513%	0.521%	0.985

The EAL results obtained directly by using the probability of exceedance results from the NLTHA of each asset are presented in Table 3.3 as "EAL Individual," where it can be seen how the calculations made with the PGA sets lead to an increased estimation of EAL over the entire inventory when compared to the AvgSa sets, which can be attributed to the overestimation of POE and increased dispersion presented by the PGA results reported in Figure 3.10. It is worth noting that while this difference might seem small when considering the total cost of the inventory, the PGA estimate represents a 25% increase in EAL over the results obtained from AvgSa, which could represent a significant monetary value, when referring to numerous bridge structures.

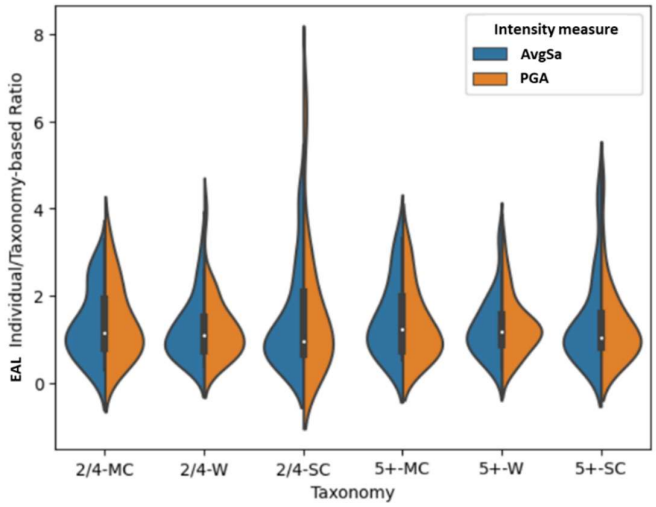

Figure 3.11. Ratio of EAL estimations made using individual fragility curve over taxonomy-based curves for each asset, divided by taxonomy-branch

The EAL calculation exercise was also conducted using the POE derived from the taxonomy-based fragility curves assigned to each asset based on their corresponding taxonomy branch. This had the purpose of investigating the differences that can be expected when using taxonomy-based curves in regional bridge risk calculations compared to having individual curves for each asset. The results of this exercise are shown in Table 3.3 as "EAL Taxonomy-Based" where it can be seen that there were negligible differences between both calculations, leading to the preliminary conclusion that this type of analysis can lead to accurate results when evaluating risk metrics over the entire inventory. However, this conclusion does not hold true when considering the differences encountered between both calculations on an asset-to-asset level, where large variations can be found between results of a specific bridge when using the individual curve when compared its taxonomy-based counterpart, as shown in Figure 3.11, independently of the IM choice.

The results presented in Table 3.3 also allowed to evaluate the performance of the choice of IM in the definition of the taxonomy-based fragility curves themselves by considering the differences obtained in EAL for the entire inventory between the individual and taxonomy-based results within the same IM choice. It can be argued that the IM that leads to the smallest difference between individual and taxonomy-based results would represent a better IM choice for taxonomy-based evaluations, however, even though the AvgSa taxonomy-based EAL calculations did provide almost exact results compared to its respective individual-based counterpart (Ind/Tax = 99.6%), very similar results were obtained with the PGA set (Ind/Tax = 98.5%), therefore, both are deemed appropriate for this purpose.

3.3.5 Road Network Case Study Evaluation

In order to evaluate the influence of the variability found in the results between fragility curves calculated with the different choices of IM in a spatially distributed scenario, a fictitious road network case study was defined by locating the bridges in the analysed inventory on the primary vehicular road system surrounding the hazard site. For this purpose, a database from OpenStreetMap OSM (2020) was mined to extract the road network layer for the Campania region and select the location of 163 bridges of the primary network (highways and trunks) as shown in Figure 3.12. The fragility properties of each of the original case study bridges were assigned to these locations, distributing the properties based on the sorted length of assets in both databases to minimize the total length difference between the OSM reported values and the assigned fragility curves. The differences between both length distributions are shown in Figure 3.13.

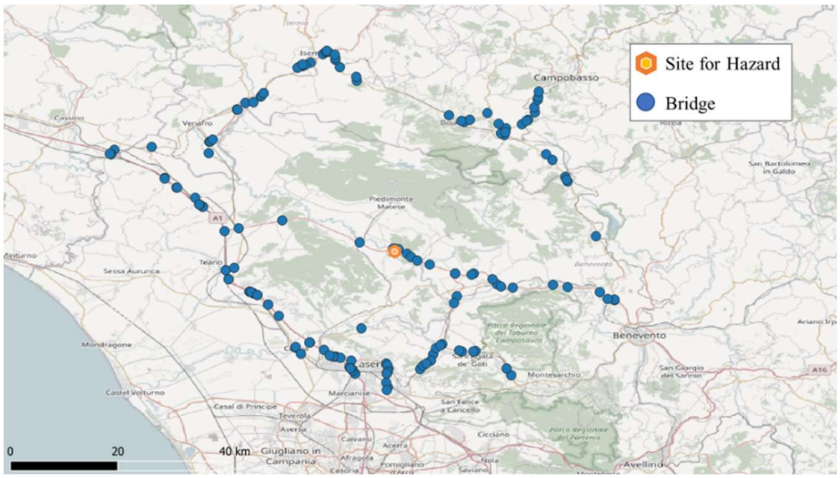

Figure 3.12. Fictional road network case study defined

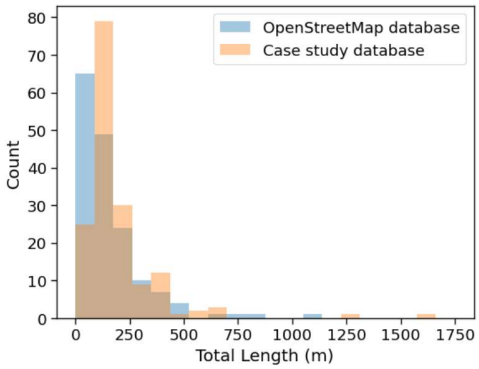

Figure 3.13. Distribution of total length between OSM and case study database

A historical seismic event was used to evaluate the differences in road network disruption that can be predicted when using both choices of IM after an earthquake. For this purpose, the 1688 Sannio Earthquake that occurred on June 5th of 1688 in the vicinity of the hazard site location was chosen. This event, whose rupture information reconstructed from historical accounts (Bucci, Massa, Tornaghi, & Zuppetta, 2005) can be seen in Table 6, was estimated to have had a moment magnitude of 7.06 M_w and accounted for extensive destruction in the near areas, as well as an estimated 10,000 human casualties.

Table 3.4. Input parameters for the 1688 Sannio Earthquake (Bucci, Massa, Tornaghi, & Zuppetta, 2005)

Latitude	41.283
Longitude	14.561
Moment Magnitude (Mw)	7.06
Fault mechanism	Normal
Depth	13 Km

This information was used as input to define an earthquake rupture model and perform a Scenario-Based Seismic Hazard Analysis (SSHA) using the Ground Motion Field Calculator available within the OpenQuake Engine (Silva, Crowley, Pagani, Monelli, & Pinho, 2014). For consistency with the hazard model used previously, the GMPE logic tree was replicated in these calculations and multiple realizations of ground shaking intensity were computed at the location of each bridge for the Sannio earthquake rupture. The mean values of shaking intensity obtained for each site and each IM choice are shown in Figure 3.14.

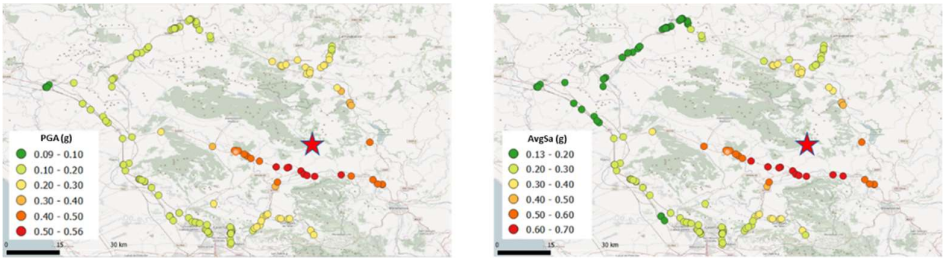

(a) **(b)**

Figure 3.14. Results for ground shaking intensity obtained from the simulation of 1688 Sannio earthquake considering: (a) PGA, (b) AvgSa(0.2s-1.0s).

Using these mean estimates of ground motion intensity, the probability of exceedance of the damage and collapse limit states were computed for each asset, considering both the PGA and AvgSa assigned fragility curves. To determine if a bridge remains operational after a seismic event based on these probabilities of exceedance, threshold values of POE were defined for the damage and collapse limit states. This simplified methodology to flag unusable bridges in a scenario assessment based on thresholds has been previously used in research projects, such as INFRA-NAT (2018) and will be used herein to provide a notion on the differences that can be expected when using such methodology under both choices of IM considered. For the sole purpose of this academic exercise, it was defined that if any

bridge in the case study that presented a POE above 90% for the damage limit state or 30% for collapse would be tagged as closed. These threshold limits, although somewhat arbitrary, are considered reasonable for comparison purposes, since the same thresholds are defined for both IM choices.

The results of bridge interruption can be seen in Figure 3.15, where 72 bridges exceeded the defined thresholds when using the fragility curves calculated for PGA as IM, in comparison to 59 closed bridges detected when using AvgSa. These results are in agreement with the findings in previous sections where metrics evaluated with the use of PGA as IM choice are consistently conservative when compared to the same values calculated with AvgSa.

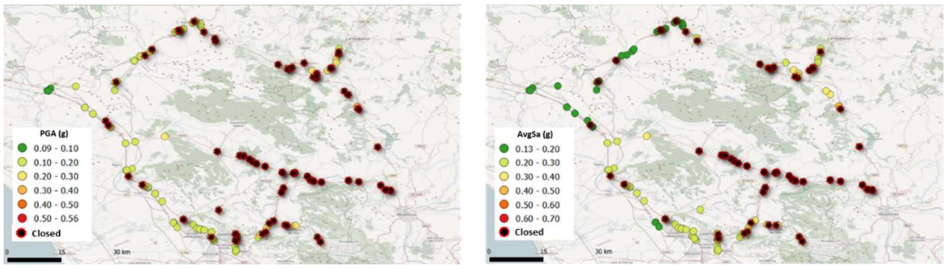

(a) (b)

Figure 3.15. Results for bridge interruption obtained from the simulation of the 1688 Sannio earthquake, considering: (a) PGA, (b) AvgSa(0.2s-1.0s).

3.4 SUMMARY AND CONCLUSIONS

In this chapter, a large inventory of existing reinforced concrete bridges with different configurations from the Italian road network was analysed through nonlinear time-history analysis (NLTHA) using hazard-consistent records, selected for both PGA and AvgSa as intensity measures. Multiple fragility and vulnerability metrics were defined to compare the impact of the choice of the IM in the statistical and structural performance of a significant number of bridge assets from individual and taxonomy-based perspectives.

Based on the results obtained by the application of the methodology defined, the following conclusions can be drawn regarding the fragility estimates obtained by making different IM choices:

- Based on the statistical evaluation of dispersion values β_{lnY} for the sets of fitted fragility curves, it is concluded that the use of AvgSa as IM consistently leads to

fitted fragility curves with an overall lower curve dispersion in comparison to equivalent results calculated using PGA as IM;

- In terms of structural response dispersion, given a certain IM level, based on the distribution of demand over capacity ratios obtained from NLTHA for multiple return periods and limit states, it was concluded that the use of AvgSa as IM leads to lower mean values of structural behaviour dispersion in comparison to results obtained using PGA as IM for all limit states and return periods considered, making AvgSa a more efficient choice for IM than PGA;
- Regarding the structural mechanisms that govern the fragility of different types of bridges for the NLTHA campaign performed, the flexure mechanisms were more recurrent than shear or unseating for all taxonomy branches and limit states considered, regardless of the choice of IM;
- The use of PGA as choice for IM leads to conservative estimates of probability of exceedance of all limit states considered, which in turn may lead to direct loss estimates that are in the range of 25% higher expected annual losses over the entire bridge inventory. This is an economically important outcome, as one can have a more accurate estimate of costs, particularly when having, for instance, limited resources with which to improve the seismic performance of the bridge inventory of a certain region;
- Calculations of average annual losses over an entire bridge inventory made with appropriately defined taxonomy-based fragility curves lead to almost exact overall results in comparison to calculations made with specifically calculated fragility curves for each asset in the inventory, regardless of the IM choice. However, large differences were observed on an asset-to-asset level and therefore it is not recommended to use taxonomy-based curves for a structure independent assessment;
- When performing the simplified exercise of assigning arbitrary but equal thresholds between choices of IM to detect closed bridges in a scenario-based case study, the use of PGA as the choice for IM lead to conservative estimates for road network interruption, which is in line with and confirms the observed trend on the probabilistic metrics that were analysed.

Overall, the outcomes of this study highlight AvgSa as an efficient IM over the more traditionally used PGA for regional seismic risk analysis, herein evaluated for the first time on a large inventory of real bridges with multiple structural configurations. Furthermore, the presented research also provided further insight, beyond the choice of IM, to other factors that contribute to the decision-making process of regional risk analysis of bridges, such as governing failure mechanisms and the applicability of taxonomy-based results for this type of purpose.

4. EXPOSURE: EFFECT OF KNOWLEDGE LEVEL

4.1 INTRODUCTION

Regional seismic assessment of bridge portfolios has become an effective tool for stakeholders and decision makers to quantify the risk associated with earthquake activity on their inventories. While the specific methodologies for this type of assessment vary, the overarching philosophy relies on dividing the problem into the components of hazard, exposure and vulnerability, which are later convoluted in a probabilistic fashion to estimate the annual rates of exceeding specific thresholds of structural performance (e.g., pier shear failure) or economic losses associated with repairing the damaged bridge structure.

Given this probabilistic nature of risk assessment, uncertainty plays a key role in the process. Two main types of uncertainty are generally recognized in risk assessment: aleatory uncertainty, which refers to the inherent random effects present in natural phenomena and therefore cannot be reduced; and epistemic uncertainty, which refers to the lack of knowledge associated with each component of risk. In the case of the exposure component, which deals with the number and characteristics of the physical assets included in the assessment, lack of structural information in terms of geometrical dimensions of elements, material properties or structural component configurations constitute a source of epistemic uncertainty that ultimately affects the accuracy of the overall risk assessment results. While it is possible to reduce this uncertainty by performing data collection and surveying campaigns, these require a large effort, time and cost, causing most practical seismic risk assessment applications for both bridges and buildings to be carried out with incomplete information.

Common practice when addressing the lack of specific structure-level information is to use macro taxonomy-based approaches that average fragility information of assets with similar configurations, which are expected to have similar performance or observed damage when subjected to equal levels of seismic demands. Such practice is the basis for the HAZUS (F.E.M.A., 2013) and SYNER-G (Pitilakis, Franchin, Khazai, & Wenzel, 2014) methodologies, for example. In order to do this, taxonomy branches are defined by grouping key structural parameters that are assumed to influence structural capacity and seismic response. Subsequently, multiple representative structures within each taxonomy branch are analysed in detail with the intention of capturing the variability of the behaviour in each class and defining an average fragility curve. Such a curve can then be applied to

each element in the inventory that have been identified as members of the class without the necessity of performing specific analysis for every individual asset.

While this practice is frequent and generally recommended for the regional assessment of buildings (D'Ayala, et al., 2015), a recent study conducted on bridges (Stefanidou & Kappos, 2019) concluded that the use of taxonomy-based fragility curves can significantly affect the accuracy of predictions for individual assets in a portfolio. Another study (Abarca, Monteiro, O'Reilly, Zuccolo, & Borzi, 2021) performed on an inventory of bridges with full information, confirmed their inaccuracy in bridge specific predictions, while also concluding, nevertheless, that the use of taxonomy-based curves leads to accurate estimates of the total direct losses for the entire portfolio. This means that these types of curves can potentially be a good alternative to assess aggregated losses over entire inventories if enough representative structures are used to accurately capture the variability within each taxonomy branch.

The number of structures that should be included in the detailed analysis to fully represent a taxonomy branch will depend on the classification scheme that is used to define the branches and the inherent variability in behaviour present in each resulting branch. Much debate exists on the appropriate bridge parameters to use to group bridge classes. While HAZUS is very popular (F.E.M.A., 2013), as evidenced by recent research (Mangalathu, Soleimani, & Jeon, 2017; Nielson & DesRoches, 2007) and regularly used in risk projects worldwide (Chen, Branum, & Wills, 2013; Yue, Zonta, Bortot, & Zandonini, 2010; Nielson & DesRoches, 2007), other options have been proposed (Mangalathu, Soleimani, & Jeon, 2017; Joint Research Centre, 2013) and researchers typically define their own classification depending on the specific characteristics of the inventory to be analyzed. Furthermore, since the inherent variability present in each classification is not known beforehand, the number of structures chosen to represent each branch is typically defined arbitrarily depending on the amount of information available for each specific case and inventory. All of this leads to an unknown level of uncertainty in the accuracy of the results obtained.

In the current chapter, the database of 308 existing bridges from the Italian road network detailed in Section 2.1.1 is used to define multiple realizations of the case study presented in Section 2.1.4, located in the province of Salerno. This portfolio is used to evaluate the uncertainty that can be expected in the total direct economic losses calculated over the entire portfolio of each case study realization when increasing portions of the inventory are known. The intention is to provide researchers and practitioners dealing with seismic risk assessment of bridge inventories with a better understanding of the uncertainty level surrounding the results obtained when a fixed percentage of their inventory has full information available. This information can also guide the early stages of the regional assessment process, in defining the number of structures that should be properly surveyed and analysed to obtain a desired level of accuracy in direct loss calculations.

Furthermore, recent developments in machine learning applications to risk assessment projects have been shown to be promising to increase the accuracy in predictions of earthquake-related damage and losses. Mangalathu et al. (2019) tested the performance of multiple algorithms to predict the limit state of bridges in a portfolio following a seismic event based on specific bridge attributes. They concluded that the use of these algorithms allows for the increase in damage detection accuracy by incorporating multiple parameters in the calculation other than just the intensity measure level used in typical fragility curves. Another recent study (Kalakonas & Silva, 2021) evaluated the use of artificial neural networks for the derivation of seismic vulnerability models for building portfolios and observed an overwhelming improvement in the reliability and accuracy in risk assessment predictions when compared to the traditional regression models, further highlighting their potential for risk assessment applications.

Also, the evaluation of the exposure knowledge impact when using a taxonomy-based approach is presented here. It is then used to train a machine learning model with the non-linear time-history analysis results of the known portions of the inventory and to subsequently estimate the fragility curves of each unknown asset. The results obtained using these predicted curves are also evaluated in terms of the uncertainty in the total direct economic losses calculated over the entire portfolio and compared with the results obtained using the traditional taxonomy-based approach.

4.2 METHODOLOGY

The methodology defined for this chapter, depicted graphically in Figure 4.1, initially consists of creating multiple networks with different configurations of bridges located in a case-study region. This is done by taking the assets from the portfolio of 308 real bridges with fully known information and randomly locating them within an existing road network, thus creating multiple synthetic case study realisations. Each bridge is then analysed in its respective location in each case-study realisation according to detailed risk assessment procedures, enabling the determination of the direct economic losses (average annual losses, AAL) for the entire portfolio, which serves as a benchmark to evaluate the uncertainty that can be expected when incomplete information of the inventory is available.

After the bridge database is used to create the baseline case study presented in Section 2.1.4 and the NLTHA process described in Section 2.2.3 is performed, the fragility curves for the collapse limit state are obtained for each bridge in the case study. These fragility curves were then integrated with the hazard curves of each site to obtain the annual probability of collapse of each bridge. This was then multiplied by an estimate of the replacement cost of the bridge to determine their collapse-based AAL. A sampling process was then adopted, whereby portions of the database of results were randomly removed and the remaining ones used to calculate taxonomy-based fragility curves, which were then assigned to each

asset of the realisations with removed information. Exposure rates between 5% and 100%, defined as the ratio between the number of assets with complete information and the total number of assets in the inventory, were evaluated by performing 40 different random samples for each exposure rate to capture the uncertainty in the calculation of total AAL using the taxonomy-based curves on the assets with incomplete information.

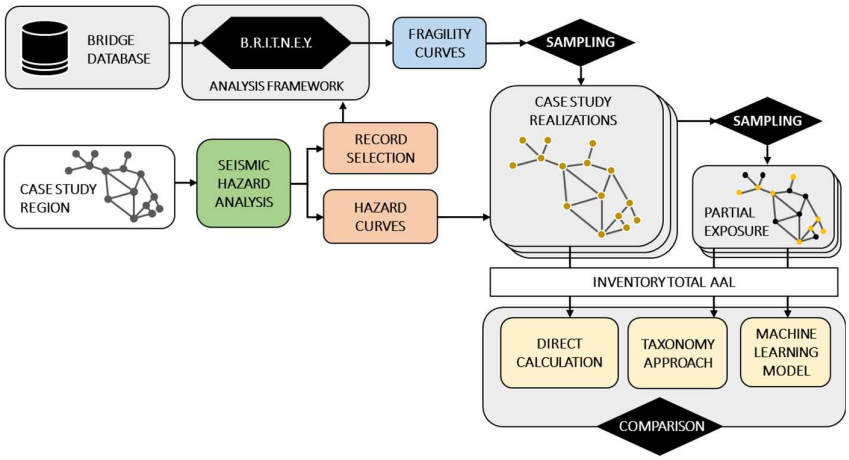

Figure 4.1. Methodology used to evaluate the effect for exposure knowledge for bridge inventories

Additionally, the same sampling process was repeated but the known portions of the inventory at each iteration were used to train a machine learning model for each bridge class to predict the collapse probability at specific IM levels for the bridges with incomplete information based on simple geometric properties of the actual structures. These predictions were then used to determine continuous fragility functions for each asset with incomplete information and estimate the total AAL of the entire inventory at each iteration. Finally, statistical trends of the uncertainty associated with each exposure rate when applying both the taxonomy-based approach and the machine learning model were defined and compared to determine the relative performance of each method. Recommendations are also provided on which method to use, depending on the percentage of known information and corresponding accuracy.

4.3 CASE STUDY GENERALIZATION

In order to generalize the case study used for this study, and strengthen the results of the current research, ten different case studies were created by repeating the sampling procedure used to allocate the 308 bridges from the database in the position of the 617 bridges in the case study region of Salerno, hence obtaining ten different configurations of

asset types in the road network. In order to maintain the validity of the fragility results and avoid having to run NLTHA with different earthquake record sets for the same bridges, the sampling process was carried out considering fixed combinations of seismic zones and soil types for each bridge. Examples of two case-study realisations are shown in Figure 4.2 with respect to the resulting spatial distribution of the taxonomy branches and the number of occurrences of each branch in the realisation.

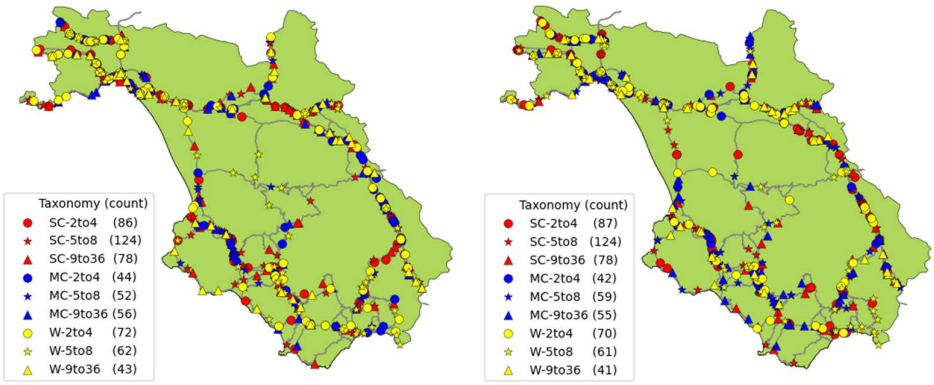

(a) **(b)**

Figure 4.2. Examples of sampling used to define Case Study realisations: (a) Case Study realization number 1, (b) Case Study realization number 3.

4.4 RESULTS

4.4.1 Fragility Curves and Direct Loss Assessment

After the application of the NLTHA process described in Section 2.2.3 is performed, the fragility curves for the collapse limit state are obtained for each bridge in the database. The results of this exercise are shown in Figure 4.3, separated by taxonomy branch, where the mean fragility curve calculated as per Equation 2.5 through Equation 2.8 is shown for reference.

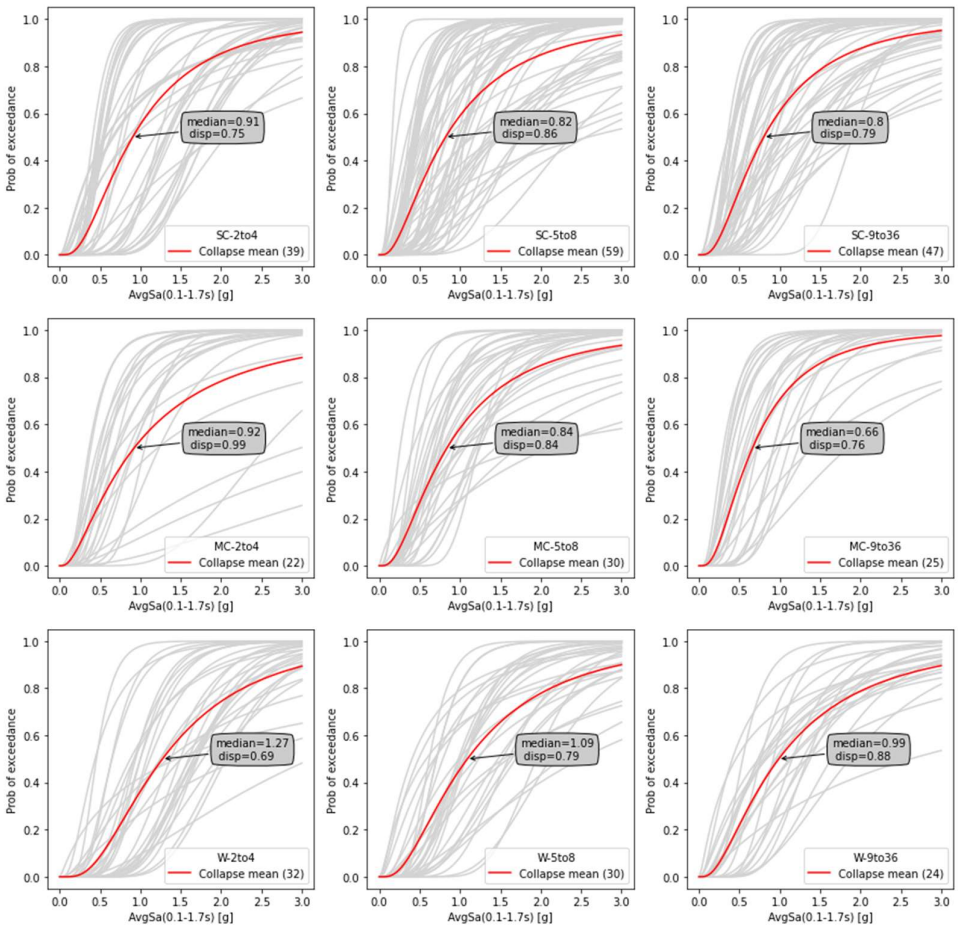

Figure 4.3. Fragility curves for Collapse Limit State obtained for the 308 bridges in the database separated by taxonomy branch

The calculation of AALs associated with the collapse limit state was carried out using the formulation from the Pacific Earthquake Engineering Research Center's Performance-Based Earthquake Engineering (PEER PBEE) framework (Porter K. A., 2003). A very straightforward implementation of the formulation is possible by including only the collapse limit state, where the product of the annual probability of exceedance of the limit state times the direct replacement cost will result in the direct collapse-based AAL, as described by Equation 4.1.

$$\text{AAL} = p(LS_C) \cdot €L|LS_C = APE_C \cdot €RC \qquad \text{Equation 4.1}$$

where:
LS_C: Collapse Limit State
$p(LS_C)$: probability of occurrence of LS_C
$€L|LS_C$: direct economic losses associated to LS_C
APE, LS_C: annual probability of exceedance of LS_C
€RC: bridge replacement cost

The annual probability of exceedance (APE) for the limit state was obtained by convoluting the fragility and hazard curves obtained for each bridge in each case study. The replacement cost for each bridge was taken as proportional to the deck area, considering a generic cost per square meter of €930, taken from the mean replacement cost per area assumed by Perdomo et al. (2020) for a similar Italian bridge inventory. The results for collapse-based direct AAL are show in Figure 4.4 for the two example case studies previously presented in Figure 4.2, whereas Table 4.1 summarizes the total AAL calculated for the entire portfolio configuration in each case-study realization. These aggregated loss values per case study will be used as a benchmark to evaluate the uncertainty related to the exposure knowledge level in the following sections.

Table 4.1. Summary of baseline total portfolio direct loss per case study

Case Study Realization	Total Direct Loss
1	€ 2,552,567
2	€2,240,684
3	€2,291,323
4	€2,525,752
5	€2,296,542
6	€2,338,223
7	€2,332,061
8	€2,314,442
9	€2,211,758
10	€2,277,621

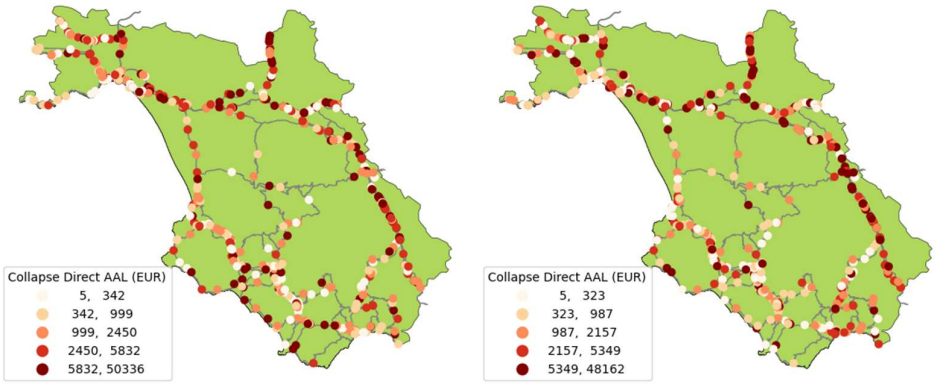

(a) **(b)**

Figure 4.4. Results for collapse AAL: (a) Case Study realization number 1, (b) Case Study realization number 3.

4.4.2 Evaluation of Exposure Uncertainty

4.4.2.1 *Taxonomy-based Approach*

The use of taxonomy-based curves is rooted in the assumption that assets with similar configurations will have a similar performance or damage when subjected to equal levels of seismic demand. Therefore, macro fragility curves created for classes of structures can be used for assets within the class without detailed analysis. As shown schematically in Figure 4.5, if all the assets in a case study were of the same taxonomy branch, specific analysis could be carried out on the bridges for which complete structural information is available. This then allows the individual fragility curves for each of them to be obtained. Subsequently, a mean fragility curve can be assembled by accounting for the mean responses, along with the inter and intra dispersion of the curves, given by Equation 2.5 through Equation 2.8. This would constitute the taxonomy-based fragility curve for the class that can be used for all the remaining assets in the taxonomy branch that have incomplete information.

While this assumption is generally accepted for regional-level seismic risk assessments, it is expected that such a simplification will introduce a non-negligible level of uncertainty, depending on the classification scheme that is used to define the branches and the number of bridges per branch with complete information specifically analysed. Since there is no consensus on a definitive classification system, or on the number of bridges required to be analysed to properly characterise a taxonomy branch, risk analysts will typically make these decisions based on the information that is available.

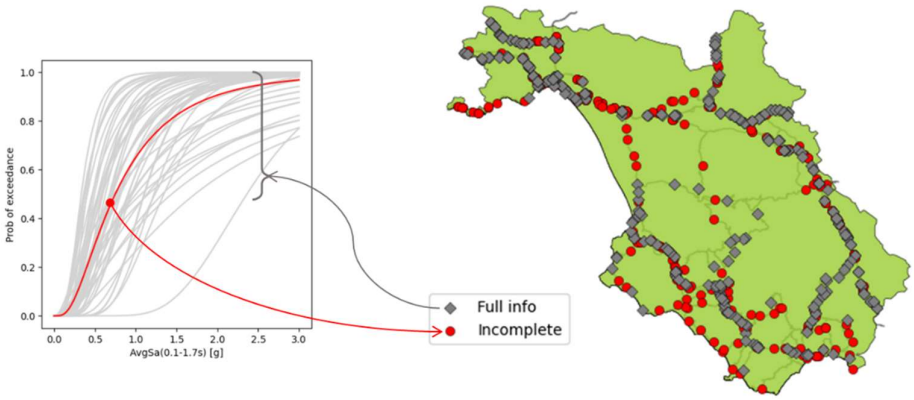

Figure 4.5. Schematic representation of taxonomy-based fragility curve assignment on assets of the same taxonomy branch with incomplete information

In order to have a comprehensive evaluation of the inherent accuracy of the use of taxonomy-based approaches, the classification system introduced in Table 2.2 is used to assign a taxonomy branch to each asset in the case-study portfolio realisations described in Section 4.3. Once this is done and a baseline collapse-based direct AAL estimate for each case study is performed, increasing portions of the portfolio's results are randomly removed. The remaining values are used to calculate taxonomy-based fragility curves that are then assigned to each asset of the case studies with removed information based on their classification. The ratio of known over unknown portions of the inventories explored in this study, hereinafter referred to as exposure rates, ranges from 5% to 100% in 5% increments, leading to 20 different exposure rates.

Additionally, the taxonomy-based curves calculated for each exposure rate will change depending on the specific assets available in the known portion of the portfolio. This is illustrated in the example shown in Figure 4.6, where four different samples of the same exposure rate for the assets in a taxonomy branch from a case-study realisation will yield slightly different mean curves. To account for this, 40 different random samples of assets with full information are taken for each exposure rate.

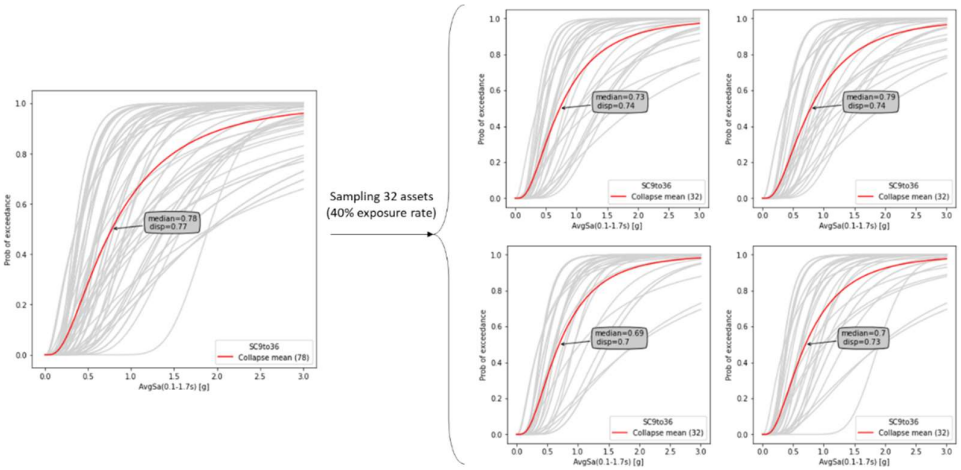

Figure 4.6. Example of variation in taxonomy-based curves obtained by sampling a 40% exposure rate from the RC-SC-9to36 taxonomy branch for Case Study realization 1

For each combination of the 10 case study realizations, 20 exposure rates and 40 known asset samples (8000 iterations in total), a recalculation of losses was carried out using the specific curves determined for the known portions of the assets. The taxonomy-based curves were then applied to the unknown assets, leading to a new estimate of the total direct AAL for the entire portfolio that can be compared to the baseline calculation for each case study realization. Results obtained for the inaccuracy in calculation with each exposure rate evaluated are shown in Figure 4.7. It can be seen that, as expected, the uncertainty in the calculation of total direct collapse AAL for the entire portfolio reduces as the proportion of assets with full information increases. Furthermore, the uncertainty associated with ±2 standard deviations has a highly nonlinear trends up to an exposure rate of about 30%, after which the reduction becomes almost linear. As such, the 30% threshold seems to be a good threshold for the minimum amount of assets within a portfolio that should be analysed when using taxonomy-based fragility curves, since obtaining more complete exposure information above this point leads to a much lower increase in accuracy in the overall results. In addition to the uncertainty estimates, median values of prediction, calculated using taxonomy-based curves, are consistently close to the baseline results calculated with individual curves specific to each asset. This is in line with findings made in previous studies (Abarca, Monteiro, O'Reilly, Zuccolo, & Borzi, 2021) and further demonstrates that the use of taxonomy-based curves can lead to accurate mean estimates of the total direct losses for the entire portfolio.

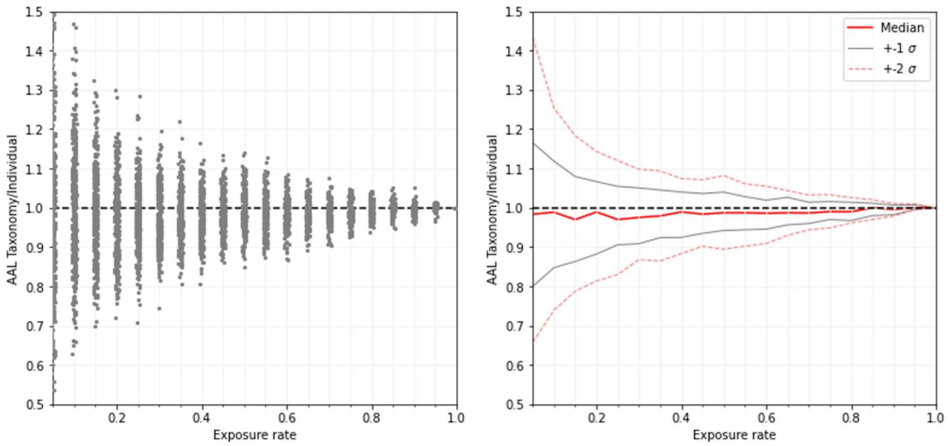

(a) (b)

Figure 4.7. Results of total inventory direct AAL Taxonomy over Individual based on different exposure knowledge percentages: a) results for each iteration, b) statistical trends observed in results.

4.4.2.2 *Machine Learning Model*

A supervised machine learning model was evaluated in terms of its capacity to reduce the uncertainty in calculations deriving from the lack of exposure data to assess individual structures in a portfolio. The objective of this evaluation was to predict the fragility curves of assets with unknown information within the same sets of taxonomy branches by using simple structural geometrical parameters. These parameters differentiate each asset within the class and are used to predict a suitable fragility curve for each bridge, using the results from the portion of the inventory with full information. This contrasts with the taxonomy-based approach that uses the same mean fragility curve for all the unknown assets within the taxonomy branch, regardless of the variations between geometric characteristics of elements within the same class that could also influence their structural performance.

For this purpose, a machine learning model is built for each taxonomy branch and trained using the database of NLTHA results of assets with full information to predict the probability of exceeding the collapse limit state given simple bridge geometrical parameters and an IM level. These models are then used for each bridge with incomplete information to predict their probability of exceedance of the limit state at discrete points of IML, after which a continuous fragility curve is fitted and assigned to each corresponding bridge.

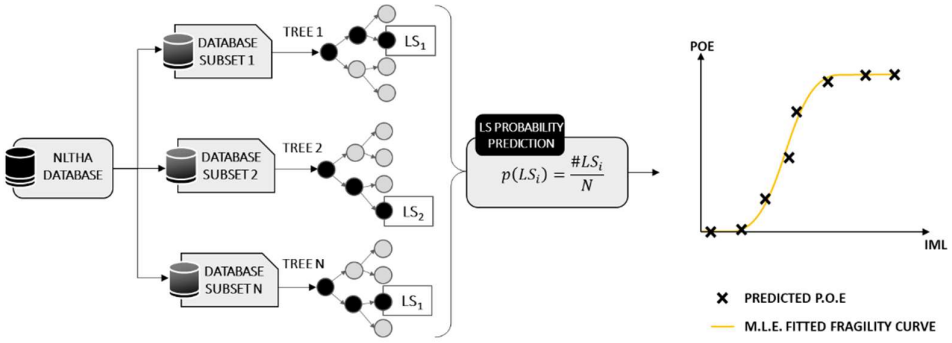

Figure 4.8. Schematic representation of random forest algorithm prediction methodology

A Random Forest Classification Model was chosen given its good performance when compared to other machine learning algorithms for similar endeavours recently demonstrated by (Mangalathu, Hwang, Choi, & Jeon, 2019). This type of algorithm uses a collection of decision trees built with bootstrapped subsets of the NLTHA database. Each tree is fitted to provide predictions of the occurrence of collapse based on its sub-sample and all predictions provided by each tree are later weighted to determine the probability of exceedance of the collapse limit state, as depicted graphically in Figure 4.8. This type of model, as with most supervised machine learning models, uses a labelled dataset that has both its independent variables (inputs) and its outcomes. Moreover, it progressively calibrates its own numerical properties to produce an inferred function that makes predictions about the output values.

The same combinations between case study realizations, exposure rates and known asset samples used for the taxonomy-based approach were analysed. The NLTHA results of the known portions of the inventories were used to train the random forest models and their prediction results were employed to determine the fragility curves of the assets with incomplete information. Subsequently, an estimate of the total direct AAL for the entire portfolio was computed and compared to the baseline calculation for each case-study realization, as done previously for the taxonomy-based approach.

For each iteration and each model, a database was assembled using the results for each bridge that was sampled as having complete information. The occurrence of collapse as a binary operator (i.e., 1: Collapse, 0: Non-collapse) representing the dependent variable (target) and a vector of independent variables (or features) was retrieved for each ground motion result obtained during the NLTHA process. A set of six features were used: number of spans, total length, average span length, maximum pier height, deck width and the IM level of each ground motion record. Given that these variables, to be processed by the

Random Forest algorithm, have different units and orders of magnitude, each was modified using a minimum-maximum scaling process that transforms the data of each feature by scaling the values within the 0 and 1 range.

In terms of the properties assigned to the Random Forest algorithm, a different model is created for each of the nine taxonomy branches at each of the performed 8000 iterations and determining and implementing optimal parameters for each model would be unpractical. As such, the same settings shown in Table 4.2 were used for all models; these values were determined by averaging the optimised settings for a discrete set of tests performed during a calibration stage.

Table 4.2. Main parameters selected for the Random Forest Algorithm's implementation

Parameter	Value
Number of estimators	20
Maximum Tree Depth	12
Maximum Features	$\sqrt{\#\ features}$
Minimum Leaf Samples	2
Minimum Split Samples	2

The resulting performance of the models changes depending on the exposure rate: the lack of data present when evaluating lower exposure rates leads to a very low accuracy in the prediction of the probability of occurrence of collapse, which reflects on the definition of the fragility curves for the unknown assets. In turn, as higher rates are evaluated the performance improves. As an intermediate example, the performance of a single model, evaluated on the assets with incomplete information and created for the RC-SC-9to36 taxonomy branch, using an exposure rate of 50%, is shown in Table 4.3 and Figure 4.9.

Table 4.3. Example performance of Random Forest model iteration on Case Study realization 1, Exposure rate = 0.5, RC-SC-9to36 taxonomy branch

Classification Confusion Matrix

	NC	C	Recall
NC	4459	389	0.92
C	671	1831	0.73
Precision	0.87	0.82	**0.86**

Prediction of Probability of Collapse

Root-mean-squared error (RMSD)	0.151
Mean absolute error (MAE)	0.078
Median absolute error (MedAE)	0.021
Coefficient of determination (R2)	0.829

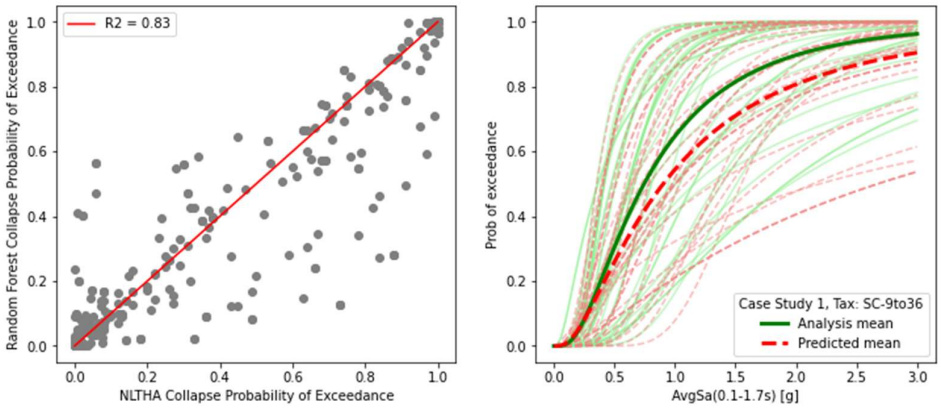

(a) (b)

Figure 4.9. Example performance of Random Forest model iteration on Case Study realization 1, Exposure rate = 0.5, RC-SC-9to36 taxonomy branch: a) Prediction of collapse probability of exceedance for unknown bridges, b) Collapse fragility curves fitted from probability predictions.

The confusion matrix for the classification of the intermediate example is also presented in Table 4.3. It consists of a table that records the number of correct and incorrect predictions given by an algorithm, and can be used to evaluate the performance of the model to predict the occurrence of collapse. In this table, the predicted results (organized in columns) are correlated with the actual assignments (organized in rows), while the resulting diagonal elements represent the limit state assignments that were correctly predicted by the model. It can be seen that the accuracy of the model, calculated as the ratio of the assignments that are correctly predicted to the total data, is 86%. This is rather good performance and is in line with similar previous research exercises (Mangalathu, Hwang, Choi, & Jeon, 2019). A reduction in performance is observed in terms of the prediction of the probability of occurrence of the collapse limit state, as demonstrated by the metrics provided in Table 4.3 and Figure 4.9 (a). In fact, it can be seen that, while the typical magnitude of the prediction inaccuracy (described through the mean absolute error) is relatively low at 8%, the performance does not seem to be uniform across the possible range of exceedance probabilities with intermediate values showing larger residuals with a trend towards underprediction.

Using the predictions of probability of exceedance to determine the fragility curves of the assets with unknown information in the intermediate example gives the results shown in Figure 4.9 (b). It can be seen that the predicted curves have a similar distribution as the calculated curves for the same bridges, with a slight tendency to underestimate the 'real'

fragility of the assets, which is in line with the underprediction of probability of exceedance mentioned previously.

Overall, the processing of direct collapse AAL for the entire case study over each iteration leads to the results shown in Figure 4.10. In this case, as with the taxonomy-based approach, the uncertainty in the calculation of total AAL, with respect to the benchmark, decreases as the inclusion of more assets with complete information increases. While a behaviour similar to the taxonomy-based results is observed, i.e. an initial nonlinear reduction of uncertainty can be seen for lower levels of exposure knowledge, the shift to a linear trend for the ±2 standard deviations occurs at an exposure rate of 50%, after which the results seem to have a much lower increase in accuracy. This behaviour is attributed to the attainment of sufficient data in the pool of assets with known information starting at the 50% exposure rate mark, which allows the adequate training of the machine learning models to predict probabilities of collapse. It is important to note that the same trend is found for the taxonomy-based curves at a 30% exposure rate, which is a significant difference in the amount of information required to obtain a substantial reduction in uncertainty. This leads to the preliminary conclusion that taxonomy-based approaches have an advantage over machine learning models to assess total direct losses in portfolios with limited information and the latter should only be considered when significant portions of the inventory have complete information.

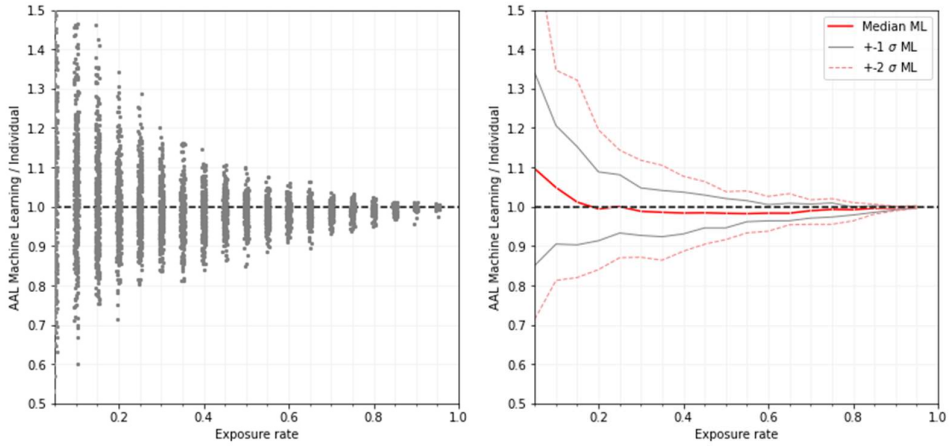

Figure 4.10. Results of total inventory direct AAL Machine Learning over Individual based on different exposure knowledge percentages: a) results for each iteration, b) statistical trends observed in results.

4.4.2.3 *Result Comparison*

A comparison between the statistical trends observed in the uncertainty of the calculation of total collapse-based direct AAL using the taxonomy-based approach and the machine learning models is presented in Figure 4.11 in terms of normalized difference with the benchmark instead of ratios. It can be seen that median values are generally stable when using taxonomy-based curves, even for low exposure rates, while the use of the machine learning models tends to overpredict median losses below the 15% exposure rate mark. Furthermore, even though similar trends are observed using both methods, the machine learning models definitively outperform the taxonomy-based curves only after achieving an exposure rate of 40%, a point where both methods display an accuracy of approximately ±10% for the ±2 standard deviations in uncertainty. It is important to note that, while this improved comparative performance of machine learning models at the 40% mark is apparent from the results, the behaviour of the uncertainty for ±2 standard deviations is still nonlinear at this point, changing to a linear trend until the 50% exposure rate as mentioned previously. This means that, while it does perform better than the taxonomy-based case, there is still a significant reduction in uncertainty by increasing the exposure knowledge from 40% to 50% for the machine learning case. All of this strengthens the conclusion that for cases where low rates of exposure knowledge are present in the inventory, the use of taxonomy-based curves should be preferred to the use of machine learning models.

It is important to note that the machine learning results were obtained using the same model settings for every iteration, independently from taxonomy branch and exposure rate. This represents a limitation in the interpretation of the results since a calibration process for each model would be done in a real case study, which would probably improve the accuracy of the results, making these models potentially more recommendable at lower exposure rates. However, it is also important to mention that the use of machine learning models requires greater expertise and computational resources to build, calibrate, interpret and deploy the algorithms, when compared to the use of taxonomy-based curves. Consequently, analysts should consider the increased effort together with the slight decrease in uncertainty before deciding on a methodology, depending on the available information.

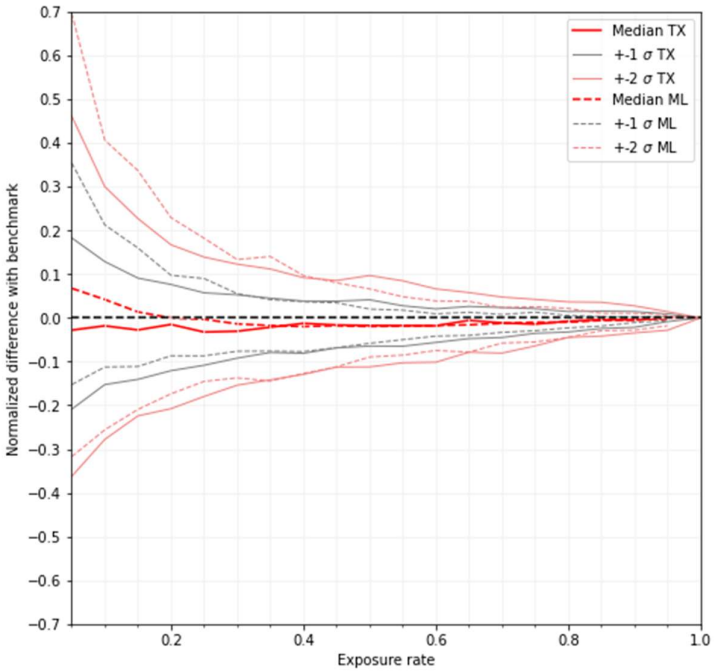

Figure 4.11. Comparison of results of total inventory direct AAL using a traditional taxonomy-based approach and machine learning models for different exposure knowledge percentages

In general, for both cases, the presence of a nonlinear behaviour in the reduction of uncertainty in ±2 standard deviations when low exposure rates are considered can be used as a decision variable to determine the amount of assets in an inventory that should be analysed. For example, when dealing with the seismic risk assessment of bridge inventories with only 10% of assets with full knowledge, the cost of increasing the knowledge of the inventory to 20% could perhaps be justified knowing that, according to the results obtained, this would result in a significant reduction in uncertainty (from ±30% to ±20% using taxonomy-based curves). On the other hand, if 50% of the inventory would have complete information, the same additional cost that would be incurred to increase this value to 60% would only lead to a reduction in uncertainty from ±10% to ±8%, when using the same approach.

4.5 SUMMARY AND CONCLUSIONS

In this chapter, the database of 308 bridges with complete structural information was used to generate 10 realizations with different configurations of the case study presented in Section 2.1.4, by randomly assigning an asset from the database to each of the 617 locations of bridges in the primary and secondary road networks of the province of Salerno, Italy. The seismic risk level of these case studies, in terms of the total direct average annual losses (AAL) associated to the collapse limit state, was assessed. These results were then used as a benchmark metric to test the implementation of popular and innovative methods in assessing regional bridge portfolios with limited information. For this purpose, the uncertainty that can be expected when considering different percentages of knowledge levels using a taxonomy-based approach as well as a machine learning model was estimated and analysed. Furthermore, the exploration of these results led to the characterization of the trends that can be expected in uncertainty depending on different rates of exposure knowledge, as well as the definition of useful exposure rate thresholds to be used in practical applications to define the amount if exposure information required to obtain a desired level of accuracy in direct loss results.

Based on the results obtained by the application of the different approaches, the following conclusions can be made regarding the epistemic uncertainty that is introduced to regional seismic assessment of bridge portfolios by partial exposure knowledge:

- The use of taxonomy-based curves that average fragility results of assets with similar configurations can lead to accurate median estimates of the aggregate losses over an entire portfolio. This was demonstrated by the results, which show how the median estimates of AAL are consistently close to the benchmark results calculated using structure specific curves, independently from the exposure rate considered;
- When considering the use of taxonomy-based curves, based on the results of this case-study, a complete knowledge of a minimum of 30% of the inventory is recommended to avoid the large uncertainty associated with lower exposure rates. The same effect was observed when using machine learning models, however the significant reduction in uncertainty happens after 50% of the inventory is known in this case. Furthermore, the same results showed that, when the known portions of the inventory are larger than these thresholds, incurring in expensive surveying campaigns to increase exposure knowledge becomes less attractive, since it will lead to a lower decrease of uncertainty;
- The use of machine learning algorithms to predict the fragility curves of bridges with incomplete information can outperform typical taxonomy-based approaches only when sufficient results from assets with full information are available to properly train the models. For the case studies explored here, a 40% exposure rate

was found to be the minimum at which the use of machine learning becomes comparatively attractive. However, the results from both approaches are similar and practitioners should consider the added complexity and computer power required to use these models when seeking for an (often slight) increase in performance.

5. VULNERABILITY: SIMPLIFIED INDIRECT LOSS ASSESSMENT

5.1 INTRODUCTION

Road transportation networks are a major contributor to the economic development of modern society and play an important role in the everyday life of its users. Whether they are used for transportation of goods, daily commutes of people, or accessibility of emergency services following a disaster, the importance of their proper functionality is undeniable. Modern and developed countries tend to have very dense and robust transportation networks that can include hundreds of thousands of kilometres of roads, typically built over several decades (Pinto & Franchin, 2010) (Calvi, et al., 2019). Along with these roads, there is a large amount of supporting infrastructure, such as bridges and viaducts, whose structural integrity is susceptible to natural hazards or general ageing and deterioration. Recent bridge collapses in Italy have demonstrated the large impact that these interruptions can have on the functionality of the surrounding road network for extended periods of time. The collapse of the Polcevera (Morandi) bridge, for example, caused indirect losses of €359,1 million in the immediate wake of the collapse, with estimated annual losses to the Italian economy in the vicinity of one trillion euros (Camera di Commercio di Genova, 2018). This has increased public interest in these structures and have thus placed pressure on governments and bridge management agencies to assess and identify vulnerable elements in the network, quantify their fragility to multiple hazards, and determine their respective impact on the overall system. Recent notable efforts led the Italian Superior Council of Public Works, within the Ministry of Infrastructure and Transport (MIT), to issue a technical report with guidelines on risk classification and management, safety assessment and monitoring of existing bridges (Consiglio Superiore dei Lavori Publici, 2020). These guidelines have already become part of the mandatory legislation for bridge management institutions and concessionaries in Italy (Ministero delle Intrastrutture e dei Trasporti , 2020).

While the probabilistic assessment of a bridge collapse under seismic hazard has been object of research in many past studies (Lupoi, Franchin, & Schotanus, 2003) (Borzi, et al., 2015), the direct consequences related to the economic cost of repairing or replacing the structure are usually focused on. The indirect component of loss, which addresses the economic impact incurred when there is a disruption in the road network, remains a less-explored field for researchers and practitioners. Indirect losses have the particularity of being very distributed over a large number of users throughout extended periods of time

and many decisions that influence the duration of the interruption are often political and not technical in nature. Also, transportation modelling requires some degree of technical expertise and a large amount of information on both the characteristics of the network and the travel demands of the users, which are not always readily available.

Different quantitative approaches have been considered in past research to calculate the effects of infrastructure vulnerability on the performance of transportation systems. Earlier studies aimed to quantify a variety of metrics that can provide insights to the consequences of infrastructure disruption, such as accounting for the loss of connectivity between origin and destination pairs (Dueñas-Osorio, Craig, & Goodno, 2007), the increase in travel distance (Chang, Shinozuka, & Moore, 2000) or travel delays after the occurrence of disastrous events (Kiremidjian, et al., 2007); these methodologies, however, do not directly account for economic losses. More refined approaches have been proposed, performing a large number of event simulations (Shinozuka, Murachi, Dong, Zhou, & Orlikowski, 2003) (Kilanitis & Sextos, 2018). They account for economic losses in a probabilistic fashion by exploring the effects of events on a transportation network model, even providing estimates of the evolution of the recovery process in time. More recent studies, such as the one performed by Miller and Baker (2016), go into great detail by accounting for post-disaster changes in travelling demands and evaluating consequences using activity-based travel models. This permits an analysis that goes beyond economic losses alone, but also the identification of geographic and demographic groups that may be disproportionately affected by certain events. Some more recent efforts (Gehl, Cavalieri, & Franchin, 2018) evaluate the use of approximate Bayesian networks, trained on results from earthquake simulations influencing an infrastructure system, to predict system performance metrics that can include indirect losses. These studies have the disadvantage of being hazard-specific and requiring a great amount of input data and computational power, which limits their wider applicability to other case studies.

With the above challenges and gaps in mind, this chapter presents a methodology to calculate the economic impact of interruptions induced in a road network due to the collapse of individual bridges, as well as a simplified alternative to identify the relative importance of the different bridges in a road network portfolio, based on the indirect losses associated to the collapse of each structure. Both alternatives are hazard independent and useful for prioritization purposes since, as it will be detailed in the following sections, they only evaluate a partial account of the consequences of disruption in the road network on a bridge-by-bridge level. Furthermore, even if the simplified alternative does require the use of a transportation network model, it is straightforward and less resource demanding than other currently available methodologies.

5.2 METHODOLOGY

The procedure used in this chapter to evaluate the proposed indirect loss quantification methodology and its simplified alternative, consists of initially creating the transportation network model for the case-study region (i.e., case study 2 located in the province of Salerno, Italy). As can be seen in Figure 5.1, two models were considered herein: a refined one, for the detailed methodology, which considers travel demand data and appropriate road modelling parameters to account for congestion in the network; and a less detailed version of the same model, for the simplified alternative, which relies only on information obtained from a common open-source database (OpenStreetMap contributors, 2020) layer data.

For the detailed methodology, the calculation of the economic impact of bridge interruptions was made using the refined network model to distribute the travel demands in the system. These results were then used to calculate the operation cost of the network's use, combining nominal costs for automobile travel with the aggregated results of time spent and distance travelled daily by the users. This exercise was carried out considering the network in its baseline condition (i.e., when all bridges are operational) and was repeated afterwards by removing each bridge at a time from the model, in order to determine the increased daily operation costs associated with the disruption caused by the absence of each bridge. The total indirect loss associated with each bridge was obtained by multiplying the obtained operation costs by an estimate for the median repair time of bridges in Italy.

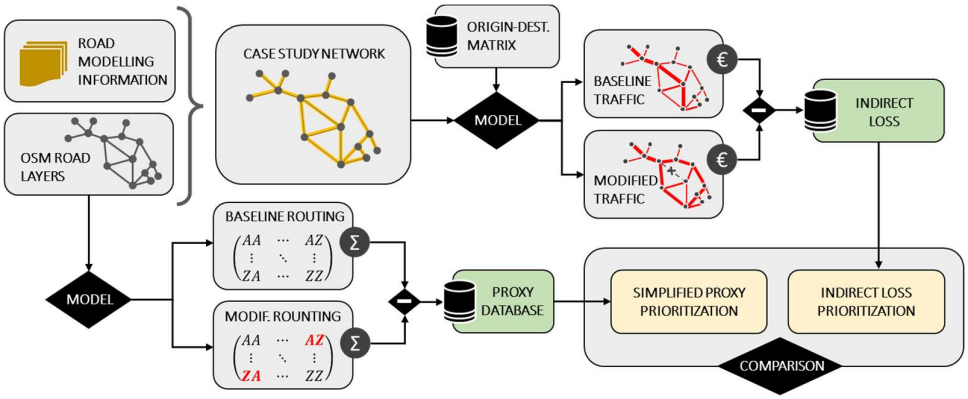

Figure 5.1. Methodology used to define a framework to estimate indirect losses and a simplified proxy-based alternative

On the other hand, the simplified version of the network model was used to obtain a travel time impedance matrix of the system, a common product used in transportation engineering that records the roundtrip duration between all possible origin and destination pairs (Tian, Chiu, Sun, & Chai, 2020). As with the refined model, this exercise was

performed for the baseline conditions of the network, as well as when each bridge was removed from the model. The sum of all indices of the matrix, indicative of the time it would take a single user to travel to and from each point of the network, was then used as a metric for each case. Finally, the increase of this sum with respect to the baseline condition was defined as a proxy of the relative importance of each bridge in the network in terms of the disruption it causes on the network. Both the detailed methodology and the simplified alternative were applied to the 617 bridges located in the highway, primary and secondary road network within the case-study province of Salerno. The results for indirect economic losses calculated using the detailed methodology were used to define the priority of each bridge in the case study, which was then used as a benchmark to evaluate the priorities obtained using the simplified proxy-based alternative.

5.3 ROAD NETWORK MODELLING

Information about the road network of Salerno was taken from the OpenStreetMap database (OpenStreetMap contributors, 2020), which comprises all roads within the highway, primary and secondary systems, including 2929 nodes and 3086 links, of which 617 represent either bridges, viaducts or overpasses (referred to herein as bridges for simplicity). The geometric centres of the 158 municipalities in the Salerno province were used as traffic attraction zones (centroids) from which all trips were assumed to originate and conclude. A graphical representation of the network is shown in Figure 5.2.

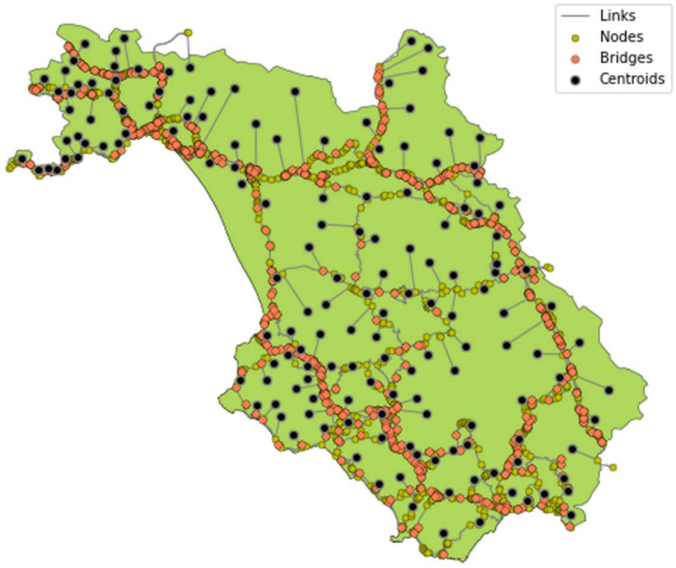

Figure 5.2. Salerno road network built from OpenStreetMap layers

A transportation network model was created using the software AequilibraE (www.aequilibrae.com), an open-source Python and QGIS package to perform transportation network analysis. Using this, the baseline traffic conditions were determined and the importance of each bridge in the network was assessed. This model is based on Static Traffic Assignment (STA), which is a simple and widely-used assignment method to determine traffic distribution on road networks (Saw, Katti, & Joshi, 2014). The accuracy of this type of model is generally perceived as insufficient in congested networks and the focus of research within the transportation field is shifting towards more refined modelling methods (Brederode, Pel, Wismans, Romph, & Hoogendoorn, 2019). Nevertheless, STA was chosen herein since it is still the preferred tool for strategic transportation planning due to its simplicity and efficiency (Saw, Katti, & Joshi, 2014). Aside from the geometric configuration of links, nodes and centroids presented in Figure 5.2, the following elements were also considered to accurately build a numerical model of the network that can generate predictions on the traffic conditions of the case-study region:

- Traffic demand information regarding the travel patterns of the users of the network between centroids;
- Information about the properties of each link, including free flow speed, nominal traffic capacity and a relationship between traffic flow and travelling speed to account for congestion.

In terms of traffic demands, a database containing travel pattern information for work and study purposes performed in 2011 was taken from the Italian Institute of Statistics (ISTAT, 2014) and used to define origin-destination demands between the municipalities of Salerno. For the current exercise, only trips performed by private car owners were considered since it represents the major contribution to transportation demands in the area and no information of freight or public transportation was available. A total of 80,562 trips, distributed in four timeframes, were identified within the case study region as shown in Table 5.1 whereas the daily total incoming trips per municipality are shown in Figure 5.3(a).

Table 5.1. Travel demands disaggregated per timeframe taken from census information

Timeframe	Number of trips
< 07:15	26,138
07:15 – 08:14	38,240
08:15 – 09:14	13,380
> 09:15	2,804
Total	80,562

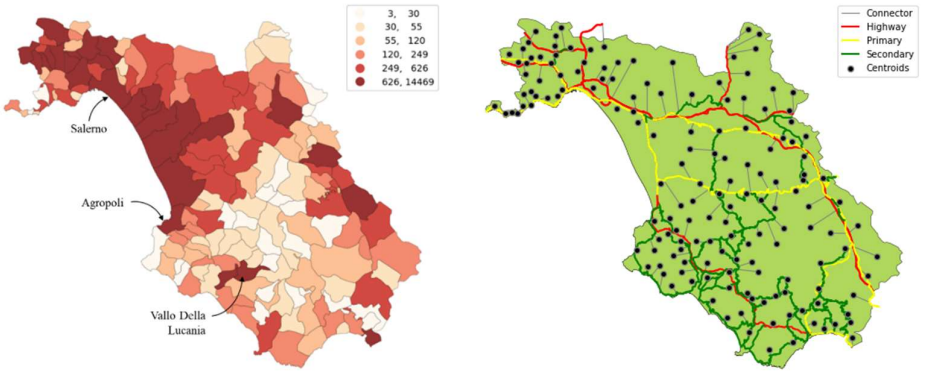

(a) **(b)**

Figure 5.3. Information used to create network model: (a) Daily inbound traffic demands taken from census data, (b) OpenStreetMap road classification.

In terms of link information, all links in the network model were first divided according to their classification (i.e., highway, primary or secondary) in OpenStreetMap as shown in Figure 5.3(b). Subsequently, the volume-delay function modelling parameters were taken from previous research regarding Italian road characteristics (Maratini, 2008), according to the commonly used BPR model (Bureau of Public Roads, 1964) for the different road types defined in the network, as shown in Table 5.2. Free flow speed was taken as the speed limit reported for each road in the OpenStreetMap database. While some studies (Zilske, Neumann, & Nagel, 2011) modify the speed limit values to try to accurately represent the free flow speed according to the case study characteristics, this was not done in this study since no precedent for acceptable modification factors was found in literature for the case study region. Moreover, the implementation of the speed limit provided good results during the validation stage, which will be demonstrated later in this section. It is important to note that detailed traffic modelling can include additional information on the nodes about intersections, such as accounting for stop-lights and turn penalties, to capture the natural delays caused by drivers making steep angle turns. In the current study, these parameters were not included since they are more relevant for the micro-modelling of urban transportation networks rather than a larger regional assessment; while this represents a limitation of the study, it is not expected that their absence will cause a significant impact on a regional model of motorway and primary roads, such as the one being proposed herein.

Table 5.2. Volume-delay function parameters used for road network modelling

Typology	Capacity (vehicles/hour/lane)	BPR Parameters	
		α	β
Highway	1600	0.28	0.93
Primary	1400	0.25	1.13
Secondary	1400	0.25	1.13

A trip distribution based on the minimization of travel time of each user was carried out using a bi-conjugate Frank-Wolfe algorithm (Mitradjieva & Lindberg, 2013) to determine the baseline traffic conditions of the fully operational road network. The results for the distribution in terms of traffic flows for each link, aggregated from each timeframe are shown in Figure 5.4(a). It can be seen that there is a large concentration of traffic flows located in the corridor connecting the Salerno and Vallo della Lucania municipalities, which is in agreement with the travel demands shown previously in Figure 5.3(a). The results in terms of trip duration were compared with the corresponding values reported in the census data to validate the model. As can be seen in Figure 5.4(b), even though the model tends to predict slightly longer travelling times when compared to the census data, overall, there is quite a good general agreement for most of the trips. The mismatch for longer travel times was expected since the model does not include the entirety of roads in the network (i.e., it excludes the local residential road system) therefore increased levels of congestion can occur artificially in the model by having to distribute the totality of the traffic demands in a reduced number of roads.

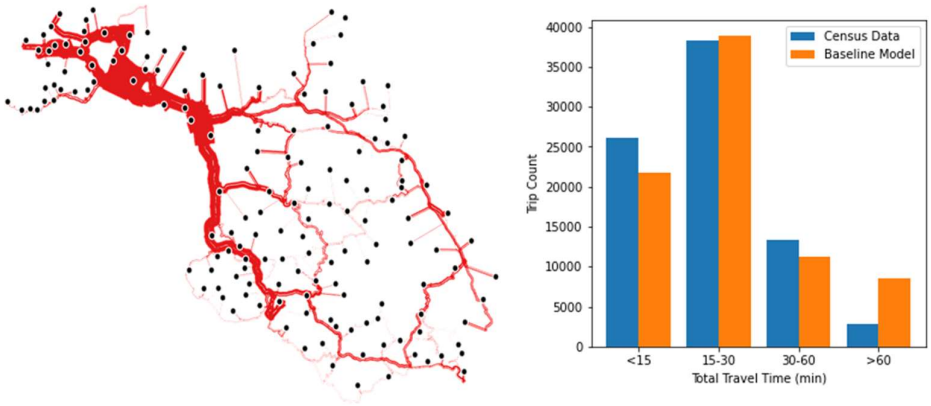

(a) **(b)**

Figure 5.4. Road network model performance: (a) Baseline traffic flows (line thickness is proportional to traffic flow), (b) Trip duration comparison of census data with baseline model results.

5.4 INDIRECT LOSS CALCULATION

5.4.1 Daily Indirect Loss

To determine the benchmark daily indirect loss associated with the collapse of each bridge in the case study, the previously described road network model, used to determine the baseline conditions of the network when all bridges are operational, was employed. Two main metrics were obtained from the model: the vehicle hours travelled (VHT), and the vehicle distance travelled (VDT), corresponding to the total amount of time and distance, respectively, that all the users in the network experience during their travels. Both metrics were then combined with reference costs for typical automobile fuel efficiency and fuel prices in Italy, as well as hourly salary rates appropriate for the Salerno province (ISTAT, 2020), as shown in Table 5.3. This allowed the calculation of a daily operation cost (DOC) of the road network in its current configuration by applying Equation 5.1.

Table 5.3. Values used for calculation of economic cost of bridge interruption

Value	Unit Cost
Car efficiency	0.075 litres / km
Cost of fuel	€1.65 / litre
Average hourly salary (Campania)	€12.9 / hour

$$DOC = F \cdot E \cdot VDT + H \cdot VHT \qquad \text{Equation 5.1}$$

where:

DOC: Daily operation cost
F: Average cost of fuel
E: Automobile fuel efficiency
H: Estimated hourly rate
VDT: vehicle distance travelled
VHT: vehicle hours travelled

Since the travel demand information that was used only included data from morning commutes, both the VDT and VHT values obtained from the trip distribution on the network were doubled to capture the total daily operation cost of the network. This of course assumes the same travel distribution occurs during the returning evening commute for all users, which might be inaccurate but serves as a reference value within the current methodology. Applying Equation 5.1 to the results obtained from the trip distribution of the baseline road network model leads to a Baseline Daily Cost (BDC) of operation for the network of approximately €1.64 million. Subsequently, the road network was modified by assuming the collapse of each bridge in the network, removing the appropriate link in the model and rerunning the daily operation cost with the modified network configuration to determine a Modified Daily Cost (MDC), associated with the collapse of each bridge, as shown in Figure 5.5. A daily interruption cost of each bridge was then calculated as the

difference between the BDC and the appropriate MDC for the bridge in question. Readers are advised to keep in mind that this calculated cost is inherently incomplete, since it does not account for all transportation modes and obviously cannot capture possible losses that the collapse of some bridges would have on local industries, due to increase logistic costs; nonetheless, the calculated costs are proposed herein as reference values of loss for prioritization purposes in a decision-making context.

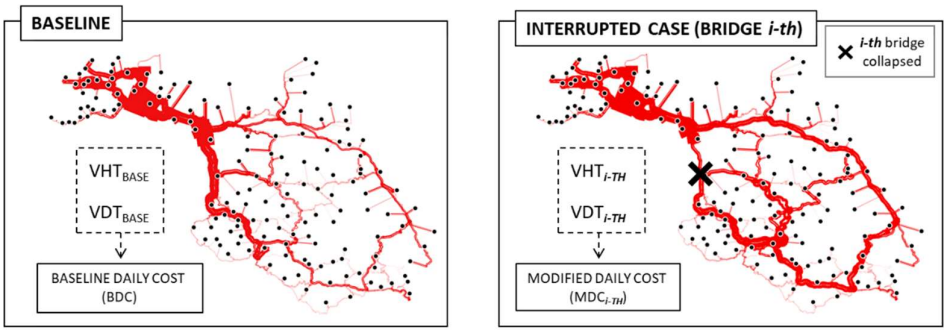

Figure 5.5. Methodology to determine Daily Indirect Loss: (a) Use of baseline traffic conditions to calculate a daily operational cost, (b) Calculation of modified daily operational cost by removing bridge *i-th*

After conducting this for the entire case study, daily interruption cost results for each bridge were obtained and are shown in Figure 5.6. It is important to note that some of the bridges in the case study, identified as essential in Figure 5.6, were located near the borders of the case-study region and did not produce interruption cost results when applying this methodology. This was because their collapse resulted in no alternative paths, causing the complete disconnection of some of the centroids. This represents a limitation of the applied methodology since alternate routes are likely available when considering neighbouring parts of the road network, as well as the residential roads that were intentionally excluded from the network model. To avoid this issue in future research, one could either extend the network model beyond the limits of the case-study regions or account for the costs of cancelled trips; however, since in the context of disaster management this disconnection would also deny access to emergency services, the decision made here was to indicate these assets as essential and focus on the remaining 531 bridges that did produce indirect loss results with the methodology used.

Furthermore, a small number of bridges yielded negative values of interruption cost, which would theoretically mean the users are experiencing a monetary benefit from the collapse of a bridge. This is caused by how the distribution algorithm minimises travel time while

the cost calculation also accounts for distance and some longer duration trips might incur in shorter distances therefore causing the overall cost to be negative for a few cases. This is deemed not to be an important limitation since the calculated negative values are negligible for. For example, the bridge with the highest calculated negative value reports a daily indirect loss of -€144, which is distributed amongst the 80,652 users considered in the network, leading to a trivial monetary value in comparison to the highest positive values calculated.

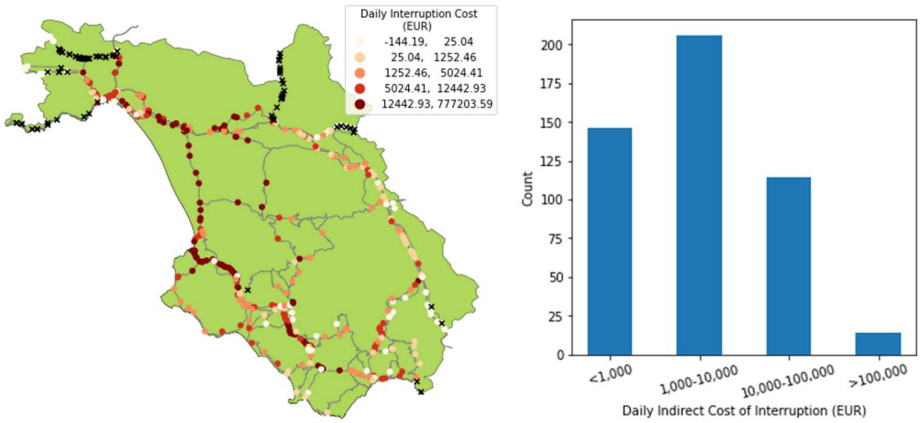

(a) **(b)**

Figure 5.6. Daily indirect cost of bridge interruption: (a) Geographical distribution, (b) Histogram.

5.4.2 Repair Time

In order to consider the total indirect loss associated to the collapse of a bridge, the total amount of disruption time incurred from the day of the collapse until the reopening of the bridge (referred to herein as repair time) needs to be accounted for. In general, the repair time of bridges varies widely from one case to another, driven mainly by economic and political decisions specific to each case. For example, a non-exhaustive list of bridge collapses in Italy since 2004, collected from reports in the media, is presented in Table 5.4. It can be seen that, for instance, the collapsed Lecco bridge in 2016 took 33 months to repair and reopen, while the much larger Morandi bridge that collapsed in 2018 took 24 months to reopen, mainly driven by the widespread media coverage of the collapse and relative importance of both bridges to their respective communities.

Previous research on this matter relied on repair time models, for which a probabilistic time is described by some function specific to each country or region, mainly defined

through expert opinion. Median repair times used in previous research range from 190 days (Shinozuka, Murachi, Dong, Zhou, & Orlikowski, 2003) to 450 days (Kilanitis & Sextos, 2018). In this study, the data from the 10 recent collapses in Italy shown in Table 5.4 was used to fit the lognormal distribution illustrated in Figure 5.7.

Table 5.4. Bridge collapses reported in Italy since 2004

#	Region	Province	Bridge Name/Location	Length (m)	Collapse Date	Re-opening Date
1	Friuli	Pordenone	Viadotto del Chiavalir	25.00	Dec-04	Jul-09
2	Liguria	Genova	Carasco	258.00	Oct-13	Apr-14
3	Sardinia	Nuoro	Oliena-Dorgali	130.00	Nov-13	Jan-20
4	Sicily	Agrigento	Lauricella-Petrulla	476.00	Jul-14	Mar-18
5	Lombardy	Lecco	Annone	56.00	Oct-16	Jul-19
6	Marche	Ancona	Ancona	45.00	Mar-17	Jun-18
7	Liguria	Genova	Viadotto Polcevera	1182.00	Aug-18	Aug-20
8	Liguria	Savona	Madonna del Monte	30.00	Nov-19	Feb-20
9	Toscana	Massa-Carrara	Albiano Magra	290.00	Apr-20	Mar-22
10	Piedmont	Novara	Romagnano Sesia	156.00	Oct-20	Aug-21

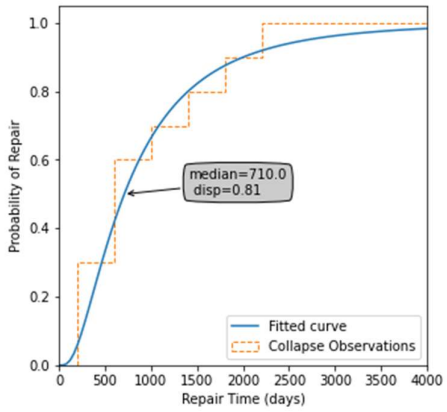

Figure 5.7. Cumulative histogram and log-normal fit for repair time observations based on recent collapses in Italy

It is important to note that the median value of 710 days obtained from the lognormal fitting shown in Figure 5.7 is much larger than the values used in previous research for other countries, however, the latter values were not based on collapse observations but on expert opinion, and their sources underline the limitations of their definitions (Shinozuka,

Murachi, Dong, Zhou, & Orlikowski, 2003). Furthermore, there seems to be a great discrepancy between observed repair times of Italian bridges, ranging from 3 to 75 months for an asset to be reopened after an unexpected collapse. This will obviously have a directly proportional impact on the total indirect loss of a collapsed bridge therefore bridge management agencies should have systems in place to reduce the repair time of assets with high daily disruption costs.

5.4.3 Total Indirect Loss Results

No evident indication of what repair time from the distribution shown in Figure 5.7 can be used for each bridge, hence the median value of 710 days obtained from the lognormal fitting was used as a fixed value for all elements in the case study. Applying this multiplier to the daily indirect loss results that were previously obtained enabled the quantification of to the median total indirect loss for each bridge in the case study, as shown in Figure 5.8. It is important to note that, instead of using a fixed value of repair time for all the bridges, an extensive sampling scheme could have been adopted by taking different random samples from the distribution shown in Figure 5.7 for each bridge in the case study and recording the total indirect loss results for the entire inventory repeatedly. However, since this parameter would be the only being modified during the sampling and its effect is linear on the total indirect loss calculation, the sampling exercise would ultimately result in a total indirect loss distribution for the entire inventory with the same distribution as the one for the repair time, with median results equal to the ones reported herein.

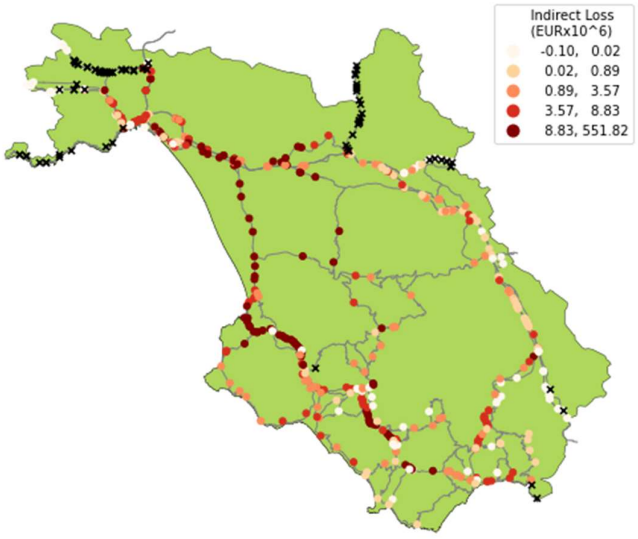

Figure 5.8. Results for median total indirect loss on the case-study network

The results indicate a median value of total indirect loss of €1.37 million, with 85% of the bridges in the inventory presenting values under €10 million, but with some bridges having very high disruption costs reaching values of €551.82 million. The geographical distribution of the indirect losses seems to closely follow the concentration of traffic flows determined for the baseline condition shown in Figure 5.4(a). That is, the bridges with highest losses are located in the corridor connecting the Salerno and Vallo della Lucania municipalities. Moreover, the calculated losses are not necessarily concentrated on highway or primary roads and seem to be greatly influenced by the absence of nearby alternate routes. This confirms that the potential indirect loss associated with the collapse of a bridge is mainly dictated by the baseline traffic demands and redundancy of the network, independently of the road typology where the bridges are located.

5.5 SIMPLIFIED METHODOLOGY PROPOSAL

Given the complexity and amount of information that is required to perform the detailed quantification of economic indirect losses derived from the disruption of a bridge in the transportation network, a simplified approach, aimed towards decision-making purposes, is explored in this section to approximately match the relative importance of bridges in an inventory in terms of indirect loss, estimated as per the methodology presented in the previous section. This simplified methodology is based on the concept of travel impedance matrices, also referred to as network cost skims, which are a widely-used concept within the transportation planning field (Tian, Chiu, Sun, & Chai, 2020). An impedance matrix reflects the inter-zonal travel costs in terms of time, distance or custom cost functions that can be expected in a network. For the simplified methodology defined in the current study, a network skim based on travel time is used to describe the time that a single user would incur to travel each possible combination of centroids as points of departure and arrival in the uncongested network.

For example, an illustrative network with three centroids, along with its respective travel time impedance matrix, is shown in Figure 5.9(a). In this case, each value in the matrix would represent the minimum time that a user would take to travel each combination of centroids. All diagonal elements in the matrix are zero values since intrazonal trips are not considered. Furthermore, the matrix is not symmetrical given that directionality is accounted for, meaning that the route and time required to travel from A to B (AB in the matrix) could be different than its reciprocal travel from B to A (BA in the matrix), depending on the network characteristics. The sum of all the values of the impedance matrix, defined herein as Baseline Vehicle Hours Travelled (BVHT), is used as a metric to evaluate the base conditions of the network when all bridges are operational. Furthermore, the exercise of deriving the skim matrix on the network when a specific bridge has been removed from the model and summing all values to define a Modified Vehicle Hours Travelled (MVHT) can be carried out to evaluate the impact that the absence of that

specific bridge will have on the network in comparison to the baseline conditions. An example is shown in Figure 5.9(b) where the removal of bridge ***i*** leads to increase the impedance of trips between zones B and C.

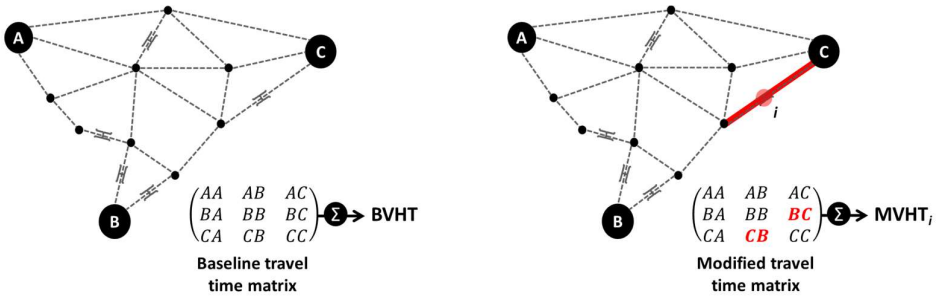

Figure 5.9. Definition of proxy value in illustrative network: (a) Determination of baseline travel time with fully functional network, (b) Modified travel times by removing individual bridge

After repeating the exercise of removing each bridge in the network and calculating its respective time skim, the algebraic difference between the MVHT of each bridge and the BVHT was defined as a proxy value, as shown in Equation 5.2, which can be used to comparatively evaluate the relative importance of each asset in terms of potential interruption time of the overall network:

$$Proxy_i = MVHT_i - BVHT \qquad \text{Equation 5.2}$$

where BVHT is the sum of all values from travel time skim matrix of the fully operational road network; and $MVHT_i$ is the sum of all values from travel time skim matrix of the road network after removing bridge *i* from the model.

The main advantage of this simplified methodology is that it requires only basic information from the road network that is typically found in open-source repositories with near worldwide coverage, such as OpenStreetMap (OpenStreetMap contributors, 2020). Information regarding link properties, used to account for congestion, as well as travel demands between zones, are not necessary since there is no traffic distribution involved, which represents a great benefit, as this information is typically unavailable, incomplete or outdated. Moreover, the determination of the impedance matrices is usually a common output, available in most traffic modelling platforms, whose calculation does not require great computational effort.

5.6 CASE STUDY EVALUATION

As described in the methodology adopted for this chapter, the proposed simplified alternative methodology was applied to the case study network in order to compare its performance with the benchmark detailed methodology calculation of indirect losses performed with the detailed methodology. The impedance matrix that represents the travel time of all possible trip combinations between each of the 158 municipalities in the case study was calculated using base conditions of the network, i.e., when all bridges are operational, and then repeated 617 times after removing each bridge in the network, as described previously. For each case, the sum of all values in the impedance matrix was used as a metric that was subtracted from the baseline case to define the proxy value. The results obtained for each bridge are shown in Figure 5.10.

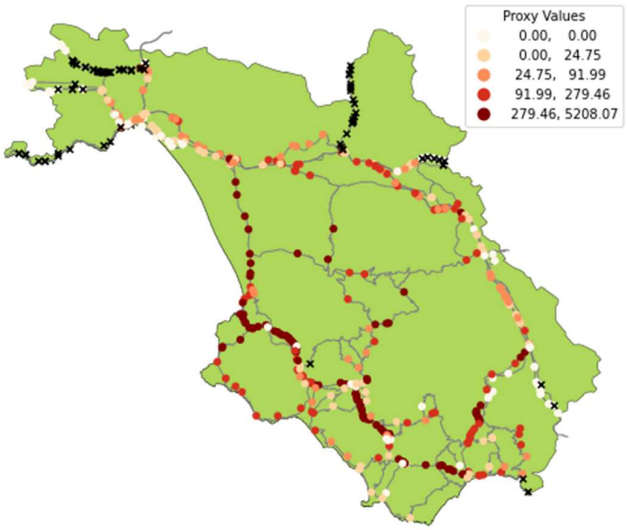

Figure 5.10. Proxy results obtained on the case study application

It can be seen that, qualitatively, the spatial distribution of bridges with higher relative proxy values is similar to the one found by the determination of indirect losses shown previously in Figure 5.8, where the higher costs of interruption are located in the Western central portion of the case study, near the coast of Salerno. Furthermore, since the same interconnectivity between network nodes is present in all models, the simplified approach also captures the effect of bridges whose collapse results in the complete disconnection of some centroids, therefore being classified as essential.

In order to quantify the comparative performance of the simplified methodology, given that the proxy values and the indirect losses cannot be directly compared with each other, for being inherently different, the comparison was made in terms of the priority that is derived by ranking the bridges based on each parameter (higher loss and proxy value). Bridges classified as essential were placed in the first positions even though they have no associated numerical results for either parameter. However, their collapse results in the complete disconnection of centroids and this was given priority. The difference in the ranking positions obtained with the detailed methodology minus the ranking obtained from the simplified methodology is shown in Figure 5.11(a). Negative and positive values in this plot represent under and over prediction in priority, respectively, of the simplified alternative, when compared to the detailed methodology. It can be seen that, while the priority rank of some assets can be severely mispredicted by the simplified methodology, the bridges located in the in the corridor connecting the Salerno and Vallo della Lucania municipalities, which presented the highest calculated indirect losses, have rank-difference values close to zero, indicating an accurate prediction of their relative importance in the case-study portfolio. Furthermore, typical regression analysis of both rankings is shown in Figure 5.11(b), while the corresponding performance metrics are presented in Table 5.5. Performance metrics for comparison between indirect losses and proxy ranking on the case study, which were calculated by treating the simplified ranking as a regression of the benchmark ranking. It can be seen that using the proxy values to determine the priority of assets and comparing it to the one defined by the indirect loss results leads to encouraging results, producing a median absolute error of 50 positions, which represent roughly 8% of the total number of assets in the case study.

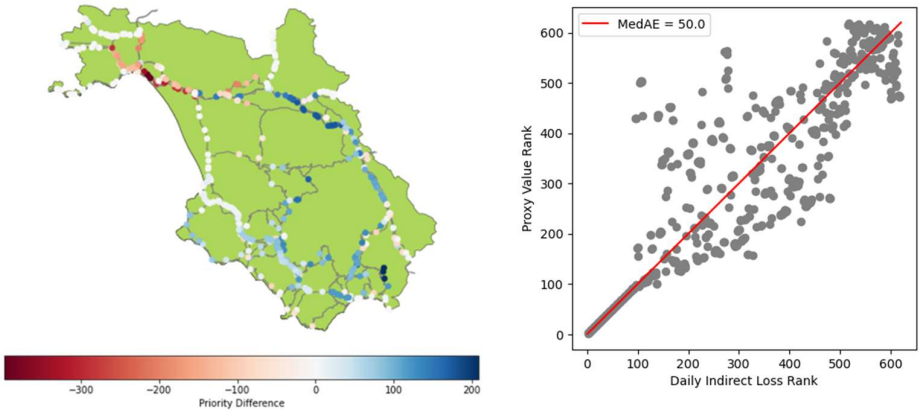

(a) **(b)**

Figure 5.11. Comparison of indirect loss and proxy-based ranking: (a) Prioritization rank difference (i.e. Indirect Loss-based rank – Proxy-based rank), (b) Comparison of priorities using both methodologies.

Table 5.5. Performance metrics for comparison between indirect losses and proxy ranking on the case study

Parameter	Value
Root-mean-squared error (RMSD)	100.1
Mean absolute error (MAE)	68.7
Median absolute error (MedAE)	50.0
Coefficient of determination (R2)	0.684

Differences between the definition of bridge ranking can be partly attributed to the fact that, when using the detailed methodology to calculate indirect losses, bridges in corridors connecting municipalities with high traffic demands will naturally incur in higher disruption costs and will be therefore prioritized. On the other hand, for the case of the simplified alternative calculation of proxy values, all municipalities have equal relative importance, making it impossible to capture this traffic concentration effect that derives from the user demands. Nonetheless, the performance of the simplified alternative methodology in terms of defining disruption prioritization of bridge inventories represents a good compromise between accuracy, complexity and information demands, in line with the objective of providing an approximate prioritization for decision-making purposes.

5.7 SUMMARY AND CONCLUSIONS

In this chapter, a quantitative methodology to calculate bridge indirect losses was outlined and tested over a case-study network comprising 617 bridges in the Italian province of Salerno, which were used to create a road network model using open-source software and travel demand data from census information. Such data was used to determine reference values for the daily operational costs of the network in the baseline conditions and when removing each one of the bridges from the model. Information about the time required to restore a bridge was collected from recent Italian collapses to estimate a reasonable disruption duration and determine the total indirect loss of each bridge. Furthermore, as a simplified alternative methodology, aimed for decision-making purposes, the total delay that a single user would experience after removing each bridge from the model, travelling to and from all possible destinations on the uncongested network was used as a proxy to determine the priority of each asset based on their importance on the road network in terms of indirect losses. Finally, this proxy-based ranking was compared to the ranking obtained using the economic values obtained using the quantitative methodology to determine its performance. Based on the results obtained via the application of the two methodologies defined, the following conclusions can be drawn:

- The calculation of the economic impact of the disruption in a road network caused by the collapse of a bridge is technically challenging and requires a large amount of information about the properties of the network and the travelling demands of its users. However, it is necessary to quantify the relative importance that bridges have in the network in terms of their functionality, a component that should be included in decision-making strategies by bridge management agencies;

- The quantitative methodology presented in this chapter to estimate indirect losses associated with the collapse of each bridge in an inventory has the ability to consistently and efficiently provide reference values of economic loss that can be used to gauge the impact of the disruption on the road network, caused by a bridge collapsing under any hazard. Nonetheless, the methodology is limited, since it excludes portions of the network and only accounts for a single mode of transportation, therefore, prospective users are advised to keep in mind the applicability of the methodology, which is intended for decision-making purposes;

- Information regarding recent collapses in Italy was used to determine a probabilistic function for repair time of Italian bridges that indicates a median replacement duration of 710 days, which is much larger than the values used in past international research. Furthermore, repair times in Italy vary widely, with past collapsed bridges being replaced anywhere between 3 and 75 months, highlighting the large differences in the way different regions manage their inventories. This parameter has a direct impact in the total indirect losses expected and it is important that bridge management agencies implement procedures so that assets with high daily interruption costs can be replaced faster, thus reducing the overall losses;

- The obtained indirect loss results indicate that these losses are governed by the baseline traffic demands and redundancy of the network, since most of the bridges with higher calculated costs were located in corridors between municipalities with high traffic demands and in portions of the network with fewer alternate routes. This is based on the results obtained from the case-study used in this research and future efforts should focus on evaluating the behaviour of indirect losses on different case-studies;

- As far as the alternative simplified methodology is concerned, it does not provide estimates of economic loss, however, it is significantly easier to deploy for large inventories than previously proposed methodologies. Moreover, it produced prioritization results with an accuracy in the range of approximately $\pm 10\%$ (median absolute error of 50 positions in the ranking order for the case study of 617 bridges), when compared to the ranking based on the detailed calculated indirect losses for each asset. This is considered appropriate for preliminary assessment of bridge importance in a decision-making context.

6.RISK MANAGEMENT: PRIORITIZATION SCHEME FRAMEWORK

6.1 INTRODUCTION

The bridge inventory of developed countries can reach thousands of assets that have been built over several decades by different administrations (Calvi, et al., Once upon a Time in Italy: The Tale of the Morandi Bridge, 2019), creating a challenge for the institutions currently managing these large portfolios of bridges for which there is incomplete information about their current structural condition and limited resources available to upgrade or maintain them. In the case of Italy, a great portion of its current infrastructure was built during a construction surge of freeways that happened all over Europe in the 1960s (Calvi, et al., Once upon a Time in Italy: The Tale of the Morandi Bridge, 2019). This coincided with a period in which the design codes of bridges referred to much lighter vehicular loads than the ones recommended for current traffic loading (Iatsko & Nowak, 2021) and the consideration of extreme demands from natural events, such as earthquakes, was still in development. Furthermore, the longevity of the current inventory, aided by the difficulties of management agencies in providing proper maintenance, has led to a generalised problem of deterioration that increases the vulnerability of these structures, a condition that has become evident by the number of bridge collapses in recent years. Recent notable cases in Italy have attracted media attention to this problem, such as the collapse of the Morandi Bridge (Viadotto Polcevera) in Genova in August 2018, but many other collapses have happened in Italy with a non-negligible effect on the road system. For example, in the list of collapses collected from reports in the media presented in Chapter 5 and detailed in Table 5.4, it can be observed that several months or even years can pass for a bridge to be reopened following its full or partial collapse. This considerably interrupts the network for an extended period, also impacting the local and wider community due to the loss of a potentially key element of the overall infrastructure system.

Considering the situation described above, there is a real need for bridge management institutions to determine rapid prioritisation methods that, based on the limited information available about assets in the inventory, allow the identification of the assets requiring special attention in the form of inspection, detailed analysis, monitoring and possible retrofitting. Such prioritisation methodologies have been the source of multiple research efforts worldwide. A summary is available in a recent technical report by the United States Department of Transportation (Chase, Adu-Gyamfi, Aktan, & Minaie, 2016). It documents the evolution and application of different bridge health indices used by bridge

management agencies interested in preserving the condition of bridge structures or prioritising the maintenance or replacement projects within their bridge inventory. Mostly, these methodologies rely on element-level information of each bridge to assess its current state and service level; however, they typically fail to include aspects of resilience and the importance of each asset on the overall network that they form a part of. Recent Italian examples include the simplified index-based methods developed by Pellegrino et al. (2011) and D'Apuzzo et al. (2019), both of which are based on detailed inspection-level information to assess the deterioration status of the bridges and combine it with the importance of each asset to the overall network by incorporating an additional index based on road typology and traffic flows. More recently, the Italian Superior Council of Public Works, within the Ministry of Infrastructure and Transport (MIT), issued a technical report with guidelines on risk classification and management, safety assessment and the monitoring of existing bridges (Consiglio Superiore dei Lavori Publici, 2020), which has already become part of the mandatory legislation for bridge management institutions and concessionaries in Italy (Ministero delle Intrastrutture e dei Trasporti , 2020). This document, which will be referred to from this point forward as the 2020 MIT Guidelines, intends to standardise the procedure with which existing bridges in Italy are assessed at a large scale by a multi-level and multi-component approach that classifies bridges in risk categories via a combination of qualitative metrics.

Among most of the sources that deal with the prioritisation of bridges in a portfolio, there are similarities about the components that should be ideally included when determining the relative importance of assets and their urgency in attention:

- Accounting for the demands deriving from multiple hazards such as: traffic loads, flooding, earthquakes and landslides;
- The overall properties of the assets, such as: structural typology, dimensions, mechanical properties, cost of the infrastructure and its relative importance to the operation of the road network;
- State of degradation, corrosion and overall expected performance of the bridge components when subjected to the considered hazards.

While these components are generally included in the available proposals for simplified prioritisation in different ways, there is a difficulty in assessing their relative importance and, therefore, the way in which they are processed is typically defined by expert opinion. When looking for an established metric that allows the consideration of the entire scope of the problem in a single value, average annual loss (AAL) is a risk metric that has seen growing use within the structural engineering community (O'Reilly & Calvi, 2019) (Shahnazaryan & O'Reilly, 2021), even being proposed as a target metric to be used in new methods for structural design and assessment (Calvi, O'Reilly, & Andreotti, 2021). AAL, also referred to in some sources as expected annual loss (EAL), is a product of risk

assessment that represents long-term expected economic losses per year, averaged over many years, that are produced by specific hazards of varying intensities and their respective annual exceedance rates, or return periods. In this chapter, a seismic risk methodology is applied to the case study of 617 bridges in the Italian province of Salerno to determine prioritisation of assets based on AAL, which is then used for two main purposes: as a benchmark to compare with the results obtained using the recent 2020 MIT Guidelines and as a possible guiding parameter to determine the relative importance of each factor affecting the determination of priority, with a view to moving towards a more optimised but still simple prioritisation approach.

6.2 METHODOLOGY

The methodology defined for this chapter, depicted graphically in Figure 6.1, initially consisted of using the synthetic case study of 617 bridges presented in Section 2.1.4 to apply detailed risk assessment procedures, leading to the calculation of the AAL for each asset, thus creating a benchmark with which to evaluate different prioritisation methodologies and the influence of multiple parameters on the overall performance of the inventory.

For this purpose, the characteristic hazard of the site of each bridge in the case study, as well as the earthquake records selected for each soil-zone combination previously described in Section 2.3.2, were considered and the numerical models created for each bridge using the BRITNEY modelling tool were analysed using the ground motion record set corresponding to the location of each asset to perform non-linear time-history analysis (NLTHA) and determine fragility curves for the collapse limit state of each case-study bridge. These fragility curves were integrated with the hazard curves of each site to obtain the annual probability of collapse of each bridge, which when can be multiplied by a replacement cost to derive AALs.

To obtain a complete account of the AALs that can be attributed to the collapse of each bridge due to seismic hazard, both the direct replacement cost as well as the indirect cost of the bridge should be considered. As presented and exemplified in Chapter 5, while the direct cost can be taken as proportional to the deck area multiplied by an average construction cost value, the indirect counterpart requires an analysis of the transportation network to evaluate the economic loss that the users would incur because of the disruption caused by the collapse of each bridge. Once the total (direct and indirect) replacement costs of each asset were calculated, they were combined with the annual probability of collapse to determine an expected AAL for each bridge, defining an AAL database that can be used as a benchmark prioritisation metric. This database was then explored through data science methodologies, including a machine learning model, to gain insights on how some of the

simple features (e.g., span length, structural typology, pier height etc.) that are commonly available for each bridge can be used as indicators to approximate the AAL-based priority.

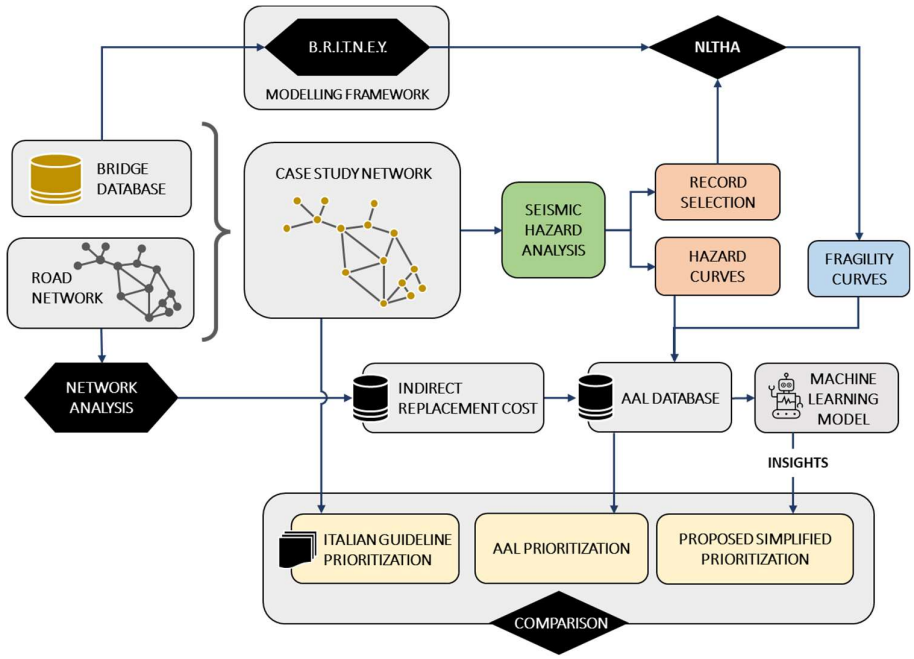

Figure 6.1. Methodology used to understand the implementation of the recent 2020 MIT Guidelines and explore improvement options

Finally, a comparison was made between the 2020 MIT Guidelines classification, the AAL-based prioritisation and the insights obtained from the database and the machine learning model, in order to evaluate the 2020 MIT Guidelines and develop a more optimised proposal with the same level of simplicity of implementation but with improved overall accuracy, when compared with the AAL ranking.

6.3 Loss Results

6.3.1 Direct Loss Assessment

The procedure to calculate direct seismic losses described previously in Chapter 4 for the research related to the Exposure component was repeated herein. In that sense, the collapse limit state fragility curves for each bridge in the database were calculated by NLTHA as described in Section 2.2.3 and shown in Figure 6.2 for reference. These fragility curves were combined with the seismic hazard at each site to determine an annual probability of

exceedance (APE), by evaluating the probability of exceedance in terms of the IML and the respective annual probability of exceeding that IML. The integration over the entire IML range results in the APE for each asset, as shown in Figure 6.3(a). As was previously considered in Chapter 4, the replacement cost for each bridge was taken as proportional to the deck area, considering a generic cost per square meter of €930, taken from the mean replacement cost per area obtained by Perdomo et al. (Perdomo, Abarca, & Monteiro, 2020) for a similar Italian bridge inventory. The results for direct collapse-based AAL are show in Figure 6.3(b), where it can be observed that higher values of loss are concentrated in the areas with higher seismic hazard.

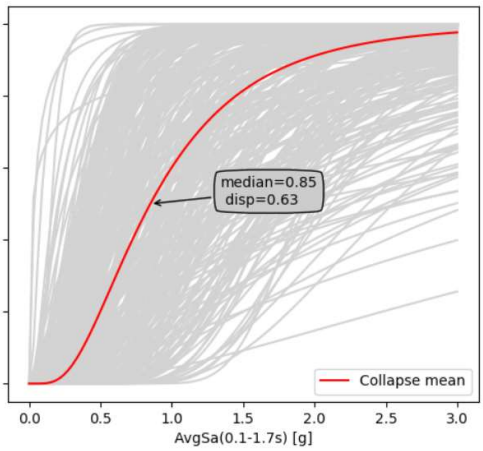

Figure 6.2. Fragility curves for collapse limit state obtained for the 308 bridges in the database

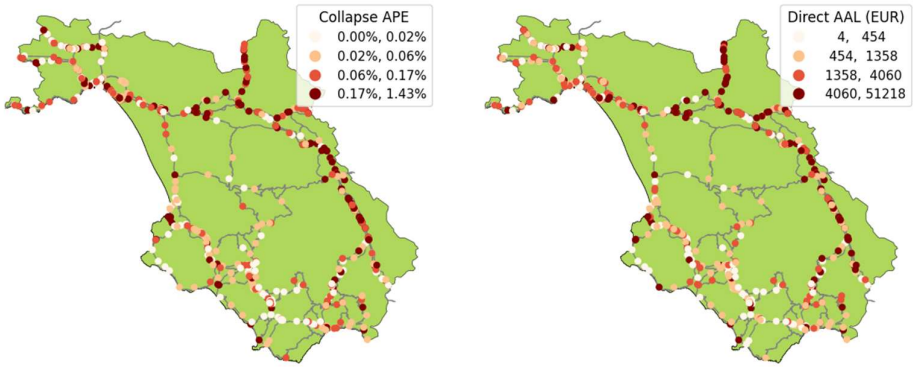

(a) **(b)**

Figure 6.3. Results for direct loss assessment on the case study inventory: (a) annual probability of exceeding collapse limit state, (b) direct collapse-based average annual losses in Euros.

6.3.2 Indirect Loss Assessment

In this case, the refined procedure to calculate indirect seismic losses described previously in Chapter 5 was repeated herein. In that sense, the road network of Salerno was analysed in its fully operational condition to determine a baseline daily operation cost, afterwhich, the analysis is repeated removing one-by-one each bridge in the network model, therefore determining the daily indirect cost that the collapse of each asset would incur on the overall network. This is multiplied by the median replacement time of 710 days, previously determined appropriate for the Italian context, to determine the total indirect loss associated to the occurrence of collapse for each bridge, results of which are shown in Figure 6.4(a) for the entire case study. By multiplying this indirect cost of collapse of each asset by the APE results shown in Figure 6.3(a), an indirect AAL is obtained for the entire inventory as shown in Figure 6.4(b).

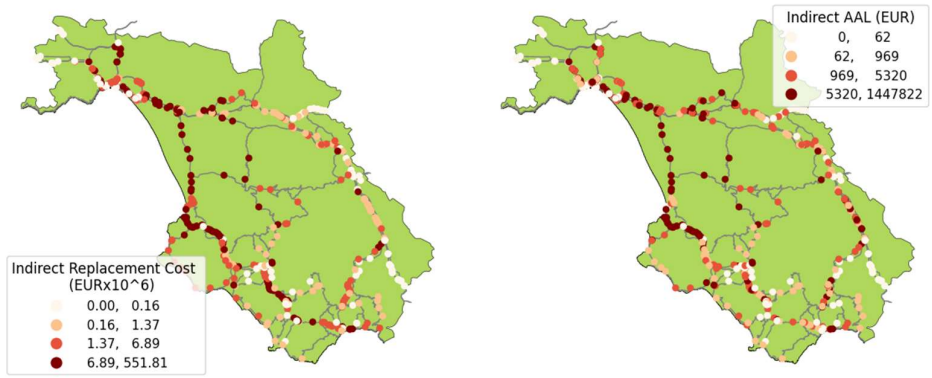

(a) **(b)**

Figure 6.4. Indirect loss results: (a) indirect replacement cost, (b) results for indirect average annual losses.

It can be seen that the indirect losses were concentrated near the coast of Salerno where the traffic is generally higher, even though the seismic hazard in this area was relatively low. This outcome can be seen as indicative that the monetary value that is incurred by the interruption of points of the road network for extended periods of time outweighs the lower seismic hazard for this case.

As was mentioned previously in Chapter 5, it is important to note that some of the bridges in the case study that were located near the edges of the Salerno region did not produce indirect loss results when applying this methodology since their collapse resulted in no alternative paths, causing the complete disconnection of some of the centroids. This is a

limitation of the applied methodology since alternate routes are likely available when considering neighbouring parts of the road network as well as the residential roads that were excluded from the network model. To avoid this issue in future research, it is possible to either extend the network model beyond the limits of the case study regions or account for the costs of cancelled trips; however, for the purposes of the present study, the analysis will focus herein on the remaining 531 bridges that did produce indirect loss results with the methodology used.

6.3.3 Total AAL Results Summary

Once both direct and indirect loss components were determined, the total collapse-based AALs were aggregated for each bridge, resulting in the distribution shown in Figure 6.5(a). Analysing the overall results, it is seen that the indirect losses represent 78% of the total losses and that the overall losses have a very similar spatial distribution to the one found for the indirect losses alone, which is expected given that these are much greater than the direct loss component.

It is important to note that, while the indirect loss component does seem to have a much larger contribution to the overall losses than the direct counterpart, the actual 78% estimate was obtained through the application of the methodology previously presented, considering all its assumptions and limitations. Changes in the repair time of assets, post-disaster travel demands, accounting for more modes of transportation and the inclusion of the residential road network will undoubtedly have an impact on the results. However, it is outside the scope of this study to provide a definitive estimate of the indirect losses but rather to provide reference values for the purpose of aiding bridge management institutions in decision-making.

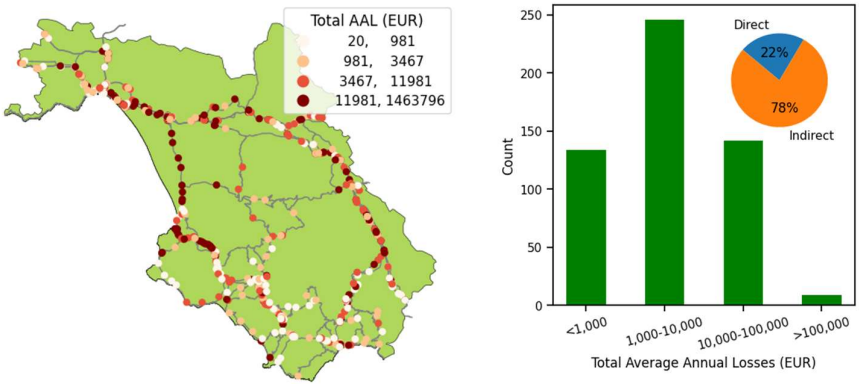

(a) (b)

Figure 6.5. Total average annual loss results: (a) total AAL results for case study inventory, (b) histogram of total AAL results.

It is also worth mentioning that a large portion of the losses are concentrated in very few assets. For example, from the histogram shown in Figure 6.5(b), only 9 bridges have loss values that are greater than €100,000 but overall, those bridges represent 42% of the total loss for the entire inventory. Such distributions in loss are mostly caused by the extreme values in indirect loss that were calculated for bridges that have a high traffic flow and very long and ineffective alternate routes. This is an important finding since bridge management agencies could use such indications to put measures in place for these assets, such as having fast-deploying temporary replacements ready to reduce the interruption duration and cost.

6.4 MACHINE LEARNING PREDICTION OF AAL-BASED RANKING

A supervised machine learning model was evaluated using the case-study AAL results presented in Section 6.3.3 to assess the feasibility of predicting losses based on limited data, and to gain insights on the effect and relative importance of simple bridge parameters on the prioritisation, defined by sorting bridges based on their individual AAL results. The intention of the machine learning modelling process is not to create a model to be used on bridges outside of the current case study, but to take advantage of the capabilities of this method to infer relationships between independent features (simple bridge parameters and reference hazard values in this case) and their impact on target values of interest (AAL estimates). It is envisaged that these can be later used to guide improvement proposals for the 2020 MIT guidelines.

6.4.1 Model and Database Characteristics

A random forest regression model was chosen given its recently demonstrated good performance when compared to other machine learning algorithms for similar applications (Mangalathu, Hwang, Choi, & Jeon, 2019), and the ability of this algorithm to evaluate the relative importance of each independent variable. This type of algorithm uses a collection of decision trees built with bootstrapped subsets of the main database, as depicted graphically in Figure 6.6. Each tree is fitted to provide predictions based on its sub-sample and all predictions provided by each tree are later averaged to improve the predictive accuracy and control overfitting. The relative importance of each independent variable is calculated by measuring their efficiency in decreasing the prediction uncertainty after each split of the branches in the tree, averaged over all trees in the forest.

This type of model, as with most supervised machine learning models, uses a labelled dataset that has both its independent variables (inputs) as well as its outcomes, and progressively calibrates its own numerical properties to produce an inferred function that makes predictions about the output values. In order to calibrate the model and evaluate its performance on external data, the dataset is split into a training set, used to fit the model

properties, and a testing set used to appraise the fitted properties. The primary model settings were calibrated by running multiple parameter options. The values shown in Table 6.1. Main parameters selected for the random forest implementation after calibration exercise performed on the testing set were chosen based on their improved prediction performance evaluated on the testing data set.

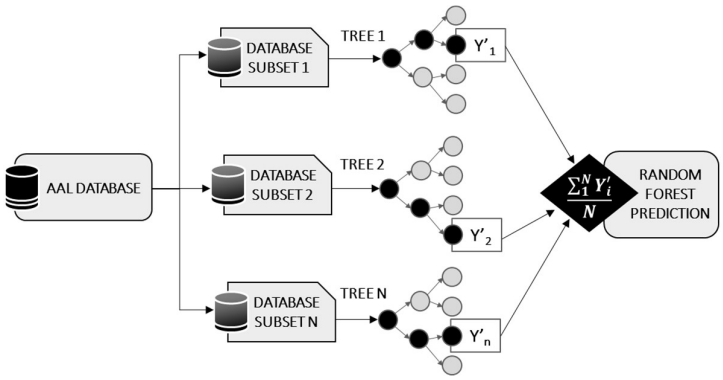

Figure 6.6. Schematic representation of random forest algorithm prediction methodology

Table 6.1. Main parameters selected for the random forest implementation after calibration exercise performed on the testing set

Parameter	Value
Training/Testing split	90/10
Number of estimators	40
Maximum Tree Depth	8
Maximum Features	$\sqrt{\#\ features}$
Minimum Leaf Samples	1
Minimum Split Samples	5

A database was assembled using the AAL results for each bridge in the case study to train the random forest model. For this purpose, the AAL representing the dependent variable (target) and a vector of independent variables (or features) was retrieved for each bridge structure. A set of six features were used for each bridge: maximum span length, maximum pier height, daily traffic flow, seismic intensity measure level for a return period of 475 years, number of spans and total replacement cost. Given that all these variables that will be processed by the algorithm have different units and orders of magnitude, each was modified using a minimum-maximum scaling process that transforms the data of each feature by scaling the values within the 0 and 1 range. The resulting database consists of

531 data rows, one for each bridge for which indirect loss results were available. It is important to note that the database created is relatively small for a regression problem, therefore the reader is encouraged to keep in mind that the model performance will be affected by this size limitation.

6.4.2 Model Performance and Insights

The evaluation of the regression model on the training and testing sets is presented in Figure 6.7, along with the relative feature importance, and a set of useful regression performance metrics is presented in Table 6.2. In general, the model does not have an ideal prediction performance, which is to be expected given the small amount of data points and features used to attempt to predict a complex value such as AAL, which depends on multiple variables that cannot be included in this type of model in a straightforward manner.

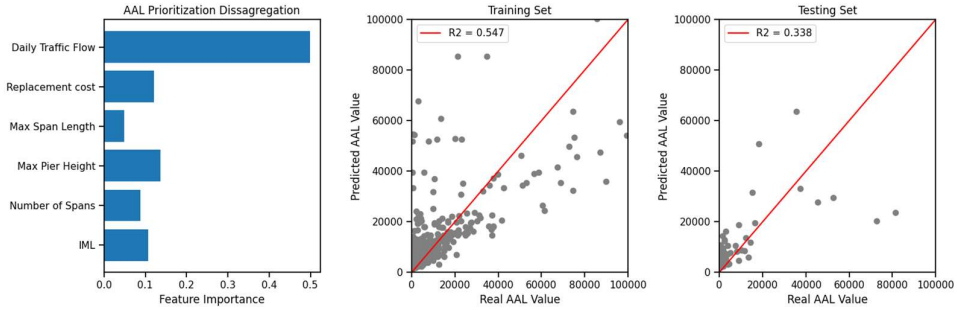

Figure 6.7. Performance of the machine learning model on the database: (a) feature importance, (b) performance of the model on the training set, (c) performance of the model in the testing set.

Table 6.2. Performance metrics for the machine learning model on the entire dataset

Parameter	Value
Root-mean-squared error (RMSD)	€ 52,279.8
Mean absolute error (MAE)	€ 10,888.2
Median absolute error (MedAE)	€ 3,398.4
Coefficient of determination (R2)	0.542
Total AAL_{pred} / AAL_{calc}	0.962

Also, in global terms, when considering the total annual losses aggregated for the entire inventory, the model exhibits a good performance, predicting a value that is 96% of the

actual calculated value, however, on the individual asset side, the model tends to overpredict the loss values for most of the elements in the case study, as seen in Figure 6.8. The underprediction in the global results contrasts with the overprediction on the individual side, however, this is explained by the fact that the expected losses for the entire inventory are governed by outlier assets that exhibit very high values of AAL. When calculated, these AAL values are not accurately predicted by the model since they are represented in the database by very few points, challenging the training of the model in this extreme range.

Overall, in terms of model performance, daily traffic flow has the highest relative importance over all the evaluated features, which is a consequence of the fact that the indirect losses represent the majority of the losses calculated and are directly related to the daily traffic. Moreover, maximum pier height was found to be the second most relevant feature when trying to predict AAL, which is a parameter that is not currently accounted for in the 2020 MIT Guidelines and has been shown to have a correlation with the dynamic properties of bridges in previous studies (Zelaschi, Monteiro, & Pinho, 2016). The maximum span length, which has a great impact in the risk classification of the 2020 MIT Guidelines, as will be shown in the following section, has the lowest relative importance as per the machine learning model exercise implemented.

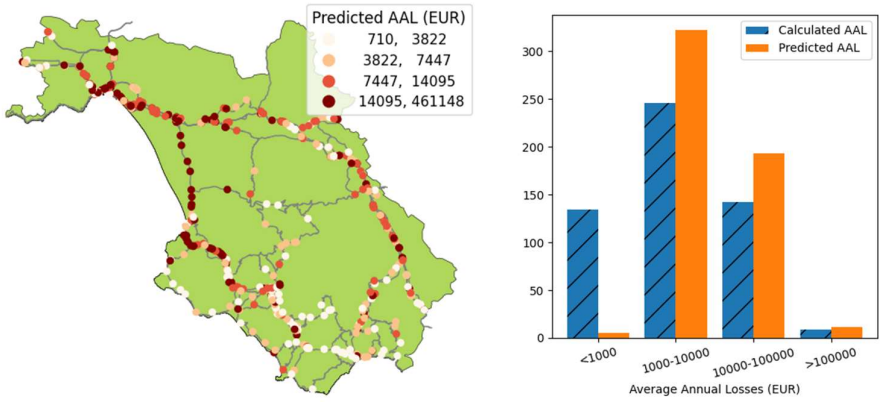

(a) **(b)**

Figure 6.8. Machine learning model results: (a) predicted AAL results for case study inventory, (b) histogram of calculated and predicted results.

Using the predicted values to determine the priority of assets and comparing it to the one defined by the AAL results actually calculated leads to encouraging results, as shown in

Figure 6.9. The application of the model to only define the relative priority of assets in the portfolio produces a median absolute error of 54 positions, which represent roughly 10% of the total number of assets in the case study.

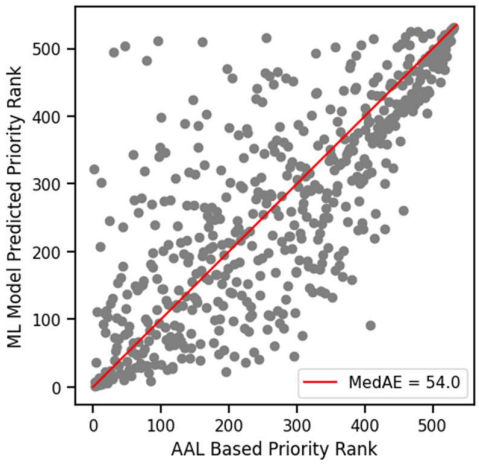

Figure 6.9. Comparison of prediction prioritisation with benchmark

6.5 ITALIAN GUIDELINES FOR BRIDGE PORTFOLIO ASSESSMENT

The 2020 MIT Guidelines propose a multi-level and multi-component approach that classifies bridges in risk categories through the processing of qualitative metrics, specific to each of the considered hazards: a) structural/foundational, including eventual degradation; b) seismic; and c) flood/landslide. These guidelines have been recently analysed and evaluated by Santarsiero et al. (2021), where a thorough summary of the entire classification methodology is presented. In such study, the simple application of the seismic and degradation components of the guidelines to an inventory of 48 bridges concluded that the obtained classification leads to conservative results.

In the study presented herein, the focus will be only on the treatment of the seismic risk classification of bridges, since it is the only component for which the benchmark AAL calculations performed in the previous sections is applicable for comparison. For what concerns seismic risk, as with the other considered risk types, the procedure is divided in the three well-known main components: a) hazard; b) exposure; and c) vulnerability, each of which being assigned one of five possible attention levels that range from low to high. This is done by processing qualitative characteristics of each bridge using a specific set of tabular values, as described in the following paragraphs. After each risk component is processed and a classification is made, all components are convoluted into an overall

seismic risk attention class. In general, the classification of each of the components of risk is determined by a preliminary class, assigned by the qualitative evaluation of primary parameters that can be further altered by secondary parameters. These may increase or decrease the preliminary classification within the available five classes. The rules for the assignment of the preliminary classes per component are summarised in Table 6.3, Table 6.4 and Table 6.5 for the hazard, exposure and vulnerability facets, respectively.

It is also important to note that structural degradation determined from inspections, availability of alternate routes and the consideration of a bridge as strategic, are also parameters used to alter the classification of a bridge according to these guidelines. These parameters are not included in the tables shown here or in their application to the case study, since this information was unavailable.

Table 6.3. 2020 MIT Guidelines' seismic risk classification – hazard

PGA (10% @ 50 years)	Topography		Soil type	
	T1, T2, T3	T4	A, B	C, D, E
0.05 - 0.10	Low	Medium-Low	+0	+1
0.10 - 0.15	Medium-Low	Medium	+0	+1
0.15 - 0.20	Medium	Medium-High	+0	+1
0.20 - 0.25	Medium-High	High	+0	+1
>0.25	High	High	+0	+1

Table 6.4. 2020 MIT Guidelines' seismic risk classification – exposure

Max Span Length (m)	Daily Traffic (vehicles)			Overpass		
	< 10000	10000-25000	> 25000	Roads	Rivers	Depressions
< 20	Low	Medium-Low	Medium	+1	+0	-1
20 - 50	Medium-Low	Medium	Medium-High	+1	+0	-1
> 50	Medium	Medium-High	High	+1	+0	-1

Table 6.5. 2020 MIT Guidelines' seismic risk classification - vulnerability for RC bridges

Spans	Max Span Length (m)		Static System		Seismic Design	
	< 20m	> 20m	Hyperstatic	Isostatic	Yes	No
Single	Low	Medium-Low	+0	+2	+0	+1
Multiple	Medium-Low	Medium	+0	+2	+0	+1

Once each component has been characterised, they are combined to determine an overall seismic risk class, as per the indications shown graphically in Figure 6.10. As noted by Santarsiero et al. (2021), the overall classification is very much affected by the vulnerability component; for example, if this component is high, then the seismic risk class will be assigned the highest category, almost regardless of the other components.

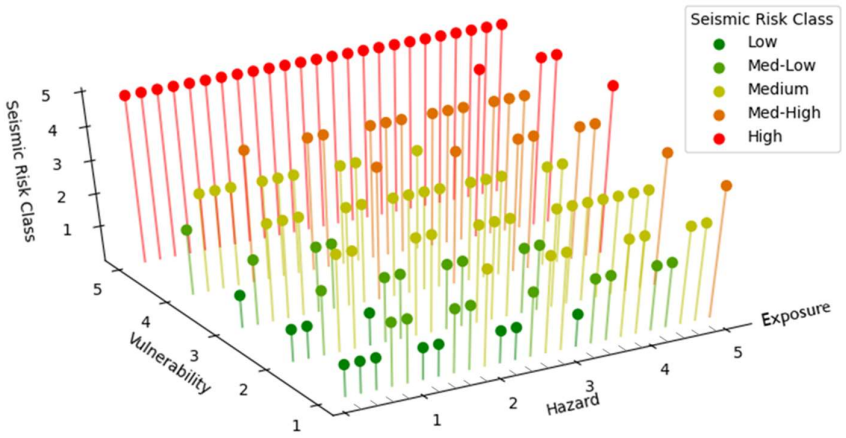

Figure 6.10. Determination of seismic risk class based on the partial classification of hazard, exposure and vulnerability, adapted from Santarsiero et al. (2021)

The methodology foreseen by the guidelines was applied to the case study inventory, providing the results shown in Figure 6.11. It can be seen that both the hazard and vulnerability components are mostly classified in the highest possible option, leading to an overall seismic risk class with mostly the high category. This is attributed to the fact that the vulnerability component dominates for simply supported bridges with spans longer than 20m that have not been seismically designed, which correspond to the predominant characteristics in the case study and to a large portion of the Italian bridge stock.

The obtained seismic category class is compared with the priority AAL rank, defined by sorting the values of AAL in an increasing ranked fashion. The bar plot in the bottom right corner of Figure 6.11 shows the seismic classification in the vertical axis (with values 1 through 5 representing low to high categories, respectively) while the AAL-based ranking of the 531 bridges in the case study is located in the horizontal axis. The assets with the highest total AAL results are plotted in the first (left) positions. Consequently, if the 2020 MIT Guidelines classification were in complete agreement with the AAL ranking, the bridges with higher risk categories would all be located on the left of the plot and the overall shape of the plot would have a descending trend.

While the classification does seem to group the high and medium-high risk categories mostly in positions that are in agreement with the AAL-based ranking, the fact that there are only two resulting categories and the predominance of the high class creates a problem for the effective implementation of these guidelines as a tool for efficient decision-making and resource prioritisation. As per the 2020 MIT Guidelines, 498 bridges from the 531 in the inventory that were classified into the high category would require the immediate development of detailed structural analysis, implementation of periodic inspections and the installation of monitoring systems. This would clearly require a great number of resources to comply with and be, in some respects, not fulfilling the need of being able to prioritise effectively.

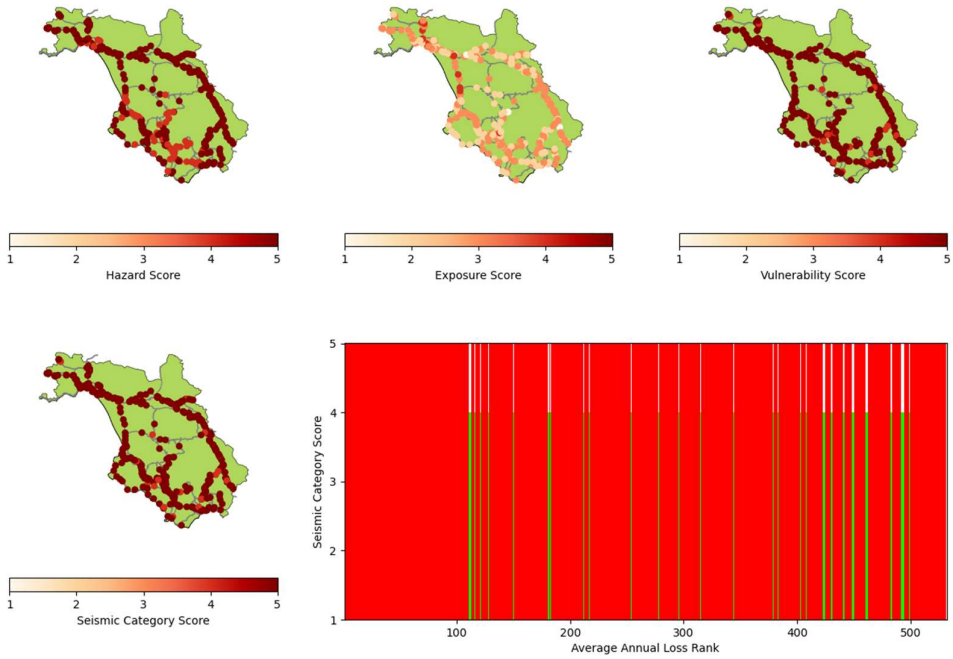

Figure 6.11. Results for application of 2020 MIT Guidelines to case study inventory

6.6 DIRECTIONS FOR IMPROVEMENT OF PRIORITIZATION SCHEME

Using the insights gained by the application of the seismic risk quantification to the case study, along with the influential features found via machine learning techniques, a possibly improved methodology to perform bridge prioritisation, based on the 2020 MIT Guidelines and their observed performance, is outlined and discussed here.

In general, the 2020 MIT Guidelines constitute a robust and well-structured methodology for bridge management. Addressing risk as a convolution of each its three components, as well as the possibility to include multiple hazards, is innovative since it allows for the disaggregation of the risk classification to identify problematic areas and consequently aid in the immediate intervention and retrofitting decision making. The shortcomings that were observed during its implementation are specifically related to the thresholds used to characterise each of its components in a simple and schematic manner, as well as the high relative importance that the vulnerability component has on the overall risk class. While this conservatism in the vulnerability component was likely a conscious decision made to prioritise bridge safety, it has the downside of classifying a large number of bridges, even those with low associated losses, in the categories of highest priority, which is not in agreement with the findings from a complete quantitative exercise based solely on economic losses. Furthermore, the definition of only five risk classes creates an additional limitation since it can be restrictive when a large, thus more diverse, inventory is considered. For example, as in the results obtained after the classification of the adopted case study, if a large number of assets is classified into a single category, the 2020 MIT Guidelines provide no indication on how they can be further prioritised so that bridge management institutions can efficiently allocate their resources in implementing the monitoring and required explicit analysis actions.

In order to potentially improve the results obtained by the application of the guidelines, the definition of fixed risk classes could be, for instance, changed to an approach based on a point system per component without establishing a limit. The overall seismic risk score would then be composed of the sum of the scores of each component with the available number of points per component being defined as proportional to the findings from the machine learning model, by giving a higher importance to the exposure component and the daily traffic flows, in order to further stress the importance of the indirect losses. In terms of the hazard component, the current thresholds values available in the guidelines are low in comparison to the seismic potential in the Italian territory according to the hazard model used (Woessner, et al., 2015). Therefore, the values could be updated as shown in Table 6.6 to be more applicable to case-study areas of high seismicity according to the hazard model used.

Table 6.6. Proposed modified seismic risk classification - hazard

PGA	Topography Class		Soil type	
(10% @ 50 years)	T1, T2, T3	T4	A, B	C, D, E
< 0.10	1	2	+0	+1
0.10 - 0.20	2	3	+0	+1
0.20 - 0.30	3	4	+0	+1
0.30 - 0.40	4	5	+0	+1
> 0.40	5	5	+0	+1

Regarding the exposure component, the thresholds for span lengths could be modified to reduce the impact of this parameter on the overall results. Also, traffic flows would be reduced to increase its sensitivity, given that this parameter was observed in Section 6.4.2 to be the most influential in the determination of annual losses. Furthermore, to provide more importance to the overall component, the total amount of awardable points would increase as shown in Table 6.7.

Table 6.7. Proposed modified seismic risk classification - exposure

Max Span Length (m)	Daily Traffic			Overpass		
	<4000	4000-10000	> 10000	Roads	Rivers	Depressions
< 25	1	+3	+5	+1	+0	-1
25 - 40	2	+3	+5	+1	+0	-1
> 40	3	+3	+5	+1	+0	-1

For what concerns the vulnerability component, the threshold values for number of spans and maximum span length could be updated as per Table 6.8, which were calibrated by iterating on different values and observing their effect in the classification performance with respect to the AAL ranking. Furthermore, the maximum pier height would be included as an additional parameter since it was recognised as a relatively important feature during the machine learning experiment, shown in Figure 6.7(a).

Table 6.8. Proposed modified seismic risk classification - vulnerability

Spans	Max Span Length (m)		Static System		Seismic Design		Max Pier Height (m)	
	< 30m	> 30m	Hyperstatic	Isostatic	Yes	No	< 15	> 15
< 3	1	2	+0	+1	+0	+1	+0	+1
3 - 10	2	3	+0	+1	+0	+1	+0	+1
> 10	3	4	+0	+1	+0	+1	+0	+1

Adopting the described modification proposals, the proposed modified methodology was applied to the same case study, leading to the results shown in Figure 6.12. It can be observed that there is a higher resolution of results for each of the components (i.e., no saturation with the high limit), which also translates in a wider range of risk scores for the overall inventory. The spatial distribution of the scores is more in agreement with the loss results and the overall prioritisation performance appears greatly improved with respect to the outcomes of the original guideline's methodology.

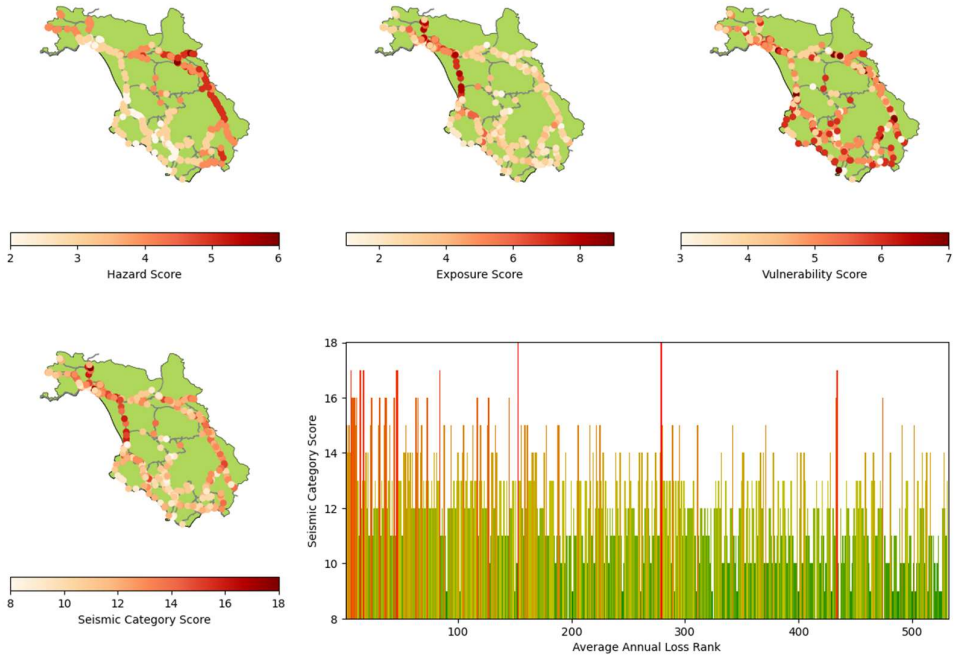

Figure 6.12. Results for the proposed modified seismic risk classification's prioritisation

It is important to note that, while the definition of the case study and its properties were designed to be considered as representative of a common typology of the bridge network of Italy, the proposed methodology was made by calibrating values from the available database therefore its applicability would be limited to real case databases that would be created following the same methodology as the one used herein, particularly in terms of road network modelling.

6.7 SUMMARY AND CONCLUSIONS

In this chapter, a synthetic case study of 617 bridges in the province of Salerno, Italy, was generated by sampling from a database of 308 bridges with complete information and was used to perform seismic risk assessment considering direct and indirect loss economic losses. The resulting database of collapse-based average annual losses (AAL) was explored using data science techniques to determine the influence of simple bridge parameters on the calculated losses and associated priorities, to ultimately use these insights to evaluate and propose improvements to the recent guidelines on risk classification and management, safety assessment and the monitoring of existing bridges (Consiglio Superiore dei Lavori

Publici, 2020) - 2020 MIT Guidelines. The application of the described methodology led to the following conclusions, regarding the prioritisation of bridge assets within a regional portfolio, even with limited information available:

- When data and analysis resources are available to consider both direct and indirect components of loss, AAL can be considered an alternative or complementary metric by which assets within a bridge portfolio can be prioritised in terms of resource allocation, inspection and retrofitting; it was seen here that this metric combines the vulnerability of each bridge, as well as the importance that each element has within the entire road network system in a single decision variable;
- Overall, it is concluded that indirect losses have a higher economic impact on the system when compared to direct losses. Given the complexity in their nature, the order of magnitude of this difference depends heavily on the assumptions made during the assessment process, such as using a single transportation mode, median repair times and excluding the residential road system; however, the large difference observed herein is expected to increase when considering all transportation modes;
- When evaluating the influence of commonly available variables in the results of total AAL, it was seen that daily traffic flow, which is related to the exposure component, seems to have the higher relative importance, in comparison to other bridge structure-specific metrics. This result appears reasonable, given the high contribution of the indirect component of loss to the overall results;
- When evaluating the 2020 MIT Guidelines that have recently been published in Italy, it was observed that the application of the methodology leads to large portions of the inventory classified to the highest-risk available category, creating a challenge in terms of its usefulness as an efficient way to classify bridge priorities and resource allocation. Different reasons can be cited for this effect, such as the limited availability of possible categories and the high importance placed on the vulnerability component that uses somewhat conservative thresholds for its classification, such as the restrictive 20m maximum span length limit;
- Using the insights gained by the analyses made, possible directions for an improved prioritisation methodology were drawn and discussed based on modifications made to the current 2020 MIT Guidelines. While further scrutiny and additional case studies are needed, such a modified prioritisation scheme performed better, when compared to a benchmark classification analytically based on AAL.

7. OVERALL CONCLUSIONS AND FUTURE DEVELOPMENTS

7.1 CONCLUSIONS

Regional seismic risk assessment of bridge portfolios has gained popularity in recent years as an effective tool for decision-making, one that is generally seen favourably by practitioners and stakeholders to quantify the expected performance of infrastructure inventories. However, many setbacks exist in the practical application side, which can lead the team performing the analysis to make decisions that will ultimately have an unknown impact on the final results of the project, for which there is little existing technical background or precedent. In this thesis, an extensive database of existing bridges in Italy was used to create large case studies and perform state-of-the-art seismic risk assessment, with the intention of evaluating some of the traditional and innovative decisions that are made in each stage of the analysis, thus quantifying their impact and making recommendations regarding best practices in each component. In the following, the main conclusions drawn from the research performed will be outlined, however, in addition to the full account of conclusions drawn in each of the main chapters in this thesis.

In terms of the hazard component:

- In the subject of choosing an appropriate intensity measure to use for the seismic assessment of bridge portfolios, the recently introduced option of average spectral acceleration (AvgSa) performs better than the traditional choice of peak ground acceleration (PGA), as its results have an overall lower dispersion while incurring in no actual additional difficulty for its implementation.

In terms of the exposure component:

- The use of taxonomy-based fragility curves does lead to overall median direct loss results that are accurate over the entire inventory analysed. However, depending on the amount of information that was used for their calculation, they induce an epistemic uncertainty (in terms of portfolio and network model knowledge) in the results that should be accounted for and properly communicated to the stakeholders.
- As a practical recommendation, it seems that the detailed knowledge of at least 30% of the inventory makes sense, since after this point the reduction of the uncertainty is less significant. The alternative use of machine learning models to

assign fragility curves to bridges with incomplete information seems to become attractive only when considerable portions of the inventory are known (at least 50%); their use does incur in an additional difficulty in comparison to the taxonomy-based approach.

In terms of the vulnerability component:

- The analysis performed in this thesis indicates that the indirect losses incurred by the users of a road network, associated to the collapse of bridges, seem to exceed the direct losses by a factor of at least 4:1. This is considered a conservative estimate since many factors were not included in the analysis; therefore, it has been confirmed that the consideration of the indirect component of loss is paramount in all regional risk assessments of bridges. This is even if their implementation does lead to an important increase in information and technical expertise demand.
- A simplified approach to approximate the relative importance of each bridge on a road network in terms of indirect losses was presented in this thesis. This method performs well, is independent of the potential hazard and has relativelly low information and technical demands; therefore, can be included as a minimum requirement on risk assessment of bridges in road networks for multiple hazards.

In terms of prioritization of bridges for an efficient resource allocation:

- When the information and resources are available to perform a full seismic risk assessment, the use of average annual losses (AAL) can be considered as an appropriate metric by which to perform a prioritization of the assets in the inventory, as it includes in its definition most of the elements desired for this purpose in a single decision variable.
- When resources are limited, as is usually the case, a simplified prioritization methodology can be defined by obtaining discreet features for each asset in the inventory and processing them considering their relative importance. An example of such methodology was presented in this thesis considering only the seismic risk component, which produced adequate results in comparison to an AAL-based benchmark.
- The methodology presented recently by the Italian Ministry of Sustainable Infrastructures and Mobility as guidelines for bridge administration institutions to perform prioritization of their assets, was demonstrated to produce overly conservative results that can present difficulties during its practical implementation, as they tend to classify most bridges to the highest category of risk.

7.2 FUTURE DEVELOPMENTS

During the development of this thesis, the following subjects were identified as important candidates for research, but were either out of the scope defined, or lacked the sufficient resources to persue them. Therefore, they are recommended to be considered in future research efforts and are listed as follows:

- While AvgSa seems to perform well in terms of efficiency and its use is recommended for the assessment of bridge portfolios, research should be performed to properly define the period range that should be used for both individual and groups of bridges. Even though there is a precedent for the rationale used in this thesis to define the range, and its use did lead to satisfactory results, no specific study for the definition of the range has been made to date, leaving each particular study open to their own interpretation and preference. It is noted that this flexibility in period range definition is also an advantage in some cases, but for practical implementation and user guidance focused on here, some indications should be pursued.
- The analysis made to evaluate the uncertainty induced by lack of exposure knowledge should be repeated to other, possibly larger, case studies to determine if the findings made herein remain valid for other cases, regions and bridge typologies.
- Even though the general typology of bridges used in this thesis (i.e. multi-span reinforced concrete bridges) represents the majority of bridges in the inventory of most countries, future research should be devoted to repeat some of the analysis made herein to other typologies such as steel, arch and cable stayed bridges, which have an important representation in some country's portfolios.
- More research should be performed in the field of indirect losses of bridge portfolios, to clearly quantify its full relative importance and hopefully aid in the development of digital tools, libraries and resources to make their consideration more feasible to risk assessment endeavours involving bridge inventories.
- It is considered imperative to perform research on the effect of ageing deterioration in conjunction with increased gravitational loads in bridges, which seems to be a likely cause of collapses observed in Italy in recent years. While many challenges exist to accurately characterize this phenomenon, it represents a predicament that will continue to grow more problematic if unattended.

REFERENCES

Abarca, A., Monteiro, R., O'Reilly, G. J., Zuccolo, E., & Borzi, B. (2021). Evaluation of intensity measure performance in the regional assessment of reinforced concrete bridge inventories. *Structures and Infrastructures*. doi:10.1080/15732479.2021.1979599

Ancheta, T., Darragh, R., Stewart, J., Seyhan, E., Silva, W., Chiou, B., & al, e. (2014). NGA-West2 database. *Earthquake Spectra*(30(3)), 989–1005. doi:DOI: 10.1193/070913EQS197M

Baker, J. W. (2011). Conditional Mean Spectrum: Tool for Ground-Motion Selection. *Journal of Structural Engineering-asce, 137*(3), 322-331. Retrieved 2 8, 2022, from https://web.stanford.edu/~bakerjw/publications/baker_(2011)_cms_overview, _jse.pdf

Baker, J. W. (2015). Efficient Analytical Fragility Function Fitting Using Dynamic Structural Analysis. *Earthquake Spectra, 31*(1), 579-599. Retrieved 10 28, 2019, from https://earthquakespectra.org/doi/abs/10.1193/021113eqs025m

Bazzurro, P., & Cornell, A. (1999). Dissagregation of Seismic Hazard. *Bulletin of the Seismological Society of America*, 501-520. doi:10.1785/BSSA0890020501

Boore, D. M. (2010). Orientation-Independent, Nongeometric-Mean Measures of Seismic Intensity from Two Horizontal Components of Motion. *Bulletin of the Seismological Society of America, 100*(4), 1830-1835. Retrieved 7 23, 2020, from https://pubs.er.usgs.gov/publication/70041869

Borzi, B., Ceresa, P., Franchin, P., Noto, F., Calvi, G. M., & Pinto, P. E. (2015). Seismic Vulnerability of the Italian Roadway Bridge Stock. *Earthquake Spectra, 31*(4), 2137-2161. Retrieved 1 18, 2019, from http://earthquakespectra.org/doi/10.1193/070413eqs190m

Bradley, B. A. (2010). A generalized conditional intensity measure approach and holistic ground-motion selection. *Earthquake Engineering & Structural Dynamics, 39*(12),

1321-1342. Retrieved 2 8, 2022, from https://onlinelibrary.wiley.com/doi/full/10.1002/eqe.995

Brederode, L., Pel, A. J., Wismans, L. J., Romph, E. d., & Hoogendoorn, S. P. (2019). Static Traffic Assignment with Queuing: model properties and applications. *Transportmetrica, 15*(2), 1-36. Retrieved 10 22, 2021, from https://tandfonline.com/doi/full/10.1080/23249935.2018.1453561

Bucci, D., Massa, B., Tornaghi, M., & Zuppetta, A. (2005). Structural setting of the 1688 Sannio earthquake epicentralarea (Southern Italy) from surface and subsurface data. *Journal of Geodynamics 40*, 294-315.

Bureau of Public Roads. (1964). *Traffic Assignment Manual.* Washington, D.C.: U.S. Department of Commerce, Urban Planning Division.

Calvi, G. M., Moratti, M., O'Reilly, G. J., Scattarreggia, N., Monteiro, R., Malomo, D., . . . Pinho, R. (2019). Once upon a Time in Italy: The Tale of the Morandi Bridge. *Structural Engineering International, 29*(2), 198-217. doi:10.1080/10168664.2018.1558033

Calvi, G. M., Moratti, M., O'Reilly, G. J., Scattarreggia, N., Monteiro, R., Malomo, D., . . . Pinho, R. (2019). Once upon a Time in Italy: The Tale of the Morandi Bridge. *Structural Engineering International, 29*(2), 198-217. Retrieved 9 20, 2021, from https://tandfonline.com/doi/full/10.1080/10168664.2018.1558033

Calvi, G., O'Reilly, G., & Andreotti, G. (2021). Towards a practical loss-based design approach and procedure. *Earthquake Engineering and Structural Dynamics*, 1-13. doi:https://doi.org/10.1002/eqe.3530

Camera di Commercio di Genova. (2018). *Effetti economici indotti dal crollo del viadotto Morandi.* Genova: Confindustria Genova.

Carozza, S., Jalayer, F., Miano, A., & Manfredi, G. (2017). Probabilistic Connectivity Analysis for a Road Network Due to Seismically-Induced Disruptions. *16th World Conference on Earthquake Engineering.* Santiago, Chile.

Chang, S. E., Shinozuka, M., & Moore, J. E. (2000). Probabilistic Earthquake Scenarios: Extending Risk Analysis Methodologies to Spatially Distributed Systems. *Earthquake Spectra*, 557–572. doi:https://doi.org/10.1193/1.1586127

Chase, S., Adu-Gyamfi, Y., Aktan, A., & Minaie, E. (2016). *Synthesis of National and International Methodologies Used for Bridge Health Indices*. McLean (VA): Federal Highway Administration. doi:http://dx.doi.org/10.13140/RG.2.1.1558.1683

Chen, R., Branum, D. M., & Wills, C. J. (2013). Annualized and Scenario Earthquake Loss Estimations for California. *Earthquake Spectra, 29*(4), 1183-1207. Retrieved 1 12, 2022, from https://earthquakespectra.org/doi/full/10.1193/082911eqs210m

Chen, W.-F., & Duan, L. (2014). *Bridge Engineering Handbook: Seismic Design*. Retrieved 10 25, 2019, from http://elib.polban.ac.id/index.php?p=show_detail&id=18431

Chiou, B., Darragh, R. B., Gregor, N., & Silva, W. J. (2008). NGA Project Strong-Motion Database. *Earthquake Spectra, 24*(1), 23-44. Retrieved 7 23, 2020, from https://journals.sagepub.com/doi/10.1193/1.2894831

Consiglio dei Ministri . (2003). *Primi elementi in materia di criteri generali per la classificazione sismica del territorio nazionale e di normative tecniche per le costruzioni in zona sismica*. Roma: G.U. n. 105 del 8 maggio 2003 - S.o. n.72.

Consiglio Superiore dei Lavori Publici. (2020). *Linee Guida per la Classificazione e Gestione del Rischio, Valutazione della Sicurezza ed il Monitoraggio dei Ponti Esistenti*. Roma: Ministero delle Infrastrutture e dei Trasporti.

Cornell, C. A. (1968). ENGINEERING SEISMIC RISK ANALYSIS. *Bulletin of the Seismological Society of America, 58*(5), 1583-1606. Retrieved 2 8, 2022, from https://pubs.geoscienceworld.org/ssa/bssa/article-abstract/58/5/1583/116673

D'Apuzzo, M., Evangelisti, A., Nicolosi, V., Rasulo, A., Santilli, D., & Zullo, M. (2019). A Simplified Approach for the Prioritization of Bridge Stock Seismic Retrofitting. *29th European Safety and Reliability Conference (ESREL)* (pp. 3277-3284). Hannover: Research Publishing Services. doi:10.3850/978-981-11-2724-3_0592-cd

D'Ayala, D., Meslem, A., Vamvatsikos, D., Porter, K., Rossetto, T., & Silva, V. (2015). *Guidelines for Analytical Vulnerability Assessment of Low/Mid-Rise Buildings*. Pavia: Global Earthquake Model. doi:10.13117/GEM.VULN-MOD.TR2014.12

Dueñas-Osorio, L., Craig, J., & Goodno, B. (2007). Seismic response of critical interdependent networks. *Earthquake Engineering and Structural Dynamics*, 285-306. doi:https://doi.org/10.1002/eqe.626

Eads, L., Miranda, E., & Lignos, D. (2015). Average spectral acceleration as an intensity measure for collapse risk assessment. *Earthquake Engineering & Structural Dynamics, 44*(12), 2057-2073. Retrieved 6 5, 2020, from https://onlinelibrary.wiley.com/doi/abs/10.1002/eqe.2575

F.E.M.A. (2013). *HAZUS-MH 2.1 Earthquake Model Technical Manual*. Washington D.C.: Federal Emergency Management Agency.

Gehl, P., Cavalieri, F., & Franchin, P. (2018). Approximate Bayesian network formulation for the rapid loss assessment of real-world infrastructure systems. *Reliability Engineering & System Safety, 177*, 80-93. Retrieved 12 1, 2021, from https://sciencedirect.com/science/article/pii/s0951832017313376

Iatsko, O., & Nowak, A. (2021). Revisited Live Loads for Single-Span Bridges. *Journal of Bridge Engineering*. doi:https://doi.org/10.1061/(ASCE)BE.1943-5592.0001647

ISTAT. (2014). *Matrici del Pendolarismo*. Retrieved from https://www.istat.it/it/archivio/139381

ISTAT. (2020). *Report condizione di vita, reddito e carico fiscale 2019*. Retrieved from https://www.istat.it/it/files/2020/12/REPORT-REDDITO-CONDIZIONI-DI-VITA-E-CARICO-FISCALE-2018_2019.pdf

Jalayer, F., Franchin, P., & Pinto, P. (2007). A scalar damage measure for seismic reliability analysis of RC frames. *Earthquake Engineering & Structural Analysis*, 2059-2079.

Joint Research Centre. (2013). *Guidelines for typology definition of European physical assets for earthquake risk assessment*. Luxemburg: European Commission.

Kalakonas, P., & Silva, V. (2021). Seismic vulnerability modelling of building portfolios using artificial neural networks. *Earthquake engineering and Structural Dynamics*, 1-18. doi:10.1002/eqe.3567

Kent, D., & Park, R. (1971). Flexural members with confined concrete. *Journal of the Structural Division, Proc. of the American Society of Civil Engineers*.

Kilanitis, I., & Sextos, A. (2018). Impact of earthquake-induced bridge damage and time evolving traffic demand on the road network resilience. *Journal of Traffic and Transportation Engineering*.

Kiremidjian, A., Moore, J., Fan, Y., Yazlali, O., Basoz, N., & Williams, M. (2007). Seismic Risk Assessment of Transportation Network Systems. *Journal of Earthquake Engineering*, 371-382. doi:http://dx.doi.org/10.1080/13632460701285277

Kohrangi, M., Bazzurro, P., Vamvatsikos, D., & Spillatura, A. (2017). Conditional spectrum-based ground motion record selection using average spectral acceleration. *Earthquake Engineering and Structural Dynamics*.

Kohrangi, M., Vamvatsikos, D., & Bazzurro, P. (2017). Site dependence and record selection schemes for building fragility and regional loss assessment. *Earthquake Engineering and Structural Dynamics*.

Lin, T., Haselton, C. B., & Baker, J. W. (2013). Conditional spectrum-based ground motion selection. Part I: Hazard consistency for risk-based assessments. *Earthquake Engineering & Structural Dynamics, 42*(12), 1847-1865. Retrieved 7 23, 2020, from http://web.stanford.edu/~bakerjw/publications/lin_et_al_(2013)_cs-based_gms_i,_eesd.pdf

Lupoi, A., Franchin, P., & Schotanus, M. I. (2003). Seismic risk evaluation of RC bridge structures. *Earthquake Engineering & Structural Dynamics, 32*(8), 1275-1290. Retrieved 12 1, 2021, from https://core.ac.uk/display/54368166

Luzi, L., Puglia, R., Russo, E., D'Amico, M., Felicetta, C., Pacor, F., . . . Zare, M. (2016). The Engineering Strong-Motion Database: A Platform to Access Pan-European Accelerometric Data. *Seismological Research Letters, 87*(4), 987-997. Retrieved 7 23, 2020, from https://pubs.geoscienceworld.org/ssa/srl/article-abstract/87/4/987/314138/the-engineering-strong-motion-database-a-platform

M.I.T., M. I. (2008). *NTC 2008 - Norme Tecniche per le Costruzioni (in Italian)*. Rome.

Mangalathu, S., Hwang, S.-H., Choi, E., & Jeon, J.-S. (2019). Rapid seismic damage evaluation of bridge portfolios using machine learning techniques. *Engineering Structures, 201*, 109785. Retrieved 9 14, 2021, from https://sciencedirect.com/science/article/pii/s0141029619328068

Mangalathu, S., Soleimani, F., & Jeon, J. (2017). Bridge classess for regional seismic risk assessment: Improving HAZUS models. *Engineering Structures*, 755-766. doi:http://dx.doi.org/10.1016/j.engstruct.2017.07.019

Maratini, R. (2008). *Strumenti per l'analisi dei sistemi di trasporto alla scala regionale:modelli di simulazione e sistemi informativi*. PhD Dissertation, Università degli Studi di Trieste. Retrieved from http://hdl.handle.net/10077/2752

McKenna, F. (2011). OpenSees: A Framework for Earthquake Engineering Simulation. *Computing in Science & Engineering*, 58 - 66.

Miller, M., & Baker, J. W. (2016). Coupling mode-destination accessibility with seismic risk assessment to identify at-risk communities. *Reliability Engineering & System Safety, 147*, 60-71. Retrieved 10 25, 2021, from https://sciencedirect.com/science/article/pii/s0951832015003117

Ministero delle Intrastrutture e dei Trasporti . (2020). *Decreto M 578 del 17-12-2020*. Roma: Consiglio Superiore dei Lavori Pubblici.

Mitradjieva, M., & Lindberg, P. O. (2013). The Stiff Is Moving---Conjugate Direction Frank-Wolfe Methods with Applications to Traffic Assignment*. *Transportation Science, 47*(2), 280-293. Retrieved 9 21, 2021, from https://pubsonline.informs.org/doi/abs/10.1287/trsc.1120.0409

Monteiro, R., Zelaschi, C., Silva, A., & Pinho, R. (2017). Derivation of Fragility Functions for Seismic Assessment of RC Bridge Portfolios Using Different Intensity Measures. *Journal of Earthquake Engineering*.

Nielson, B. G., & DesRoches, R. (2007). Analytical Seismic Fragility Curves for Typical Bridges in the Central and Southeastern United States. *Earthquake Spectra, 23*(3), 615-633. Retrieved 1 12, 2022, from https://earthquakespectra.org/doi/abs/10.1193/1.2756815

O'Reilly, G., & Calvi, G. (2019). Conceptual seismic design in performance-based earthquake engineering. *Earthquake Engineering & Structural Dynamics*, 389–411. doi:10.1002/eqe.3141

OpenStreetMap contributors. (2020, 2 20). *OpenStreetMap Planet dump*. Retrieved from OpenStreetMap: https://download.geofabrik.de/europe/italy/sud.html

OpenStreetMap contributors. (2020). *Planet dump*. Retrieved from https://planet.osm.org: https://www.openstreetmap.org

O'Reilly, G. (2021). Seismic intensity measures for risk assessment of bridges. *Bulletin of Earthquake Engineering*, 3671-3699. doi:https://doi.org/10.1007/s10518-021-01114-z

O'Reilly, G., & Monteiro, R. (2019). On the Efficient Risk Assessment of Bridge Structures. *7th ECCOMAS Thematic Conference COMPDYN*. Crete Island, Greece.

Ozsarac, V., Monteiro, R., & Calvi, G. (2021). Probabilistic seismic assessment of reinforced concrete bridges using simulated records. *Structure and Infrastructure Engineering*. doi:10.1080/15732479.2021.1956551

Padgett, J. E., Nielson, B. G., & DesRoches, R. (2008). Selection of optimal intensity measures in probabilistic seismic demand models of highway bridge portfolios. *Earthquake Engineering & Structural Dynamics, 37*(5), 711-725. Retrieved 11 30, 2020, from https://onlinelibrary.wiley.com/doi/abs/10.1002/eqe.782

Pellegrino, C., Pipinato, A., & Modena, C. (2011). A Simplified Management Procedure for Bridge Network Maintenance. *Structure and Infrastructure Engineering, 7*(5), 341-351. Retrieved 9 20, 2021, from https://tandfonline.com/doi/abs/10.1080/15732470802659084

Perdomo, C., Abarca, A., & Monteiro, R. (2020). *Estimation of Seismic Expected Annual Losses for Multi-Span Continuous RC Bridge Portfolios Using a Component-Level Approach*. Journal of Earthquake Engineering. doi:10.1080/13632469.2020.1781710

Pinto, P. E., & Franchin, P. (2010). Issues in the Upgrade of Italian Highway Structures. *Journal of Earthquake Engineering, 14*(8), 1221-1252. Retrieved 12 1, 2021, from https://core.ac.uk/display/54351613

Pitilakis, K., Franchin, P., Khazai, B., & Wenzel, H. (2014). *SYNER-G: Systemic Seismic Vulnerability and Risk Assessment of Complex Urban, Utility, Lifeline Systems and Critical Facilities*. Dordrecht: Springer. doi:10.1007/978-94-017-8835-9

Porter, K. (2009). Cracking an Open Safe: More HAZUS Vulnerability Functions in Terms of Structure-Independent Intensity. *Earthquake Spectra*.

Porter, K. A. (2003). An overview of PEER's performance-based earthquake engineering methodology. *Ninth International Conference on Applications of Statistics and Probability in Engineering*. San Francisco, California.

Santarsiero, G., Masi, A., Picciano, V., & Digrisolo, A. (2021). The Italian Guidelines on Risk Classification and Management of Bridges: Applications and Remarks on Large Scale Risk Assessments. *Infrastructures, 6*(8). doi:https://doi.org/10.3390/infrastructures6080111

Saw, K., Katti, B., & Joshi, G. (2014). Literature Review of Traffic Assignment: Static and Dynamic. *International Journal of Transportation Engineering*, 339-347. doi:https://dx.doi.org/10.22119/ijte.2015.10447

Scott, M., & Fenves, G. (2006). Plastic Hinge Integration Methods for Force-Based Beam–Column Elements. *Journal of Structural Engineering*, 244-252.

Shahnazaryan, D., & O'Reilly, G. (2021). Integrating expected loss and collapse risk in performance-based seismic design of structures. *Bulletin of Earthquake Engineering*, 987–1025. doi:10.1007/s10518-020-01003-x

Shinozuka, M., Murachi, Y., Dong, X., Zhou, Y., & Orlikowski, M. (2003). Effect of seismic retrofit of bridges in transportation networks. *Earthquake Engineering and Engineering Vibration*, 169-179.

Silva, V., Akkar, S., Baker, J., Bazzurro, P., Castro, J., Crowley, H., . . . Vamvatsikos, D. (2019). Current Challenges and Future Trends in Analytical Fragility and Vulnerability Modelling. *Earthquake Spectra*.

Silva, V., Crowley, H., Pagani, M., Monelli, D., & Pinho, R. (2014). Development of the OpenQuake engine, the Global Earthquake Model's open-source software for seismic risk assessment. *Natural Hazards, 72*(3), 1409-1427. Retrieved 7 23, 2020, from https://link.springer.com/article/10.1007/s11069-013-0618-x

Stefanidou, S. P., & Kappos, A. J. (2019). Bridge-specific fragility analysis: when is it really necessary? *Bulletin of Earthquake Engineering, 17*(4), 2245-2280. Retrieved 11 11, 2021, from https://openaccess.city.ac.uk/21190

Stergiou, E., & Kiremidjian, A. (2008). *Treatment of uncertainties in seismic risk analysis of transportation systems (PEER Report 2008/02).* Berkeley, California: Pacific Earthquake Engineering Research Center .

Tian, Y., Chiu, Y.-C., Sun, J., & Chai, C. (2020). Sunsetting skim matrices: A trajectory-mining approach to derive travel time skim matrix in dynamic traffic assignment for activity-base model integration. *Journal of Transport and Land Use*, 413–428. doi:https://doi.org/10.5198/jtlu.2020.1551

Woessner, J., Laurentiu, D., Giardini, D., Crowley, H., Cotton, F., Grünthal, G., . . . Stucchi, M. (2015). The 2013 European Seismic Hazard Model: key components and results. *Bulletin of Earthquake Engineering, 13*(12), 3553-3596. Retrieved 7 23, 2020, from https://link.springer.com/article/10.1007/s10518-015-9795-1

Woessner, J., Laurentiu, D., Giardini, D., Crowley, H., Cotton, F., Grünthal, G., . . . Stucchi, M. (2015). The 2013 European Seismic Hazard Model: key components and results. *Bulletin of Earthquake Engineering, 13*(12), 3553-3596. Retrieved 9 22, 2021, from https://link.springer.com/article/10.1007/s10518-015-9795-1

Yue, Y., Zonta, D., Bortot, F., & Zandonini, R. (2010). *Assessment of the operation level of a bridge network in post-earthquake scenarios*. Retrieved 1 12, 2022, from https://strathprints.strath.ac.uk/55998

Zelaschi, C., Monteiro, R., & Pihno, R. (2016). Parametric Characterization of RC Bridges for Seismic Assessment Purposes. *Structures*(7), 14-24.

Zelaschi, C., Monteiro, R., & Pinho, R. (2016). SIMPLIFIED PERIOD ESTIMATION OF ITALIAN RC BRIDGES FOR LARGE-SCALE SEISMIC ASSESSMENT. *ECCOMAS Conference 2016*. Crete, Greece. doi:10.7712/100016.2237.16427

Zilske, M., Neumann, A., & Nagel, K. (2011). *OpenStreetMap for traffic simulation*. Retrieved 10 21, 2021, from https://depositonce.tu-berlin.de/bitstream/11303/4976/2/zilske_neumann_nagel.pdf

Zuccolo, E., O'Reilly, G., Poggi, V., & Monteiro, R. (2021). haselREC: an automated open-source ground motion record selection and scaling tool. *Bulletin of Earthquake Engineering*, 5747-5767. doi:10.1007/s10518-021-01214-w